ArevaEPRDCPEm Resource

From: WILLIFORD Dennis (AREVA) [Dennis.Williford@areva.com]
Sent: Monday, April 29, 2013 5:18 PM
To: Snyder, Amy
Cc: Miernicki, Michael; ANDERSON Katherine (EXTERNAL AREVA); DELANO Karen (AREVA); LEIGHLITER John (AREVA); ROMINE Judy (AREVA); RYAN Tom (AREVA)
Subject: Response to U.S. EPR Design Certification Application RAI No. 547 (6499, 6359), FSAR Ch. 3 - NEW PHASE 4 RAI, Supplement 6 - Part 1 of 4
Attachments: RAI 547 Supplement 6 Response US EPR DC Part_1of4.pdf

Amy,

AREVA NP Inc. provided a schedule for a technically correct and complete response to the four questions in RAI No. 547 on July 11, 2012. On October 4, 2012, AREVA NP submitted Supplement 1 which provided a technically correct and complete final response to one (03.07.02-77) of the four remaining questions. On November 27, 2012, AREVA NP submitted Supplement 2 which changed the schedule for one of the three remaining questions. On November 29, 2012, AREVA NP submitted Supplement 3 which provided a technically correct and complete final response to one of the three remaining questions. On January 31, 2013, AREVA NP submitted Supplement 4 which provided a technically correct and complete final response to Question 03.06.01-14. On April 11, 2013, AREVA NP submitted Supplement 5 which provided a revised final response to Question 03.06.01-14 based on NRC staff feedback received during the ITAAC Public Meeting on April 4-5, 2013.

The attached file, "RAI 547 Supplement 6 Response US EPR DC – Part 1 of 4.pdf" provides a technically correct and complete final response to Question 03.07.02-78. Due to file size limitations, the remaining parts will be provided in three subsequent e-mails.

The following table indicates the respective pages in the response document, "RAI 547 Supplement 6 Response US EPR DC.pdf," that contain AREVA NP's response to the subject question. Appended to this file are affected pages of the U.S. EPR Final Safety Analysis Report in redline-strikeout format which support the response to RAI 547, Question 03.07.02-78.

Question #	Start Page	End Page
RAI 547 — 03.07.02-78	2	54

This concludes the formal AREVA NP response to RAI 547, and there are no questions from this RAI for which AREVA NP has not provided responses.

Sincerely,

Dennis Williford, P.E.
U.S. EPR Design Certification Licensing Manager
AREVA NP Inc.
7207 IBM Drive, Mail Code CLT 2B
Charlotte, NC 28262
Phone: 704-805-2223
Email: Dennis.Williford@areva.com

From: WILLIFORD Dennis (RS/NB)
Sent: Thursday, April 11, 2013 6:44 PM
To: Amy.Snyder@nrc.gov
Cc: Michael.Miernicki@nrc.gov; DELANO Karen (RS/NB); LEIGHLITER John (RS/NB); ROMINE Judy (RS/NB); RYAN Tom (RS/NB); WILLS Tiffany (CORP/QP); HONMA George (EXT); LENTZ Tony (External RS/NB)
Subject: Response to U.S. EPR Design Certification Application RAI No. 547 (6499, 6359), FSAR Ch. 3 - NEW PHASE 4 RAI, Supplement 5

Amy,

AREVA NP Inc. provided a schedule for a technically correct and complete response to the four questions in RAI No. 547 on July 11, 2012. On October 4, 2012, AREVA NP submitted Supplement 1 which provided a technically correct and complete final response to one (03.07.02-77) of the four remaining questions. On November 27, 2012, AREVA NP submitted Supplement 2 which changed the schedule for one of the three remaining questions. On November 29, 2012, AREVA NP submitted Supplement 3 which provided a technically correct and complete final response to one of the three remaining questions. On January 31, 2013, AREVA NP submitted Supplement 4 which provided a technically correct and complete final response to Question 03.06.01-14.

The attached file, "RAI 547 Supplement 5 Response US EPR DC.pdf" provides a revised final response to Question 03.06.01-14 based on NRC staff feedback received during the ITAAC Public Meeting on April 4-5, 2013.

The following table indicates the respective pages in the response document, "RAI 547 Supplement 5 Response US EPR DC.pdf," that contain AREVA NP's response to the subject question. Appended to this file are affected pages of the U.S. EPR Final Safety Analysis Report in redline-strikeout format which support the response to RAI 547, Question 03.06.01-14.

Question #	Start Page	End Page
RAI 547 — 03.06.01-14	2	18

The schedule for a technically correct and complete response to the remaining question is unchanged and is provided below.

Question #	Response Date
RAI 547 — 03.07.02-78	April 30, 2013

Sincerely,

Dennis Williford, P.E.
U.S. EPR Design Certification Licensing Manager
AREVA NP Inc.
7207 IBM Drive, Mail Code CLT 2B
Charlotte, NC 28262
Phone: 704-805-2223
Email: Dennis.Williford@areva.com

From: WILLIFORD Dennis (RS/NB)
Sent: Thursday, January 31, 2013 8:26 PM
To: Amy.Snyder@nrc.gov
Cc: Michael.Miernicki@nrc.gov; DELANO Karen (RS/NB); LEIGHLITER John (RS/NB); ROMINE Judy (RS/NB); RYAN Tom (RS/NB); WILLS Tiffany (CORP/QP); WELLS Russell (RS/NB); VANCE Brian (RS/NB); GUCWA Len (External RS/NB)
Subject: Response to U.S. EPR Design Certification Application RAI No. 547 (6499, 6359), FSAR Ch. 3 - NEW PHASE 4 RAI, Supplement 4

Amy,

AREVA NP Inc. provided a schedule for a technically correct and complete response to the four questions in RAI No. 547 on July 11, 2012. On October 4, 2012, AREVA NP submitted Supplement 1 which provided a technically correct and complete final response to one (03.07.02-77) of the four remaining questions. On November 27, 2012, AREVA NP submitted Supplement 2 which changed the schedule for one of the three remaining questions. On November 29, 2012, AREVA NP submitted Supplement 3 which provided a technically correct and complete final response to one of the three remaining questions.

The attached file, "RAI 547 Supplement 4 Response US EPR DC.pdf" provides a technically correct and complete final response to one of the two remaining questions.

The following table indicates the respective pages in the response document, "RAI 547 Supplement 4 Response US EPR DC.pdf," that contain AREVA NP's response to the subject question. Appended to this file are affected pages of the U.S. EPR Final Safety Analysis Report in redline-strikeout format which support the response to RAI 547, Question 03.06.01-14.

Question #	Start Page	End Page
RAI 547 — 03.06.01-14	2	22

The schedule for a technically correct and complete response to the remaining question is unchanged and is provided below.

Question #	Response Date
RAI 547 — 03.07.02-78	April 30, 2013

Sincerely,

Dennis Williford, P.E.
U.S. EPR Design Certification Licensing Manager
AREVA NP Inc.
7207 IBM Drive, Mail Code CLT 2B
Charlotte, NC 28262
Phone: 704-805-2223
Email: Dennis.Williford@areva.com

From: WILLIFORD Dennis (RS/NB)
Sent: Thursday, November 29, 2012 12:10 PM
To: Amy.Snyder@nrc.gov
Cc: BENNETT Kathy (RS/NB); DELANO Karen (RS/NB); LEIGHLITER John (RS/NB); ROMINE Judy (RS/NB); RYAN Tom

(RS/NB)
Subject: Response to U.S. EPR Design Certification Application RAI No. 547 (6499, 6359), FSAR Ch. 3 - NEW PHASE 4 RAI, Supplement 3

Amy,

AREVA NP Inc. provided a schedule for a technically correct and complete response to the four questions in RAI No. 547 on July 11, 2012. On October 4, 2012, AREVA NP submitted Supplement 1 which provided a technically correct and complete final response to one (03.07.02-77) of the four remaining questions. On November 27, 2012, AREVA NP submitted Supplement 2 which changed the schedule for one of the three remaining questions.

The attached file, "RAI 547 Supplement 3 Response US EPR DC.pdf" provides a technically correct and complete final response to one of the three remaining questions.

The following table indicates the respective pages in the response document, "RAI 547 Supplement 3 Response US EPR DC.pdf," that contain AREVA NP's response to the subject question. Appended to this file are affected pages of the U.S. EPR Final Safety Analysis Report in redline-strikeout format which support the response to RAI 547, Question 03.07.02-76.

Question #	Start Page	End Page
RAI 547 — 03.07.02-76	2	14

The schedule for a technically correct and complete response to the remaining 2 questions is unchanged and is provided below.

Question #	Response Date
RAI 547 — 03.06.01-14	January 31, 2013
RAI 547 — 03.07.02-78	April 30, 2013

Sincerely,

Dennis Williford, P.E.
U.S. EPR Design Certification Licensing Manager
AREVA NP Inc.
7207 IBM Drive, Mail Code CLT 2B
Charlotte, NC 28262
Phone: 704-805-2223
Email: Dennis.Williford@areva.com

From: WILLIFORD Dennis (RS/NB)
Sent: Tuesday, November 27, 2012 12:40 PM
To: Amy.Snyder@nrc.gov
Cc: BENNETT Kathy (RS/NB); DELANO Karen (RS/NB); LEIGHLITER John (RS/NB); ROMINE Judy (RS/NB); RYAN Tom (RS/NB); WELLS Russell (RS/NB)
Subject: Response to U.S. EPR Design Certification Application RAI No. 547 (6499, 6359), FSAR Ch. 3 - NEW PHASE 4 RAI, Supplement 2

Amy,

AREVA NP Inc. provided a schedule for a technically correct and complete response to the four questions in RAI No. 547 on July 11, 2012. On October 4, 2012, AREVA NP submitted Supplement 1 which provided a technically correct and complete final response to one (03.07.02-77) of the four remaining questions.

The schedule for a technically correct and complete response to the 1 of the remaining 3 questions has been changed as provided below.

Question #	Response Date
RAI 547 — 03.06.01-14	**January 31, 2013**
RAI 547 — 03.07.02-76	November 29, 2012
RAI 547 — 03.07.02-78	April 30, 2013

Sincerely,

Dennis Williford, P.E.
U.S. EPR Design Certification Licensing Manager
AREVA NP Inc.
7207 IBM Drive, Mail Code CLT 2B
Charlotte, NC 28262
Phone: 704-805-2223
Email: Dennis.Williford@areva.com

From: WILLIFORD Dennis (RS/NB)
Sent: Wednesday, October 17, 2012 2:07 PM
To: Amy.Snyder@nrc.gov
Cc: Michael.Miernicki@nrc.gov; BENNETT Kathy (RS/NB); DELANO Karen (RS/NB); LEIGHLITER John (RS/NB); ROMINE Judy (RS/NB); RYAN Tom (RS/NB); GARDNER Darrell (RS/NB) (Darrell.Gardner@areva.com); VANCE Brian (RS/NB); WELLS Russell (RS/NB)
Subject: Response to U.S. EPR Design Certification Application RAI No. 547 (6499, 6359), FSAR Ch. 3 - NEW PHASE 4 RAI, Question 03.06.01-14 - STATUS

Amy,
AREVA appreciates the initial comments received from NRC staff during our telecon on September 25th, the e-mail with additional comments received on September 27th, and the additional comments and status update on the review status of the DRAFT RAI 547 Question 03.06.01-14 response (submitted on August 17, 2012) which were provided by Mike Miernicki on October 15th. We understand that the NRC staff needs additional time to complete their review and provide final comments on the Draft response. AREVA will provide a revised schedule for submittal of the final response to this question after receipt and evaluation of all NRC staff comments.

The schedule for a technically correct and complete final response to the other 2 questions remains unchanged as shown below.

Question #	Response Date

RAI 547 — 03.06.01-14	**TBD**
RAI 547 — 03.07.02-76	November 29, 2012
RAI 547 — 03.07.02-78	April 30, 2013

Sincerely,

Dennis Williford, P.E.
U.S. EPR Design Certification Licensing Manager
AREVA NP Inc.
7207 IBM Drive, Mail Code CLT 2B
Charlotte, NC 28262
Phone: 704-805-2223
Email: Dennis.Williford@areva.com

From: RYAN Tom (RS/NB)
Sent: Thursday, October 04, 2012 1:33 PM
To: Tesfaye, Getachew
Cc: BENNETT Kathy (RS/NB); DELANO Karen (RS/NB); LEIGHLITER John (RS/NB); ROMINE Judy (RS/NB); WILLIFORD Dennis (RS/NB); ABAYAN Victor (EP/PE)
Subject: Response to U.S. EPR Design Certification Application RAI No. 547 (6499, 6359), FSAR Ch. 3 - NEW PHASE 4 RAI, Supplement 1

Getachew,

AREVA NP Inc. provided a schedule for a technically correct and complete response to the four questions in RAI No. 547 on July 11, 2012.

The attached file, "RAI 547 Supplement 1 Response US EPR DC.pdf" provides a technically correct and complete final response to one of the four remaining questions.

The following table indicates the respective pages in the response document, "RAI 547 Supplement 1 Response US EPR DC.pdf," that contain AREVA NP's response to the subject question. Appended to this file are affected pages of the U.S. EPR Final Safety Analysis Report in redline-strikeout format which support the responses to RAI 547 Question 03.07.02-77.

Question #	**Start Page**	**End Page**
RAI 547 — 03.07.02-77	2	2

The schedule for a technically correct and complete response to the remaining 3 questions is unchanged and is provided below.

Question #	**Response Date**
RAI 547 — 03.06.01-14	**October 17, 2012**
RAI 547 — 03.07.02-76	**November 29, 2012**
RAI 547 — 03.07.02-78	**April 30, 2013**

Sincerely,

Tom Ryan for
Dennis Williford, P.E.
U.S. EPR Design Certification Licensing Manager
AREVA NP Inc.
7207 IBM Drive, Mail Code CLT 2B
Charlotte, NC 28262
Phone: 704-805-2223
Email: Dennis.Williford@areva.com

From: WILLIFORD Dennis (RS/NB)
Sent: Wednesday, July 11, 2012 2:52 PM
To: Getachew.Tesfaye@nrc.gov
Cc: BENNETT Kathy (RS/NB); DELANO Karen (RS/NB); ROMINE Judy (RS/NB); RYAN Tom (RS/NB); Michael.Miernicki@nrc.gov; WELLS Russell (RS/NB)
Subject: Response to U.S. EPR Design Certification Application RAI No. 547 (6499, 6359), FSAR Ch. 3 - NEW PHASE 4 RAI

Getachew,

Attached please find AREVA NP Inc.'s response to the subject request for additional information (RAI). The attached file, "RAI 547 Response US EPR DC.pdf," provides a schedule since a technically correct and complete response to the four questions cannot be provided at this time.

The following table indicates the respective pages in the response document, "RAI 547 Response US EPR DC.pdf," that contain AREVA NP's response to the subject questions.

Question #	Start Page	End Page
RAI 547 — 03.06.01-14	2	2
RAI 547 — 03.07.02-76	3	4
RAI 547 — 03.07.02-77	5	5
RAI 547 — 03.07.02-78	6	12

The schedule for a technically correct and complete response to these 4 questions is provided below.

Question #	Response Date
RAI 547 — 03.06.01-14	**October 17, 2012**
RAI 547 — 03.07.02-76	**November 29, 2012**
RAI 547 — 03.07.02-77	**November 14, 2012**
RAI 547 — 03.07.02-78	**April 30, 2013**

Sincerely,

Dennis Williford, P.E.
U.S. EPR Design Certification Licensing Manager
AREVA NP Inc.

7207 IBM Drive, Mail Code CLT 2B
Charlotte, NC 28262
Phone: 704-805-2223
Email: Dennis.Williford@areva.com

From: Tesfaye, Getachew [mailto:Getachew.Tesfaye@nrc.gov]
Sent: Friday, June 15, 2012 2:45 AM
To: ZZ-DL-A-USEPR-DL
Cc: Xu, Jim; Thomas, Brian; Miernicki, Michael; Clark, Phyllis; Segala, John; ArevaEPRDCPEm Resource
Subject: U.S. EPR Design Certification Application RAI No. 547 (6499, 6359), FSAR Ch. 3 - NEW PHASE 4 RAI

Attached please find the subject request for additional information (RAI). A draft of the RAI was provided to you on May 17, 2012, and June 12, 2012, you informed us that the RAI is clear and no further clarification is needed. As a result, no change is made to the draft RAI. The schedule we have established for review of your application assumes technically correct and complete responses within 30 days of receipt of RAIs. For any RAIs that cannot be answered within 30 days, it is expected that a date for receipt of this information will be provided to the staff within the 30 day period so that the staff can assess how this information will impact the published schedule.

Thanks,
Getachew Tesfaye
Sr. Project Manager
NRO/DNRL/LB1
(301) 415-3361

Hearing Identifier: AREVA_EPR_DC_RAIs
Email Number: 4351

Mail Envelope Properties (554210743EFE354B8D5741BEB695E65612BFF5)

Subject: Response to U.S. EPR Design Certification Application RAI No. 547 (6499, 6359), FSAR Ch. 3 - NEW PHASE 4 RAI, Supplement 6 - Part 1 of 4
Sent Date: 4/29/2013 5:18:22 PM
Received Date: 4/29/2013 5:20:57 PM
From: WILLIFORD Dennis (AREVA)

Created By: Dennis.Williford@areva.com

Recipients:
"Miernicki, Michael" <Michael.Miernicki@nrc.gov>
Tracking Status: None
"ANDERSON Katherine (EXTERNAL AREVA)" <katherine.anderson.ext@areva.com>
Tracking Status: None
"DELANO Karen (AREVA)" <Karen.Delano@areva.com>
Tracking Status: None
"LEIGHLITER John (AREVA)" <John.Leighliter@areva.com>
Tracking Status: None
"ROMINE Judy (AREVA)" <Judy.Romine@areva.com>
Tracking Status: None
"RYAN Tom (AREVA)" <Tom.Ryan@areva.com>
Tracking Status: None
"Snyder, Amy" <Amy.Snyder@nrc.gov>
Tracking Status: None

Post Office: FUSLYNCMX03.fdom.ad.corp

Files	**Size**	**Date & Time**
MESSAGE	16838	4/29/2013 5:20:57 PM
RAI 547 Supplement 6 Response US EPR DC Part_1of4.pdf	6998904	

Options
Priority: Standard
Return Notification: No
Reply Requested: No
Sensitivity: Normal
Expiration Date:
Recipients Received:

Response to

Advanced Request for Additional Information No. 547, Supplement 6

06/15/2012

U.S. EPR Standard Design Certification
AREVA NP Inc.
Docket No. 52-020
SRP Section: 03.07.02 – Seismic System Analysis

Application Section: FSAR Section 3.7

QUESTIONS for Structural Engineering Branch 2 (ESBWR/ABWR Projects) (SEB2)

Question 03.07.02-78

Open Item

Follow-up to RAI 371, Question 03.07.02-66 and RAI 376 Question 03.08.05-28.

1. In RAI 371 Question 03.07.02-66 Item (a), the staff had asked the applicant to evaluate the impact of an analysis simplification for the seismic analysis of the Nuclear Island (NI) basemat in that zero thickness plate elements all lying in a single plane were used to represent the basemat centerline. However, the actual basemat has a thickness which varies and the centerline does not lie in a single plane. This has the potential to introduce errors in the basemat seismic loads used for design. In its response the applicant describes a revised NI 3D FEM seismic analysis model which is used to develop the basemat seismic loads. The foundation basemat is represented by five layers of solid brick elements. These elements replace the zero thickness shell elements used to represent the basemat in the SASSI model. This FEM is used to calculate moments and shears in the basemat using the ANSYS computer program. The time history inputs are the in-column motions at the level of the bottom of the basemat and are consistent with those motions used in the corresponding SASSI analysis.

   Compression-only vertical soil springs support the bottom of the basemat while horizontal contact/sliding elements are used to address the potential sliding of the model. The spring parameters were obtained from the Gazetas formulation, which were found to produce displacements and base reactions similar to the SASSI results for the dynamic case. However the comparison of displacements and base reactions was not provided with the applicant's response and should be included to allow the staff to complete its evaluation and to provide assurance that the SASSI model and ANSYS model are dynamically equivalent. In addition the applicant did not provide the properties of the contact/sliding elements used in the analysis. The applicant is requested to provide these properties and their technical basis for the staff's review.

   In the response it says that springs similar to the dynamic model were used in the static model. For static models the spring stiffness is normally set at about one-half the dynamic spring stiffness. However in a discussion of the static model soil springs the applicant says that the one-half of the strain compatible shear modulus was used for the seismic soil cases. This appears to be an editorial error in that it should state that one-half of the strain compatible shear modulus was used for the static soil cases. The applicant is requested to explain this discrepancy and correct the sentence if it is in error.

   In FSAR Section 3.7.2.3.1.4, Revision 4 Interim, on page 3.7-106 it states that the ANSYS model is loaded statically by accelerating the lumped and distributed masses before a time history analysis is performed. Presumably the time history results then include the effect of both the dynamic and static loads. The applicant should describe how the dynamic shears and moments are then extracted from this result so that they can be combined with the results of the ANSYS static model which uses spring stiffness's based on one-half of the strain compatible shear modulus.

   Lateral soil pressures along the vertical embedded walls were developed following a standard geotechnical approach. For the seismic loads, the lateral soil pressures are based on wall displacements that occur during the application of the seismic input motions. The

parameters of the lateral springs were developed to yield maximum and minimum pressures defined by the Rankine passive (Kp = 3.0)/active (Ka = 0.333) pressure states with an at-rest pressure (K0) value of 0.50. The stiffness of these springs was selected to yield a displacement at full passive pressure of 0.006H (2.799 in) and for the minimum active state a displacement of 002H (0.933 in). However, the passive pressure curve appears to be different from that used in the stability analysis of the NI presented in the response to RAI 376 Question 03.07.02-69 (see Figures 03.07.02-69-15 and -16). The applicant is requested to explain why a different passive curve was used in the basemat analysis and what effect this might have on the mat design loads.

The tendon gallery acts as a shear key under seismic loads. The seismic loads need to include the effect of any localized movement of the basemat. Determining the additional loads due to movement of the basemat is accomplished by performing two separate analyses. In the first analysis, uplift and sliding of the basemat is not allowed. In the second analysis, uplift and sliding is permitted. The difference in the pressure between these two cases is a delta pressure which is added to the lateral loads determined from the SASSI SSI analysis of the NI. For the two rock cases which appear to provide the highest sidewall pressure loads on the shear key, the applicant states that the top ring of nodes of the tendon gallery are connected to the solid element basemat using ANSYS shell to solid Multi-Point Constraints (MPCs) and have no sidewall rock springs. The bottom ring (elevation) of nodes of these shell elements that are connected to the basemat have stiff sidewall rock springs that simulate partially fixed boundary conditions. These nodes experience higher pressures and moments (stress concentration effect) typically associated with fixity. For these cases, average maximum pressure values considering a full element instead of a node are presented in Table 03.07.02-66-2. As it is not clear from the applicant's explanation which nodes or elements are being described and what is meant by partially fixed boundary conditions, the applicant is requested to provide:

- A figure depicting the boundary conditions for the shear key nodes and;
- A figure depicting maximum pressure values and average pressure values over the complete height of the tendon gallery with a description of how the average values were calculated.

2. The response to RAI 371 Question 03.07.02-66 Item (a) indicates that FSAR Tier 2, Section 3.8.5.4.2 was revised to clarify how the seismic design loads for the NI basemat are obtained from the ANSYS 3D FEM basemat foundation model. However, a review of the FSAR Section 3.8.5.4.2 markup reveals several inconsistencies and discrepancies with the information provided in the RAI response, as well as obsolete information that is no longer applicable to the applicant's current design approach for the NI. For example, the staff notes the following:

   (a) Section 3.8.5.4.2, Revision 4 Interim, first paragraph. The second sentence refers to a "static model" that is incorrectly stated as being described in Sections 3.8.1.4.1 and 3.8.5.3.

   (b) Section 3.8.5.4.2, Revision 3, second paragraph. There remains a reference to the "NI Common Basemat Structure static analysis." There is also a reference to Figure 3.8-103 that illustrates the ANSYS NI basemat model; however, the latter only shows the NI basemat itself and not the superstructure (which is also a part of the NI basemat model as shown in Figure 3.7.2-152).

(c) Section 3.8.5.4.2, Revision 3, third and subsequent paragraphs. An explanation is provided as to how the vertical soil/rock springs were developed using the Gazetas formulation and the elliptical variation of stiffness across the foundation footprint. However, specific information is only provided for the static springs (i.e., springs used in the static analysis for gravity loads, Table 3.8-13). No information is given for the dynamic springs (i.e., springs used in the time-history seismic analysis). Furthermore, there is no mention of the horizontal soil/rock springs that represent the soil/rock pressures on the embedded sidewalls (including the tendon gallery), or the fact that the ANSYS basemat model captures nonlinear effects due to sliding and uplift.

(d) Section 3.8.5.4.2, Revision 3, pg. 3.8-134, bottom paragraph. References to Figures for obsolete soil cases such as 1u, 2u, 4u, 3r3u, etc., remain in the text.

(e) Section 3.8.5.4.2, Revision 3, pg. 3.8-135, first paragraph. The text indicates that the results of the soil spring analyses are used in determining the acceptability of the supporting soil media under static loading conditions; however, as indicated in the response to RAI 376 Question 03.08.05-28, soil bearing pressures are computed using the SASSI 3D FEM model for both static and dynamic cases.

(f) Section 3.8.5.4.2, Revision 3, pg. 3.8-135, third and subsequent paragraphs. The discussion switches from consideration of the ANSYS basemat model to the NI stability analysis, and then to the discussion of differential settlement evaluation, without a clear indication to the reader that the corresponding analytical models are different and use different computer codes. The applicant should consider using different sub-headings for each of the different discussions.

(g) Although indicated in the response, the staff could not identify in Section 3.8.5.4.2, Revision 3 or 4 Interim, the explanation of how the design forces for the NI basemat (bending moments and shears) are obtained from the analysis results of the ANSYS basemat model, for all analysis cases and loading conditions.

In light of the above, it appears that the changes made to FSAR Tier 2, Section 3.8.5.4.2, from Revision 0 through Revision 3, have resulted in a text that could be confusing to a reader who is not familiar with the various modifications made to the applicant's initial design approach. Therefore, the applicant is requested to provide a complete revision of FSAR Tier 2, Section 3.8.5.4.2 that clearly explains the ANSYS 3D FEM Basemat Foundation Model: its description, characteristics, purpose, limitations, and difference with the ANSYS Fixed Base 3D FEM Superstructure Model. This revision should be consistent with the information provided in the RAI response and with the new FSAR Tier 2, Section 3.7.2.3.1.4. This revision should also include a clear explanation of how the design forces for the NI basemat (moments and shears) are obtained from the analysis results of the ANSYS basemat model, for all analysis cases and loading conditions.

In addition, the applicant is requested to review FSAR Tier 2, Sections 3.8.1 through 3.8.5 and identify all references to the "NI Common Basemat Structure model" or to the "static model." For each identified reference, determine whether it applies to the ANSYS 3D FEM Basemat Foundation Model or to the ANSYS Fixed Base 3D FEM Superstructure Model. A clear differentiation between these two models should be evident in the text; otherwise, provide a revision to the text.

3. The response to RAI 371 Question 03.07.02-66 Item (a) indicates that soil pressures used for designing embedded walls due to seismic loading are obtained from the SSI analysis. It is also indicated that these loads are scaled up such that their magnitude is at least equal to the corresponding Rankine passive pressures (Kp = 3.0) for the corresponding soil case. These pressures are then applied to the ANSYS Fixed Base 3D FEM Superstructure Model to perform the design of the embedded walls. This is consistent with FSAR Tier 2, Section 3.8.5.4.2, Revision 4 Interim.

   On the other hand, the response to RAI 376 Question 03.08.05-28 Item 3 indicates that wall pressures calculated from SSI analysis, elastic solution by Wood, and those required for sliding stability are considered in the design of embedded walls. It adds that each soil case is analyzed, dynamically and statically, and design loads and controlling loads for each wall are used in the design. This is consistent with FSAR Tier 2, Section 3.8.5.4.1, Revision 3, but appears to be inconsistent with FSAR Tier 2, Section 3.8.5.4.2, Revision 4 Interim.

   The response to RAI 376 Question 03.08.05-28 also provides Figures 03.08.05-28-4 through 03.08.05-28-41, and Figures 03.08.05-28-60 through 03.08.05-28-97, which compare the total soil pressures applied to the ANSYS Fixed Base 3D FEM Superstructure Model (scaled SSI pressure profiles) to the passive pressures developed for the stability analysis and to Wood's solution. The applicant indicates that, for each soil case, the passive pressures from the stability analysis are always bounded by the scaled SSI pressure profiles. The staff also notes that Wood's solution is always bounded by the scaled SSI pressure profiles. This appears to address the inconsistency noted in the two preceding paragraphs. However, since the results of the comparative study are required to ensure the adequacy of the embedded wall design, in accordance with the guidance in SRP 3.8.4 and 3.8.5, the applicant is requested to provide the following additional information:

   (a) To ensure that the referenced figures in RAI 376 Question 03.08.05-28 provide a consistent comparison, confirm that all the pressure profiles shown represent the combined effect of static plus surcharge plus seismic loads, including the profiles identified as Wood's solution. How are the static and surcharge loads combined with the scaled SSI pressures and to the passive pressures from the stability analysis?

   (b) Provide a graphical explanation of the scaling of the SSI pressure profiles. Clarify whether this scaling is done at each depth so that the scaled SSI pressure profiles always bound the linear Kp=3.0 pressure profile, or whether the scaling is done at one depth only using a single scaling factor applied to the entire profile. (It is stated that the maximum pressure on each wall is at least equal to the passive earth pressure of Kp=3.0).

   (c) A review of the referenced figures indicates that, for a given wall, soil, and analysis case, it does not appear to be always true that the scaled SSI pressure profile always bounds the pressures required by the sliding stability analysis. For example, in Figure 03.08.05-28-5 (Wall 2, "cracked" analysis) the vertical "4uem Stability Kp" profile (blue line) is greater than the "4uem" profile (magenta line) at depths between approx. 5 ft. and 25 ft. A similar situation is observed in Figure 03.08.05-28-61 (Wall 2, "uncracked" analysis). This is due to the difference in the relative shape of the two pressure profiles. Since the applicant indicates that it is not using an envelope of all soil cases (such as the ones shown in Figures 03.08.05-28-42 through 03.08.05-28-59 and Figures 03.08.05-28-98 through 03.08.05-28-115), but is considering each soil case independently, explain how

it is ensured that the scaled SSI pressure profile used in wall design always bounds the pressures required by the sliding stability analysis for each soil case.

(d) It appears that the additional pressures due to the localized sliding/uplift of the basemat (i.e., the "delta pressures" described in the response to RAI 371 Question 03.07.02-66, listed in Tables 03.07.02-66-1 and 03.07.02-66-2) were not included in the referenced figures in RAI 376 Question 03.08.05-28. It therefore does not provide the staff with an accurate representation of the total soil pressures acting on the walls, which was the intent of the original RAI. Therefore, the applicant should provide a revised version of the figures in RAI 376 Question 03.08.05-28 that includes the SSI pressures, the delta pressures, and the combination of the two for all embedded walls including the tendon gallery. The information provided should be consistent with the information requested under Question (1) of this RAI.

(e) The response to RAI 371 Question 03.07.02-66 Item (a) indicates that static soil pressures corresponding to at-rest conditions (K_0=0.5) are applied separately to the ANSYS Fixed Base 3D FEM Superstructure Model. Since the soil pressures shown in the referenced figures in RAI 376 Question 03.08.05-28 represent the combined effect of static plus surcharge plus seismic loads, and it is indicated that they are applied separately to the ANSYS model, clarify how the static soil pressures are differentiated from the seismic soil pressures for the purposes of design load combinations.

(f) Clarify the apparent inconsistency between FSAR Tier 2, Section 3.8.5.4.1, Revision 3 and FSAR Tier 2, Section 3.8.5.4.2, Revision 4 Interim identified in the first two paragraphs of Question (3) above.

4. The response to RAI 376 Question 03.08.05-28 Attachment 1 indicates that, for rock case 5aeh, the methodology for designing embedded sidewalls due to seismic loading deviates from the methodology used for all other soil cases. Instead of soil pressures applied directly to the ANSYS Fixed Base 3D FEM Superstructure Model, this model is modified with additional nodal constraints applied to the out-of-plane X and Y directions of sidewall nodes that are in contact with the excavation, and the seismic loads are applied statically to the model. It is indicated that these additional constraints simulate the contact of the sidewalls with the surrounding hard rock, while at the same time, allowing for vertical movement of these walls to adequately represent overturning effects.

   (a) The above statements imply that the critical member forces for sidewall design occur at an elevation immediately above the top of rock, and that member forces computed by the analytical model below the top of rock, which could be locally very high, are ignored. Clarify whether this is the case, and if so, clarify whether the portions of the sidewalls below the top of rock are uniformly designed for the same member forces as the portions immediately above the top of rock.

   (b) Attachment 1 of the RAI response also indicates that inward (away from the rock) movement of the sidewalls is only expected to occur under hydrostatic or seismic (on the side of the building opposite of the earthquake direction) loading, and that this will be considered in local design. The applicant should explain how this effect is accounted for in local design. For seismic loading and global design, explain why the additional nodal constraints on the analytical model are not removed from the side of the building

opposite of the earthquake direction since the wall would move away from the rock foundation.

(c) In light of the deviation from the methodology used for all other soil cases and to ensure the adequacy of the design approach for rock case 5aeh, provide a comparison of wall member forces obtained using the alternate approach for rock case 5aeh to the wall member forces obtained by applying the following pressure profiles to the ANSYS Fixed Base 3D FEM Superstructure Model (without additional nodal constraints below the top of rock): (i) pressures obtained from the SASSI analysis and (ii) pressures considered in the sliding stability analysis. This comparison may be performed for a set of critical walls.

(d) Update the FSAR to indicate that rock case 5aeh is treated as a special case and to describe the alternate methodology.

5. The response to RAI 371 Question 03.07.02-66 Item (a) indicates that the tendon gallery is designed to resist maximum shear obtained by imposing the corresponding envelope pressure from the SASSI analysis, Wood's solution, and hydrostatic pressure.

   On the other hand, the response to RAI 376 Question 03.08.05-28 Item 3 indicates that the results from the analysis using the ANSYS basemat model with static soil springs are used to develop design loads for the foundation mat, including the tendon gallery. The applicant is requested to clarify the inconsistency with the response to RAI 371 Question 03.07.02-66 Item (a), as well as the inconsistency between what is stated above and what is shown in Figures 3.8.5-28-34 through 3.8.5-28-41 and Figures 3.8.5-28-90 through 3.8.5-28-97 in RAI 376 Question 03.08.05-28. Also, clarify what is meant by the phrase "ANSYS basemat model with static soil springs."

   The response to RAI 376 Question 03.08.05-28 provides figures showing the lateral pressures used to design the tendon gallery sidewalls. However, Figures 3.8.5-28-34 through 3.8.5-28-41 ("cracked" seismic analysis case) only show results for soil cases 1n2ue and 2sn4uem, while Figures 3.8.5-28-90 through 3.8.5-28-97 ("uncracked" seismic analysis case) only show results for case 4uem. Provide updated figures which include all relevant soil/rock cases, including the rock cases 1n5aeh and 5aeh, which appear to result in the highest sidewall pressures (as described in the response to RAI 371 Question 03.07.02-66 Item (a)). Also, add the additional pressures due to the localized sliding/uplift of the basemat (i.e., the "delta pressures" described in the response to RAI 371 Question 03.07.02-66, listed in Tables 03.07.02-66-1 and 03.07.02-66-2) that were not included in the figures. The information provided should be consistent with the information requested under Question (1) of this RAI.

6. The response to RAI 376 Question 03.08.05-28 Item 5(c) indicates that the foundation static and dynamic bearing pressure demands computed for the Nuclear Island (applicable to all Seismic Category I structures) are provided in Table 3E.1-40 of FSAR Tier 2. The response also provides Figures 3.8.5-28-A through 3.8.5-28-D, which show bearing pressure contour plots for different seismic analysis cases. Since the maximum bearing pressures observed in Figures 3.8.5-28-A through 3.8.5-28-D exceed the values listed in Table 3E.1-40 of FSAR Tier 2 by a significant margin (approx. 56 ksf in Figure 3.8.5-28-C vs. 31.9 ksf maximum "edge" pressure in Table 3E.1-40), the applicant is requested to provide the following additional information:

(a) Explain what is meant by the term “edge” used in Table 3E.1-40. Was any averaging process used to determine the reported values? Where is this explained in the FSAR?

(b) For the bearing pressure contour plots shown in Figures 3.8.5-28-A through 3.8.5-28-D, provide the technical basis for the process used to average the corner pressures, toe pressures, and any other localized pressure “hotspots.”

(c) Explain the discrepancy between the values listed in Table 3E.1-40 and the results observed in Figures 3.8.5-28-A through 3.8.5-28-D. Item 5(c) of the RAI response asserts that (i) isolated corner pressures that exceed the tabulated edge pressures are acceptable as the pressures will redistribute due to localized yielding of the soil, and (ii) there is sufficient margin in the ultimate allowable edge pressure to accommodate the redistribution increases. This explanation is not acceptable for the following reasons: (i) redistribution of pressures is already accounted for in the values shown in Figures 3.8.5-28-A through 3.8.5-28-D, and (ii) it is not acceptable to reduce the factor of safety of the design to accommodate the reported differences between the values shown in Table 3E.1-40 and those shown in Figures 3.8.5-28-A through 3.8.5-28-D.

(d) Item 5(e) of the RAI response indicates that the ANSYS 3D FEM basemat model results were compared to the SASSI FEM model results. Since the reported bearing pressures are obtained from the SASSI FEM model results, provide bearing pressure contour plots similar to those in Figures 3.8.5-28-A through 3.8.5-28-D, obtained from the ANSYS 3D FEM basemat model. Discuss the comparison between the two sets of results.

(e) Clarify the definition of “dead” load used in Figures 3.8.5-28-A through 3.8.5-28-D and Table 3E.1-40. Identify the applicable gravity loads that were considered in the estimates of static and dynamic bearing pressures, and confirm that they are consistent with FSAR Tier 2, Revision 3, Sections 2.5.4.10.1 and 3.8.5.4.1.

7. Since SSI analyses are used to compute the seismic driving forces in the sliding and overturning stability analyses, clarify whether the factors of safety reported in FSAR Tier 2, Table 3E.1-39, Revision 3, correspond to “cracked” or “uncracked” analysis cases, or to the governing (i.e., minimum) of both cases. This information should be added to the FSAR.

Response to Question 03.07.02-78:

1. As described in the Response to RAI 371, Question 03.07.02-66 Item (a), a separate NI Common Basemat Structure Foundation 3D FEM (ANSYS) Model was developed with nonlinear foundation springs for the analysis and design of the NI common basemat. U.S. EPR FSAR Tier 2, Section 3.7.2.3.1.4 has been updated to clarify the description of the NI Common Basemat Foundation Model. The following clarifications are provided, as requested in RAI 547, Question 03.07.02-78:

   - The ANSYS basemat model was validated against the SASSI seismic analysis to ensure that the two models are dynamically equivalent. The validation was performed by comparing the driving shears, dynamic bearing pressure, and basemat uplift area. Table 3.7.2-78-1 shows the comparison of the driving shears obtained from the ANSYS and SASSI analyses. Time histories of the total dynamic driving forces acting on the NI structures in the x-, y- and z-directions were calculated by adding all the co-directional dynamic soil spring forces at the bottom and sidewalls (equivalent to the dynamic soil reaction forces at all soil/structure interaction nodes in the SASSI model). In general, the driving shear values in the ANSYS basemat foundation model are higher than the SASSI.

Table 3.7.2-78-1: Comparison of Driving Shears

Analysis Case	ANSYS Basemat Driving Shear Values			SASSI Basemat Driving Shear Values		
	F_X (lbf)	F_Y (lbf)	F_Z (lbf)	F_X (lbf)	F_Y (lbf)	F_Z (lbf)
4uem	4.647E+08	4.112E+08	3.989E+08	3.830E+08	3.872E+08	3.489E+08
5aeh	3.340E+08	3.555E+08	3.159E+08	3.186E+08	3.608E+08	3.591E+08
1n2ues	2.010E+08	2.119E+08	2.879E+08	1.770E+08	1.872E+08	2.552E+08
2sn4uem	3.986E+08	3.145E+08	3.759E+08	3.385E+08	2.962E+08	3.488E+08
1n5aeh	2.807E+08	2.951E+08	3.246E+08	3.131E+08	3.084E+08	3.475E+08

Table 3.7.2-78-2 shows a comparison of the dynamic bearing pressures generated from ANSYS and SASSI analyses.

Table 3.7.2-78-2: Maximum Dynamic Bearing Pressure Comparison

Soil Case	ANSYS Max (Edge) Bearing Pressure (kip/ft^2)	SASSI Max (Edge) Bearing Pressure (kip/ft^2)
1n2ues	29	30
1n5aeh	45	27
2sn4uem	34	31
4uem	42	30
5aeh	45	27

Finally, a comparison of the uplift area of the basemat, as estimated by ANSYS and SASSI analyses, is shown in Table 3.7.2-78-3. The uplift area from the SASSI analysis is determined by tracking the nodes that are in tension. If the calculated net total vertical force acting on a basemat node (the sum of the dead load, buoyancy force and z component of the dynamic soil interaction force) is positive, then that node is considered to be in tension (i.e. uplifting). Otherwise, the node is in compression and there is no uplift. The percentage of the total basemat area due to uplift is reported at each time step. The maximum uplift ratio for the duration of the seismic event is reported in Table 3.7.2-78-3.

Table 3.7.2-78-3: Maximum Basemat Uplift Area Comparison

Soil Case	ANSYS Uplift Ratio (%)	SASSI Uplift Ratio (%)
1n2ue	0.0	3.9
1n5aeh	12.9	13.5
2sn4uem	27.2	6.4
4uem	32.4	11.3
5aeh	27.9	16.3

The Response to RAI 547, Question 03.07.02-76, addresses the compatibility of the 3D FEM ANSYS basemat model (with the structure) and the SASSI model.

- In the NI common basemat structure foundation analysis model, also referred to as BMAT model herein, the contact interface between the NI concrete basemat and soil springs is modeled with a sliding friction coefficient value of $\mu = 0.5$ consistent with the value reported in U.S. EPR FSAR Tier 2, Table 2.1-1.

  The coefficient of friction between the bottom of the NI common basemat concrete surface and top of the soil surface is modeled using ANSYS 3D node-to-node contact element, CONTA178. CONTA178 elements are more efficient and stable than node-to-surface and surface-to-surface contact elements for large problems such U.S. EPR NI common basemat structures and offer better chattering and penetration control. The NI common basemat includes 8-noded hexahedron elements (brick elements) with matching mesh pattern between the basemat and bottom soil springs. Because of smaller sliding magnitude and rotation behavior of the nonlinear problem, CONTA178 elements were selected. A coefficient of friction value of 0.5 was used in both static and dynamic (sliding) conditions.

  The Response to RAI 371, Question 03.07.02-66 Item (a), stated that: "Soil springs for the static basemat analysis are developed similarly to the dynamic seismic analysis soil springs except one half of the strain compatible shear modulus was used for the seismic soil cases." The stiffness of the static springs for the soil cases considered in the static analysis is equal to one-half of the corresponding dynamic stiffness. The above clarification is consistent with the following statement in U.S. EPR FSAR Tier 2, Section 3.8.5.4.2: "Although Gazetas addresses the dynamic stiffness of the foundation basemat, the use of one-half the dynamic shear modulus in the equation approximates the total stiffness of the supporting soil medium under static conditions." U.S. EPR FSAR

Tier 2, Table 3.8-13 has been revised to include the static and dynamic soil springs for the generic and high frequency soil cases.

- The initial conditions (dead load, 25% live load, 75% precipitation load, hydrostatic forces, and at-rest earth pressures) to the basemat foundation model (nonlinear) are input by performing multiple static analysis load steps prior to the start of the dynamic load. Static load steps are performed in a transient analysis by turning off the transient time integration effects. The static analysis time-steps are performed at solution times less than 0.005 sec. The transient itself is started by turning on the time integration effects at time = 0.005 sec to the end of the acceleration time-history input.

  The seismic time-history analysis starts from time = 0.005 sec. The effects of the seismic loads are obtained by subtracting the results at time-history data points with the static analysis baseline results. The maximum seismic loads are obtained by determining the maximum/minimum design loads for the basemat and tendon gallery (TG) for each of the elements/nodes over all time points of the transient analysis.

  In addition to the seismic load, the BMAT model is analyzed with static soil springs for static load cases:

  – Normal loads (e.g., dead, live, soil/lateral earth pressure, thermal load, pipe reaction, post- tension loads, relief valve loads, etc.).

  – Construction loads.

  – Test loads for the reactor containment building.

  – Severe environmental loads (e.g., wind).

  – Extreme environmental loads (e.g., tornado).

  – Abnormal loads (e.g., internal flood, buoyant pressure, accident pressure, etc.).

  The basemat foundation and TG walls are designed for the combined effects of the various load combinations. U.S. EPR FSAR Tier 2, Sections 3.8.1 through 3.8.4, list the appropriate load combinations used in the design of Seismic Category I structures. The analysis of the basemat foundation and TG walls is described in the enclosed markup of U.S. EPR FSAR Tier 2, Section 3.8.5.4.2.

- The passive pressure curves for the embedded walls of the BMAT model were based on the guidelines presented in Foundations & Earth Structures, Design Manual 7.02 (NAVFAC DM-7.02) from Naval Facilities Engineering Command and are used to compute the sidewall soil springs. The key differences between the above approach (i.e., regular spring approach) and the one used in the stability analysis (i.e., alternate spring approach) are the following:

  – The NI basemat foundation analysis sidewall springs are based on established geotechnical properties (NAVFAC DM-7.02) used in common practice, whereas the alternate springs in NI stability analysis are derived by performing soil capacity analyses using ADINA code.

  – The alternate springs have Ka = 0 instead of Ka = 0.33 used in basemat foundation model.

  – The at-rest earth pressure coefficients, Ko are approximately 0.5 in both models.

– The passive pressure coefficient, Kp for the alternate springs are about 3.5 which is marginally higher than Kp value of 3.0 used in NI basemat foundation analysis.

Table 3.7.2-78-4 and Table 3.7.2-78-5 compare maximum sliding distances for soil cases 2sn4uem and 1n5aeh in the X and Y directions, respectively. The results for the regular springs are denoted as "ANSYS" and the alternate springs as "ADINA." The minimum factor of safety against sliding for 2sn4uem case is 1.07 (regular springs) and 1.10 (alternate springs). For case 1n5aeh, the minimum factor of safety against sliding is 1.20 for both regular and alternate springs. The global behavior of the models is similar for regular and alternate springs. For soil case 2sn4uem, the slope of the alternate passive pressure curves is higher when compared to DM-7.02 curves; and the sidewalls resist slightly higher forces, as seen in slightly lower amount of sliding displacement. However, for local behavior such as local maximum bearing pressures, sliding displacement, and uplift ratios are similar for ANSYS and ADINA as shown in Table 3.7.2-78-6 and Table 3.7.2-78-7. Hence, the use of alternate soil springs in BMAT model is expected to have minimal to no impact on mat design loads, as the seismic design loads represent the maximum forces and moments across the entire time-history duration.

Table 3.7.2-78-4: Comparison of Maximum Sliding Displacement in the X-Direction (EW)

Soil Case	ANSYS Results at Max X-Dir Sliding Displacement Time				
	Local Max Bearing Pressure (kip/ft^2)	Max X-Dir Sliding Movement (in)	Max Y-Dir Sliding Movement (in)	Max Z-Dir Movement (in)	Basemat Area Uplift Ratio (%)
1n5aeh (ANSYS)	60.5	0.055	0.046	0.008	0.00
1n5aeh_alt (ADINA)	64.8	0.050	0.051	0.019	1.80
2sn4uem (ANSYS)	47.3	0.310	0.094	0.046	1.39
2sn4uem_alt (ADINA)	46.4	0.273	0.085	0.078	3.15

Table 3.7.2-78-5: Comparison of Maximum Sliding Displacement in the Y-Direction (NS)

Soil Case	ANSYS Results at Max Y-Dir Sliding Displacement Time				
	Local Max Bearing Pressure (kip/ft^2)	Max X-Dir Sliding Movement (in)	Max Y-Dir Sliding Movement (in)	Max Z-Dir Movement (in)	Basemat Area Uplift Ratio (%)
1n5aeh (ANSYS)	70.3	0.042	0.061	0.011	1.21
1n5aeh_alt (ADINA)	70.0	0.039	0.060	0.011	1.36
2sn4uem (ANSYS)	43.8	0.228	0.182	0.064	2.40
2sn4uem_alt (ADINA)	49.0	0.141	0.187	0.007	0.00

Table 3.7.2-78-6: Comparison of Maximum Dynamic Bearing Pressure

Soil Case	ANSYS Results at Max Bearing Pressure Time				
	Local Max Bearing Pressure (kip/ft^2)	Max X-Dir Sliding Movement (in)	Max Y-Dir Sliding Movement (in)	Max Z-Dir Movement (in)	Basemat Area Uplift Ratio (%)
1n5aeh (ANSYS)	99.2	0.026	0.025	0.026	2.70
1n5aeh_alt (ADINA)	101.0	0.022	0.025	0.031	2.99
2sn4uem (ANSYS)	58.7	0.253	0.149	0.068	0.86
2sn4uem_alt (ADINA)	62.5	0.141	0.179	0.072	1.07

Table 3.7.2-78-7: Comparison of Maximum Uplift Ratio

Soil Case	ANSYS Results at Max Uplift Ratio Time				
	Local Max Bearing Pressure (kip/ft^2)	Max X-Dir Sliding Movement (in)	Max Y-Dir Sliding Movement (in)	Max Z-Dir Movement (in)	Basemat Area Uplift Ratio (%)
1n5aeh (ANSYS)	55.7	0.025	0.020	0.034	12.89
1n5aeh_alt (ADINA)	51.9	0.031	0.023	0.023	9.83
2sn4uem (ANSYS)	47.1	0.243	0.179	0.241	27.19
2sn4uem_alt (ADINA)	48.0	0.169	0.153	0.254	28.64

- The TG walls are modeled using shell elements (ANSYS SHELL43 elements) and connected to the solid element basemat (ANSYS SOLID45 elements) using ANSYS shell to solid Multi-Point Constraints (MPCs). Figure 3.7.2-78-1 shows the shell to solid MPCs. The bottom of the NI basemat solid elements is located at different elevations. The outer TG walls connect to the Balance of Nuclear Island portion of the NI common basemat at elevation -41ft and the inner TG walls connect to the RBIS/RCB portion of the NI common basemat at elevation -36 ft. Table 3.7.2-78-8 lists the nodes at different elevations of the TG and their boundary conditions.

Table 3.7.2-78-8: Boundary Conditions for Tendon Gallery Walls

Inner Tendon Gallery Wall Nodes		Outer Tendon Gallery Wall Nodes	
Elevation (ft)	BCs	Elevation (ft)	BCs
-36	Shell to Solid MPCs, No sidewall springs	-	-
-39	Sidewall springs with correction factor to account for missing soil contact areas	-	-
-41	Sidewall springs	-41	Shell to Solid MPCs, No sidewall springs
-45	Sidewall springs	-45	Sidewall springs with correction factor to account for missing soil contact areas
-49	Sidewall springs	-49	Sidewall springs

Inner Tendon Gallery Wall Nodes		Outer Tendon Gallery Wall Nodes	
Elevation (ft)	**BCs**	**Elevation (ft)**	**BCs**
-52	Sidewall springs, bottom springs and contact elements	-52	Sidewall springs, bottom springs and sliding/contact elements

Figures 3.7.2-78-2 through 3.7.2-78-6 show the delta pressures on TG walls due to sliding for soil cases 1n2ue, 2sn4uem, 4uem, 1n5aeh and 5aeh, respectively. Table 3.7.2-78-9 lists the delta pressures on the TG walls for the soil cases 1n2ue, 2sn4uem and 4uem.

For the two rock cases 1n5aeh and 5aeh, the delta pressures are much higher because of their use of rock springs for the TG. The top ring of the nodes of the TG are connected to the solid element basemat using ANSYS shell to solid MPCs. These are located at elevations - 36 ft and -41 ft for the inner and outer TG, respectively. These nodes cannot be modeled to have sidewall rock springs as they are constrained to the solid element basemat nodes by MPCs. To compensate for the lateral resistance against sliding, the participating area of the top nodes is added to the line of nodes one level below the top nodes; i.e., the participating areas used for calculating the sidewall springs at elevation -39 ft of the inner TG wall and -45 ft for the outer TG wall are increased. Due to the regular mesh size, the participating areas of the line of nodes at -39 ft and -45 ft are 1.5 times their actual participating areas. Hence, the sidewall springs at the above elevations of the TG are stiffer sidewall rock springs. Due to the high stiffness of the springs, these impose higher reactions typically associated with support nodes. These nodes experience higher sidewall forces and moments (stress concentration effect) typically associated with fixity. For these cases, average maximum values are calculated by dividing the maximum ΔPr by a factor of 1.5 which is equal to the original increase to their contributing areas (see Table 3.7.2-78-10). No other averaging is performed for the remainder of the TG wall elevations.

Table 3.7.2-78-9: Maximum Delta Pressure Due to Sliding on Tendon Gallery Walls for Soil Cases

Case	Condition	Inner TG Wall ΔPr (kip/ft^2)	Outer TG Wall ΔPr (kip/ft^2)
1n2ue	Cracked	0.036	0.031
2sn4uem	Cracked	0.346	0.241
4uem	Cracked	0.764	0.554

Table 3.7.2-78-10: Maximum Delta Pressure Due to Sliding on Tendon Gallery Walls for Rock Cases

Case	Condition	Maximum ΔPr (kip/ft^2)		Average Maximum ΔPr (kip/ft^2)	
		Inner TG Wall	Outer TG Wall	Inner TG Wall	Outer TG Wall
1n5aeh	Cracked	26.165	12.552	17.443	12.552
5aeh	Cracked	69.613	27.092	46.408	27.092

The results shown in Tables 3.7.2-78-9 and 3.7.2-78-10 are different than those reported in response to RAI 371, Question 03.07.02-66 (Tables 3.7.2-66-1 and 3.7.2-66-2) due to the following reasons:

1. The BMAT has been updated to incorporate changes made to the NI 3D Finite Element Model for Dynamic Analysis (SASSI Model) described in U.S. EPR FSAR Tier 2, Section 3.7.2.3.1.2 addressing the static and dynamic model compatibility considerations (Response to RAI 547 Question 03.07.02-76), and

2. Addition of the surcharge load on the TG walls due to the self-weight of the NI.

Figure 3.7.2-78-1: Shell to Solid MPCs for Tendon Gallery and Basemat Connection

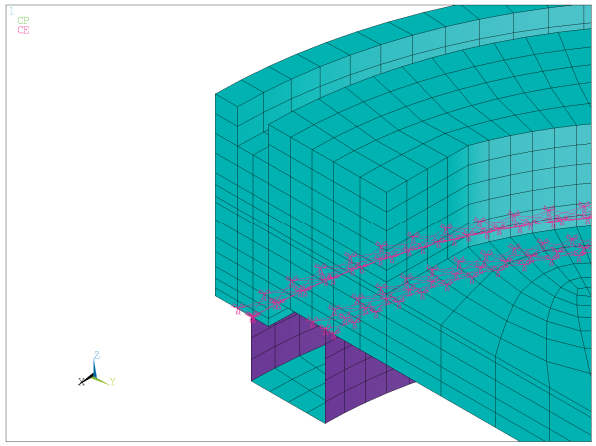	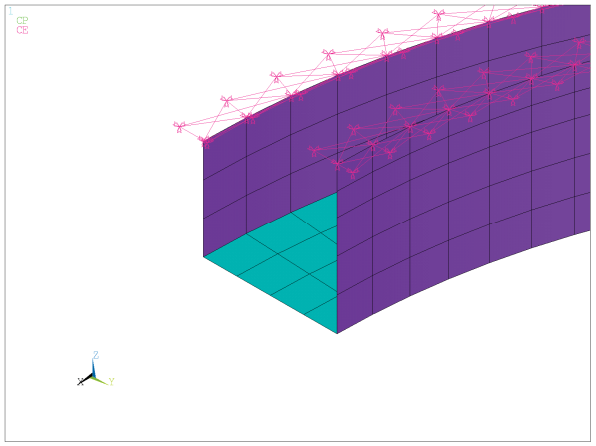
Cross section view showing TG shell elements, basemat solid elements and MPCs	Cross section view showing TG shell elements and MPCs
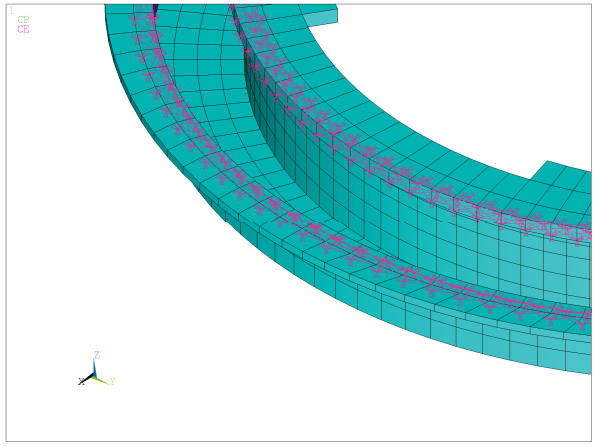	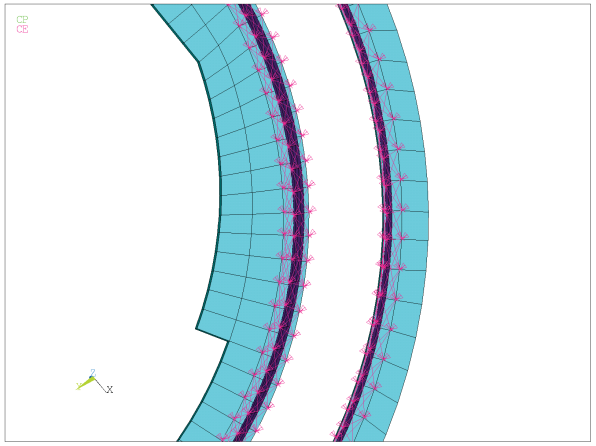
Isometric view showing TG shell elements, basemat solid elements and MPCs	Bottom view showing Shell to Solid MPCs

Figure 3.7.2-78-2: Case 1n2ue, Cracked, Additional (Delta) Pressures Due to Sliding on the Tendon Gallery Walls

Delta Pressure Due to Sliding on the Tendon Gallery Walls in ksf.		
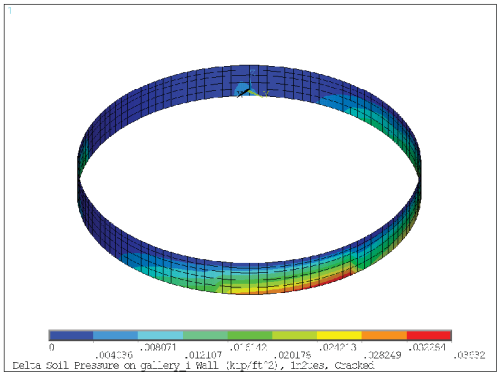	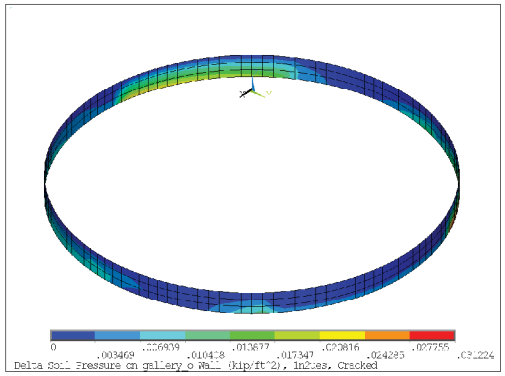	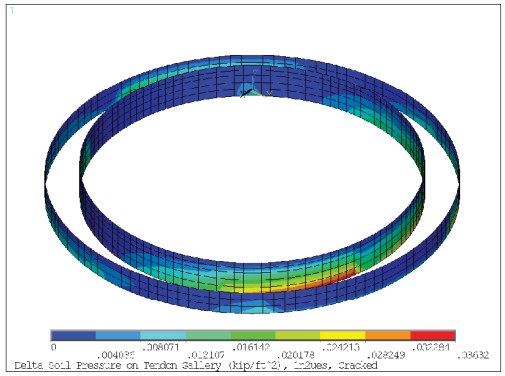
Inner Tendon Gallery Wall	Outer Tendon Gallery Wall	Outer & Inner Tendon Gallery Walls

Figure 3.7.2-78-3: Case 2sn4uem, Cracked, Additional (Delta) Pressures Due to Sliding on the Tendon Gallery Walls

Delta Pressure Due to Sliding on the Tendon Gallery Walls in ksf.		
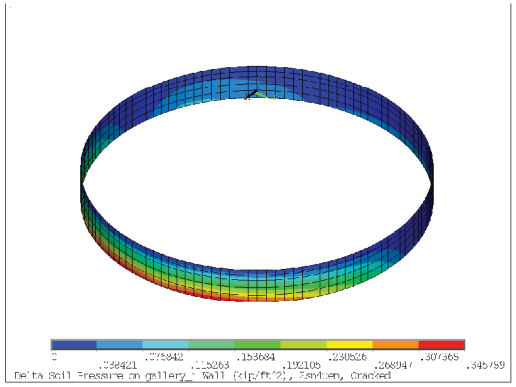	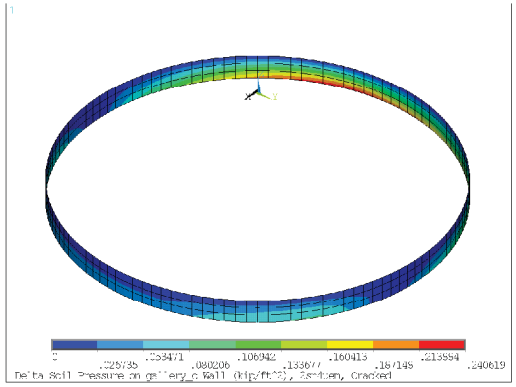	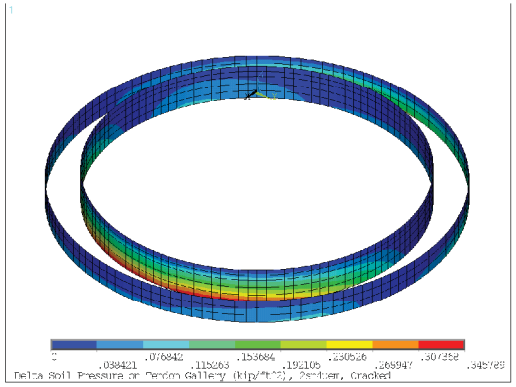
Inner Tendon Gallery Wall	Outer Tendon Gallery Wall	Outer & Inner Tendon Gallery Walls

Figure 3.7.2-78-4: Case 4uem, Cracked, Additional (Delta) Pressures Due to Sliding on the Tendon Gallery Walls

Delta Pressure Due to Sliding on the Tendon Gallery Walls in ksf.		
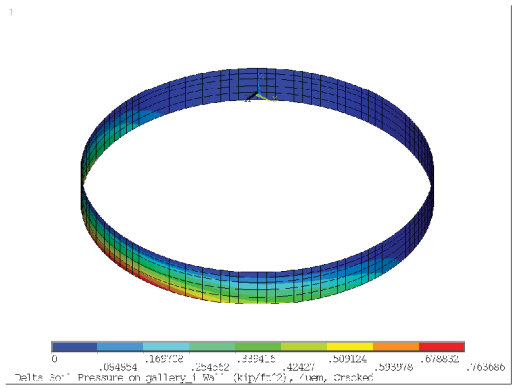	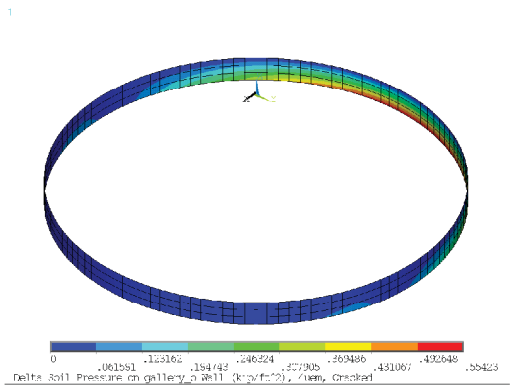	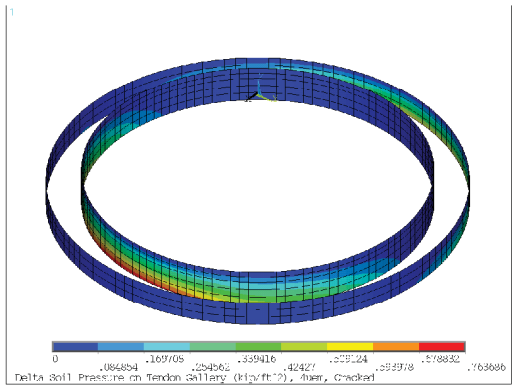
Inner Tendon Gallery Wall	Outer Tendon Gallery Wall	Outer & Inner Tendon Gallery Walls

Figure 3.7.2-78-5: Case 1n5aeh, Cracked, Additional (Delta) Pressures Due to Sliding on the Tendon Gallery Walls

<table>
<tr><td colspan="3">Delta Pressure Due to Sliding on the Tendon Gallery Walls in ksf.</td></tr>
<tr><td> 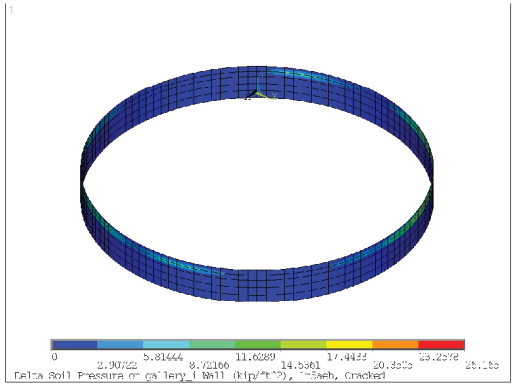 </td><td> 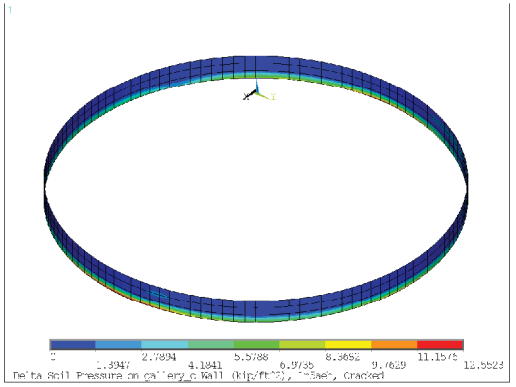 </td><td> 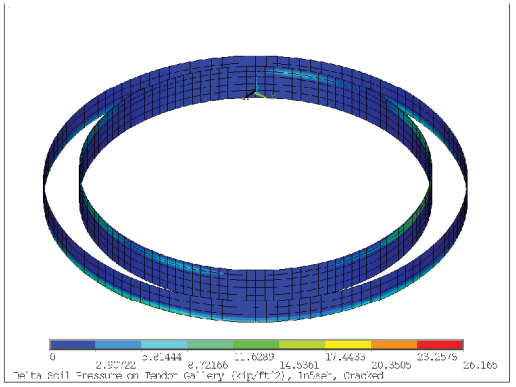 </td></tr>
<tr><td>Inner Tendon Gallery Wall</td><td>Outer Tendon Gallery Wall</td><td>Outer & Inner Tendon Gallery Walls</td></tr>
</table>

Figure 3.7.2-78-6: Case 5aeh, Cracked, Additional (Delta) Pressures Due to Sliding on the Tendon Gallery Walls

Delta Pressure Due to Sliding on the Tendon Gallery Walls in ksf.		
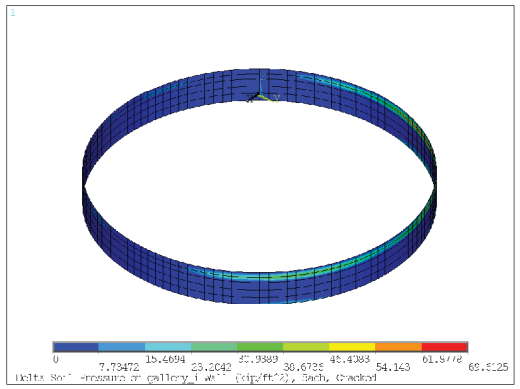	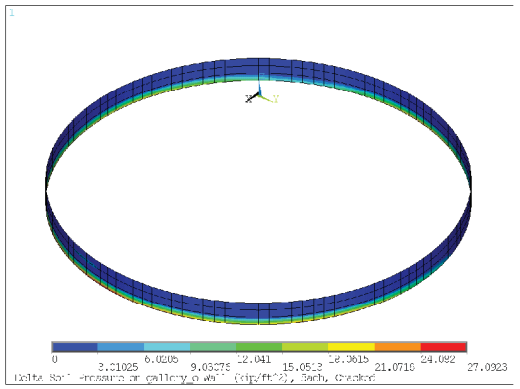	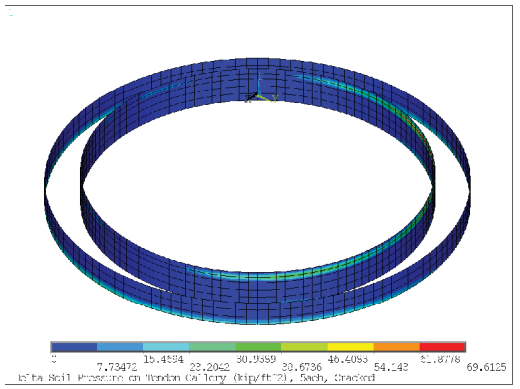
Inner Tendon Gallery Wall	Outer Tendon Gallery Wall	Outer & Inner Tendon Gallery Walls

2. As requested, U.S. EPR FSAR Tier 2, Section 3.8.5.4.2, will be revised (see enclosed FSAR markups) to clarify the issues identified in the RAI as described below:

   (a) Deleted references to U.S. EPR FSAR Tier 2, Sections 3.8.1.4.1 and 3.8.5.3. To avoid duplication of information in U.S. EPR FSAR Tier 2, Sections 3.7 and 3.8, structural model-related information including the finite element representation of the NI Common Basemat Foundation Model (static and dynamic) are addressed in Section 3.7.2.3.1.4. Analysis and design considerations for the basemat are included in U.S. EPR FSAR Tier 2, Section 3.8.5.4.2.

   (b) Reference to "NI Common Basemat Structure Static Analysis" has been deleted (see also item (a) above). A reference has been added to U.S. EPR FSAR Tier 2, Section 3.8.5.4.2 to Figure 3.7.2-151 that shows the basemat portion of the model and to U.S. EPR FSAR Tier 2, Figure 3.7.2-152 that shows the full model including the superstructure.

   (c) Additional information has been provided for the basemat foundation dynamic springs and the side soil/rock springs used in the basemat foundation model. In addition, clarification has been provided addressing the nonlinear effects due to sliding and uplift.

   (d) References to figures of obsolete soil cases (1u, 2u, 3r3u) have been deleted.

   (e) U.S. EPR FSAR Tier 2, Section 3.8.5.4.2 and Appendix 3E.1, will be revised (see enclosed FSAR markups) to clarify that the acceptability of the supporting soils is based on the results of the SASSI analysis (described in U.S. EPR FSAR Tier 2, Section 3.7.2) and not the BMAT model analysis.

   (f) U.S. EPR FSAR Tier 2, Section 3.8.5.4.2, will be revised (see enclosed FSAR markups) to include sub-headings.

   (g) The methodology for extracting seismic shears and moments from the combined static and dynamic analysis of the foundation basemat and TG has been added to U.S. EPR FSAR Tier 2, Section 3.8.5.4.2. In addition to the dynamic loads, the foundation basemat model is analyzed for the static load cases. The design of the basemat and TG is based on the appropriate load combinations as listed in U.S. EPR FSAR Tier 2, Section 3.8.1 through 3.8.4.

      Also, see response to Part 1 of Question 03.07.02-78 above.

   (h) U.S. EPR FSAR Tier 2, Sections 3.8.1 through 3.8.4, will be updated as part of the overall consistency check and will be documented in a future U.S. EPR FSAR revision.

3. The following clarifications and supplemental information are provided related to the design of the embedded walls and the TG:

   (a) The NI embedded walls are designed for passive soil pressures from SASSI analysis scaled to a K_p=3 as well as design pressures consisting of combined static, surcharge, delta pressures and scaled SSI pressures for each soil case in U.S. EPR FSAR Tier 2, Table 3.7.1-6. Figure 3.7.2-78-8 through Figure 3.7.2-78-45 show pressure profiles for the embedded walls for the following load cases: static and surcharge, scaled SSI, Woods solution and surcharge as well as design pressures consisting of combined static, surcharge, delta pressures and scaled SSI pressures. The embedded walls,

excluding the TG, are designed using the scaled SASSI analysis pressure values to which the delta loads due to sliding and uplift are added. The TG walls are designed using the result from the nonlinear analysis of finite element model for the NI Common Basemat Foundation which includes the delta loads. The details are explained in response to part 3(e) of this RAI response.

The high frequency soil cases are bounded by the generic soil cases. Therefore, the figures in the Response to RAI 376, Question 03.08.05-28, corresponding to the high frequency soil cases (hflb, hfub and hfbe) were not updated in this response. However, the same procedure is followed for all soil cases and the design is performed considering all soil cases. In addition, Figure 03.08.05-28-42 through Figure 03.08.05-28-59 for "Max/Min Soil Pressures" in the Response to RAI 376 Question 03.08.05-28 were intended only for additional information; and, therefore, are not updated in the Response to RAI 547.

(b) .Figure 3.7.2-78-7 illustrates the scaling of SSI pressures for a typical wall (Wall 2) and soil case (1n2ue). The scale factor for a given soil case corresponds to the ratio of the maximum passive pressure to the maximum SSI pressure along the depth of the embedded wall. The (single) scale factor is applied to the SSI pressure profile (along the depth of a wall) for a given soil profile. For Wall 2 with soil case 1n2ue, the maximum SSI pressure (at depth of -38.9 ft) is 5,054 psf, and the maximum passive pressure at this depth is 15,835 psf. The scale factor is calculated as 3.13. This scale factor is applied to the SSI pressures (labeled "Unscaled SSI") at various depths to arrive at the scaled SSI pressures (labeled "Scaled SSI").

Figure 3.7.2-78-7: SSI Pressure with and without scaling for Wall 2, Soil Case 1n2ue

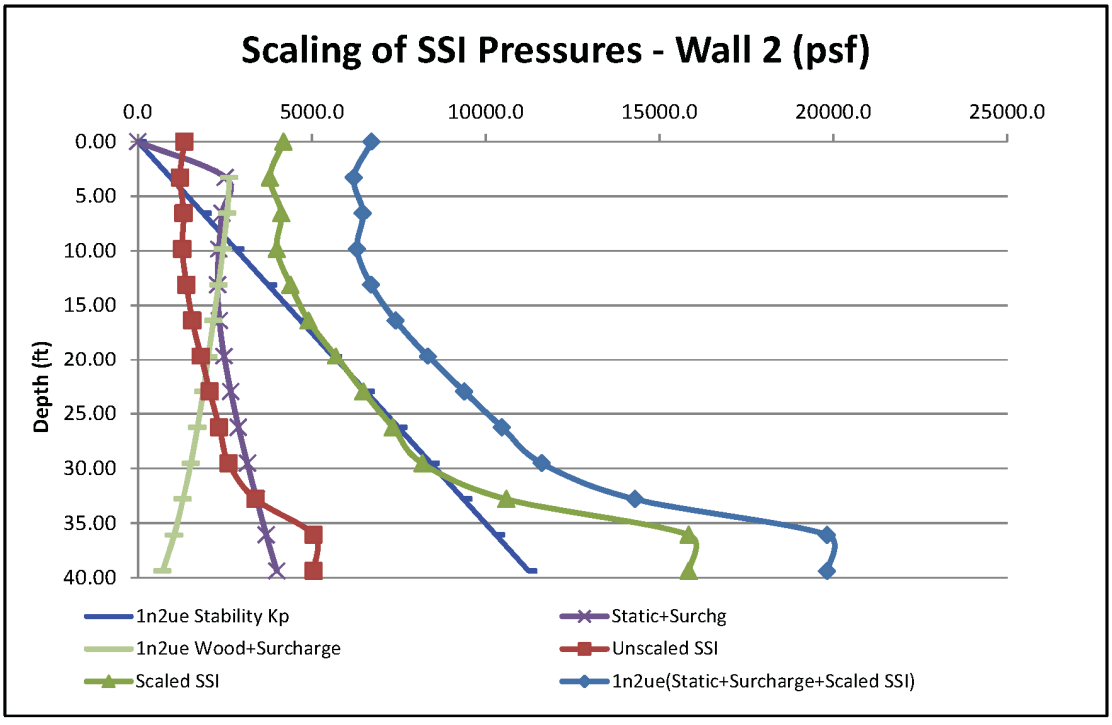

(c) The combined static, surcharge, delta pressure, and scaled SSI pressures generally bound the pressures required by the sliding stability analysis (SSI analysis). The example cited in the Response to RAI 376, Question 03.08.05-28, corresponds to the soil case 4uem for which a uniform soil pressure of 43.5 psi for the walls and 50 psi for the TG was applied to provide the minimum factor of safety for sliding. Note that for soil case 4uem, the scaled SSI pressure with static, surcharge and delta pressures do not bound the stability pressure case at certain local sections of the wall (between roughly 5 ft. and 25 ft. from the top). However, Figure 3.7.2-78-46 through Figure 3.7.2-78-55 show that other soil cases would govern the design of the walls; and, in fact, exceed the stability pressure requirements of soil case 4uem. In soil case 2sn4uem for walls 5 and 11, only minor sections of the wall were not bounded by the scaled pressures. However, the design of the wall would be governed by the larger sidewall pressures at the top and bottom of the walls where the scaled SSI pressures are significantly greater than the stability pressures.

(d) Figure 3.7.2-78-8 through Figure 3.7.2-78-37 show the stability (K_p); static and surcharge; Wood's and surcharge; static, surcharge, scaled SSI and additional (delta) pressure due to localized sliding/uplift of the basemat; and the combined delta pressure, scaled SSI, static and surcharge for the embedded walls. .

Figure 3.7.2-78-8: Wall 2 - Soil 1n2ue & 1n5aeh (Cracked Concrete Case)

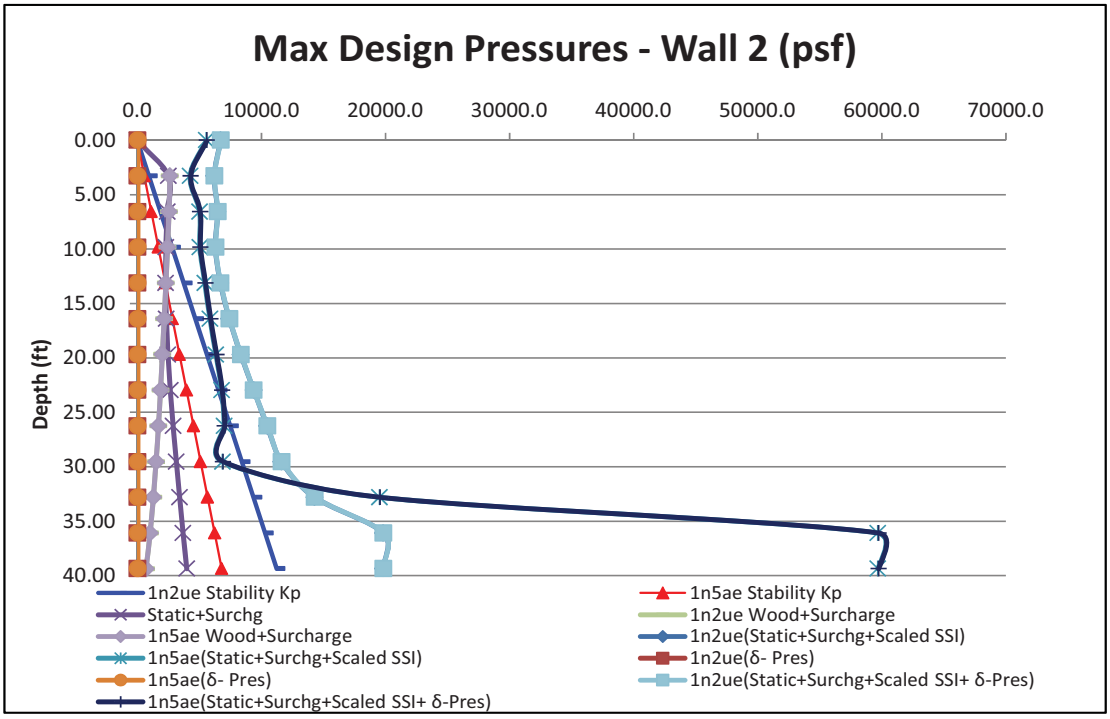

Figure 3.7.2-78-9: Wall 2 - Soil 2sn4uem (Cracked Concrete Case)

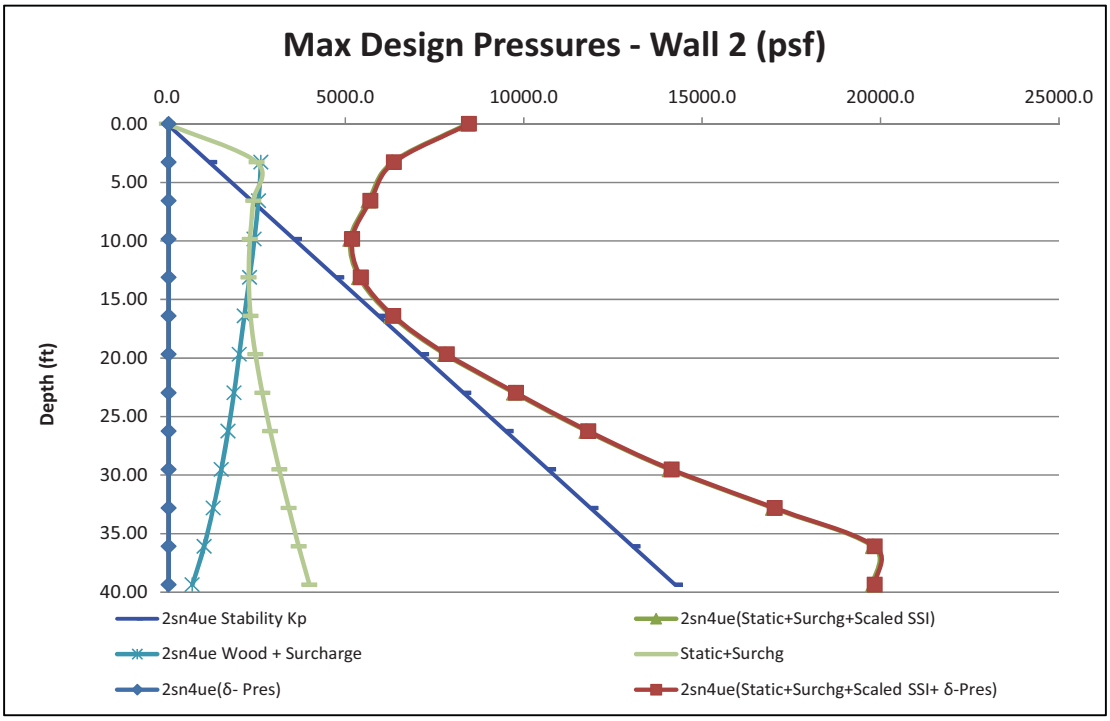

Figure 3.7.2-78-10: Wall 2 – 4uem (Cracked Concrete Case)

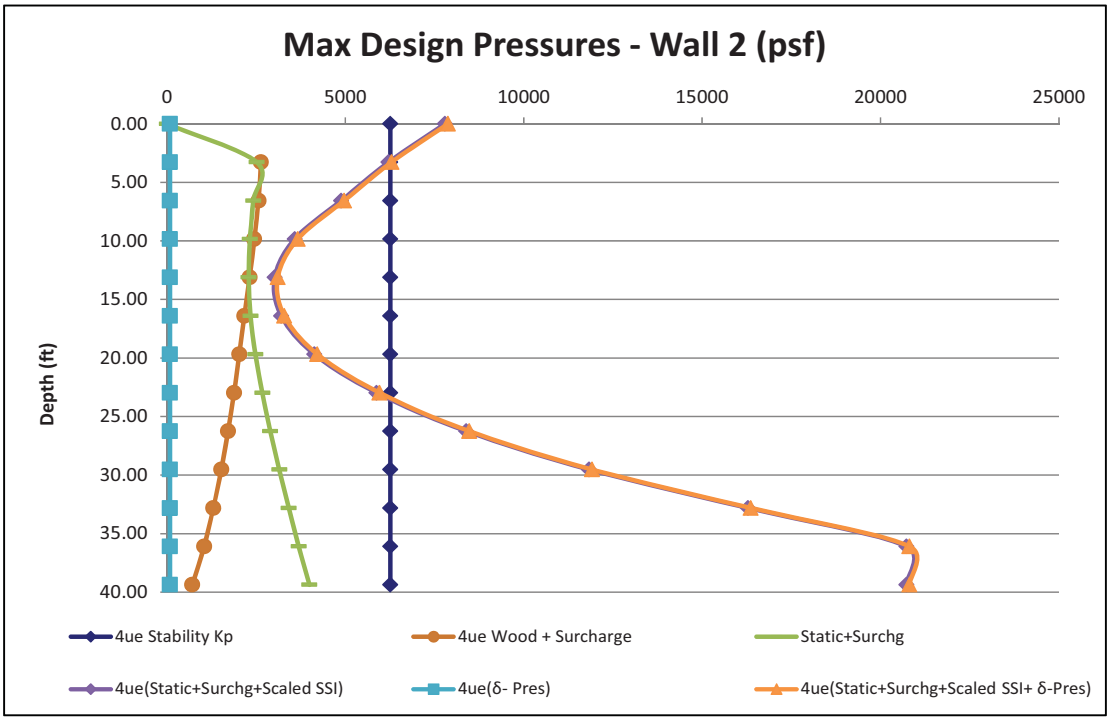

Figure 3.7.2-78-11: Wall 3 - Soil 1n2ue & 1n5aeh (Cracked Concrete Case)

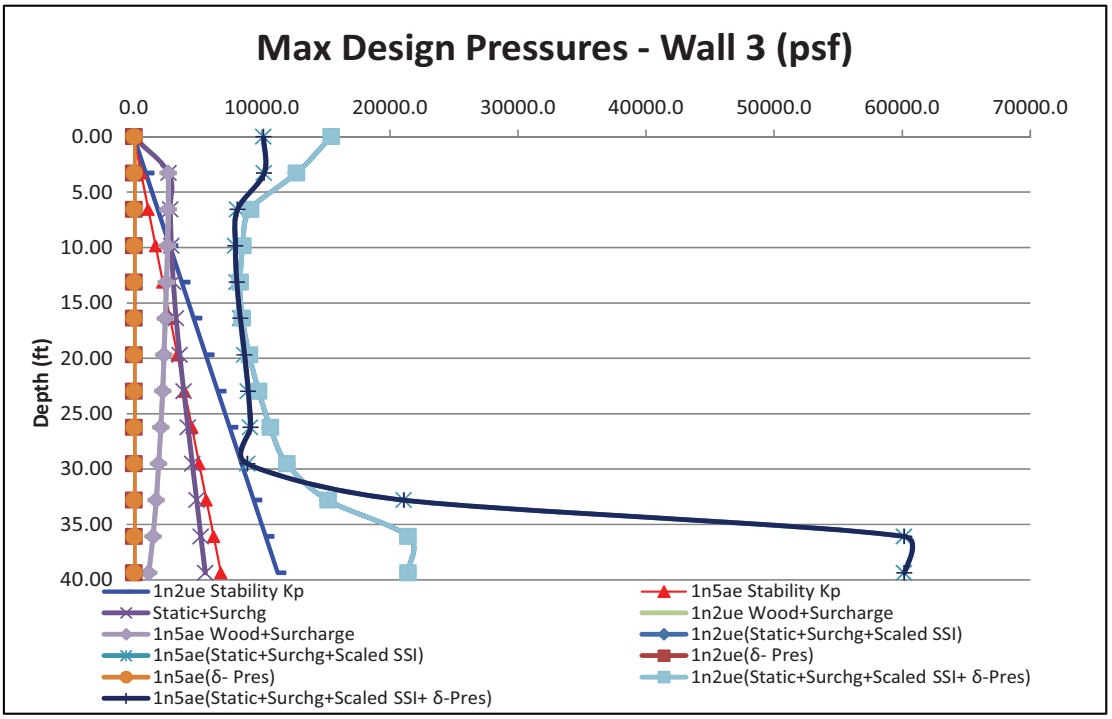

Figure 3.7.2-78-12: Wall 3 - Soil 2sn4uem (Cracked Concrete Case)

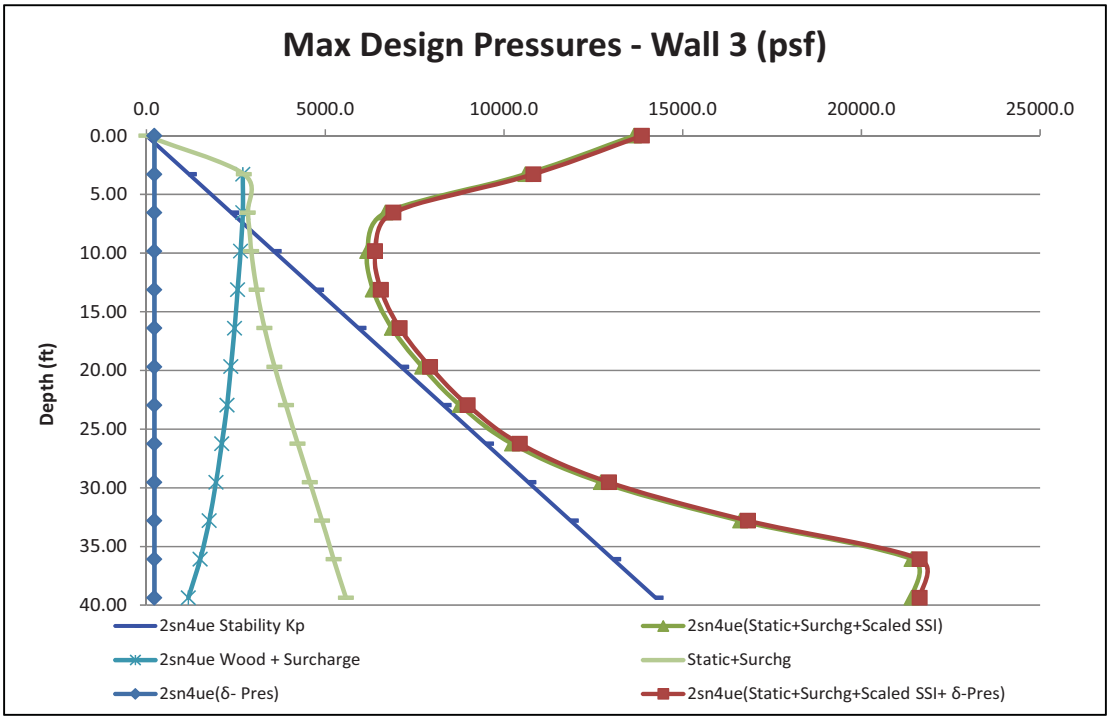

Figure 3.7.2-78-13: Wall 3 – 4uem (Cracked Concrete Case)

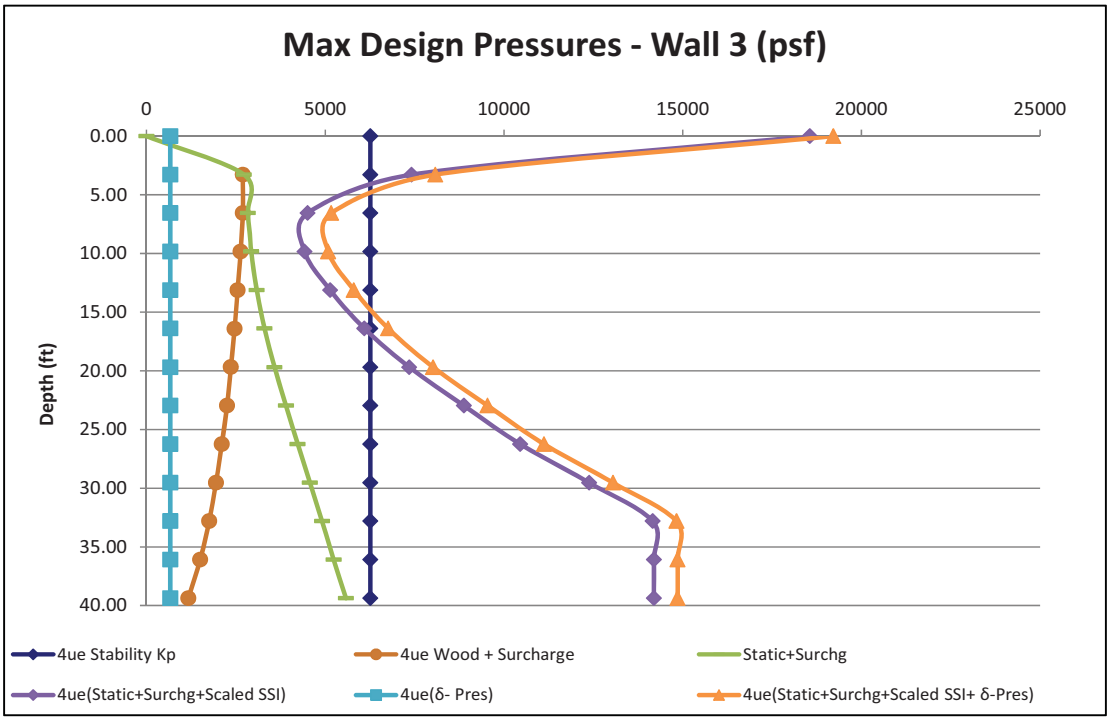

Figure 3.7.2-78-14: Wall 4 - Soil 1n2ue & 1n5aeh (Cracked Concrete Case)

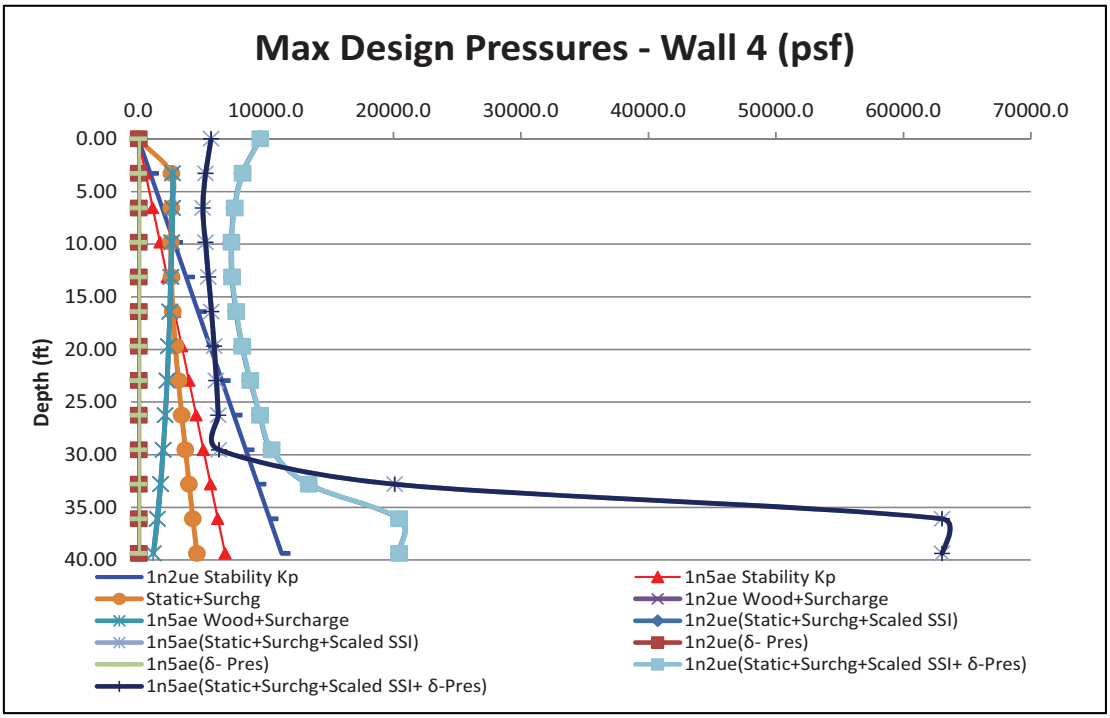

Figure 3.7.2-78-15: Wall 4 - Soil 2sn4uem (Cracked Concrete Case)

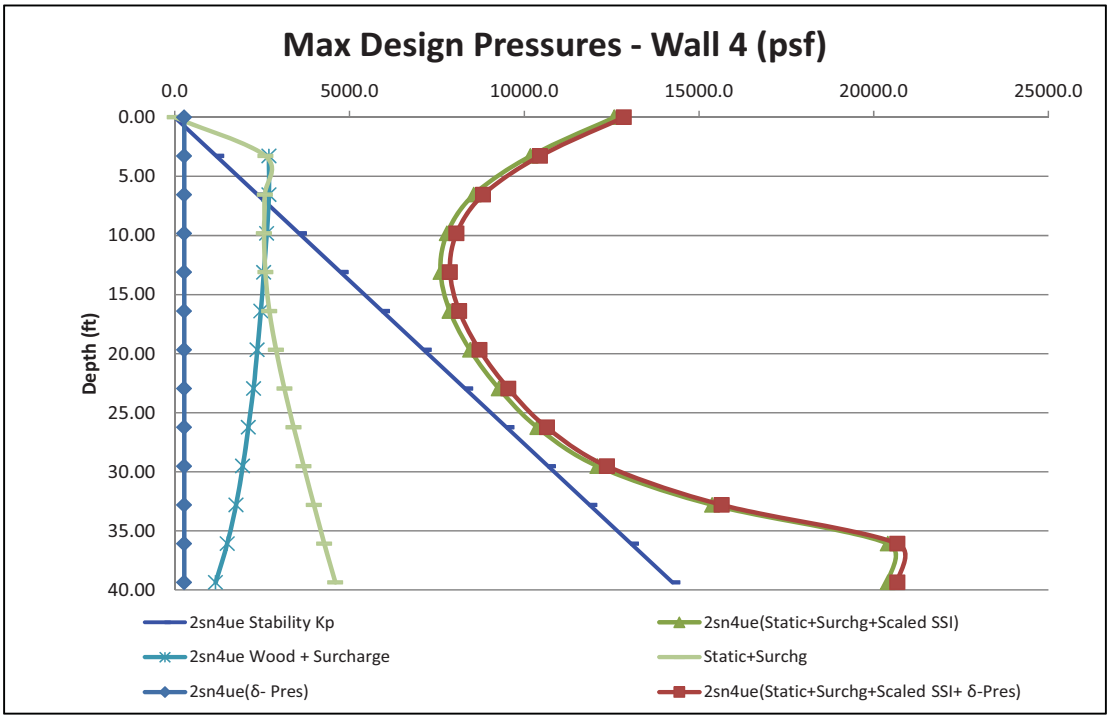

Figure 3.7.2-78-16: Wall 4 – 4uem (Cracked Concrete Case)

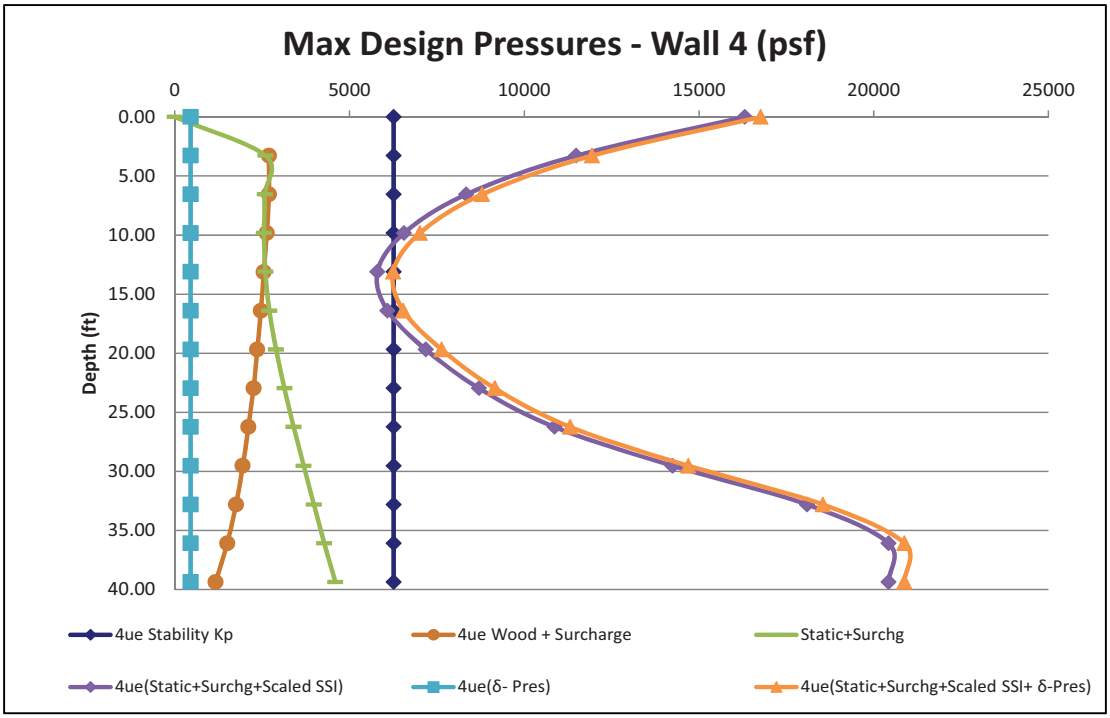

Figure 3.7.2-78-17: Wall 5 - Soil 1n2ue & 1n5aeh (Cracked Concrete Case)

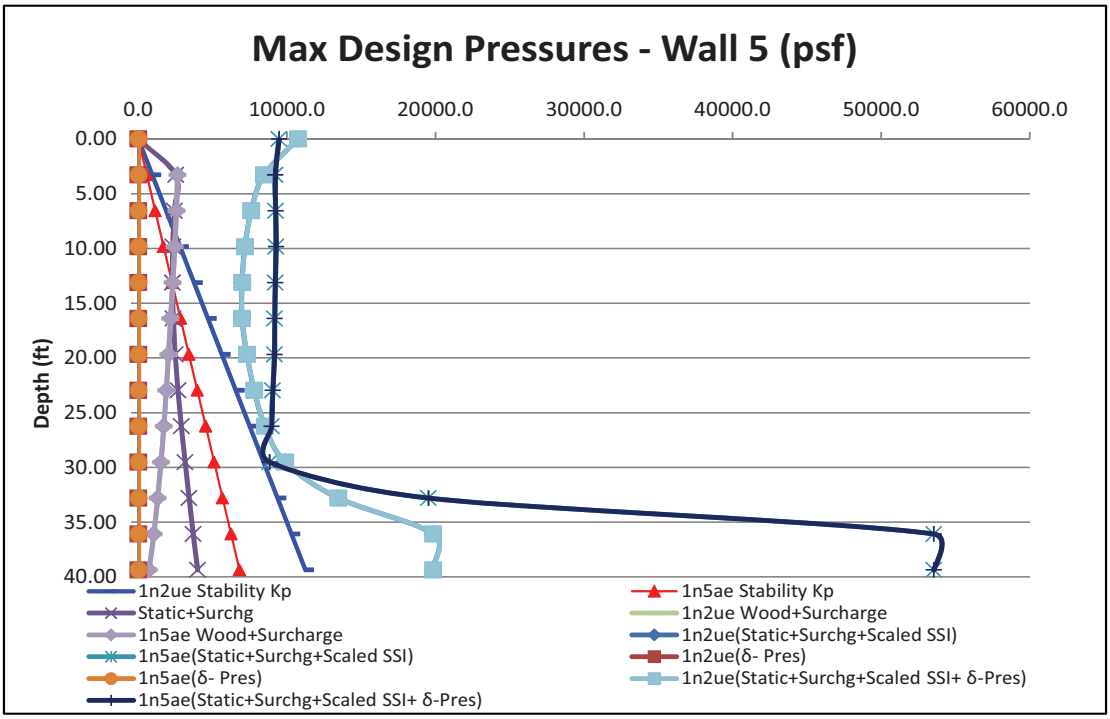

Figure 3.7.2-78-18: Wall 5 - Soil 2sn4uem (Cracked Concrete Case)

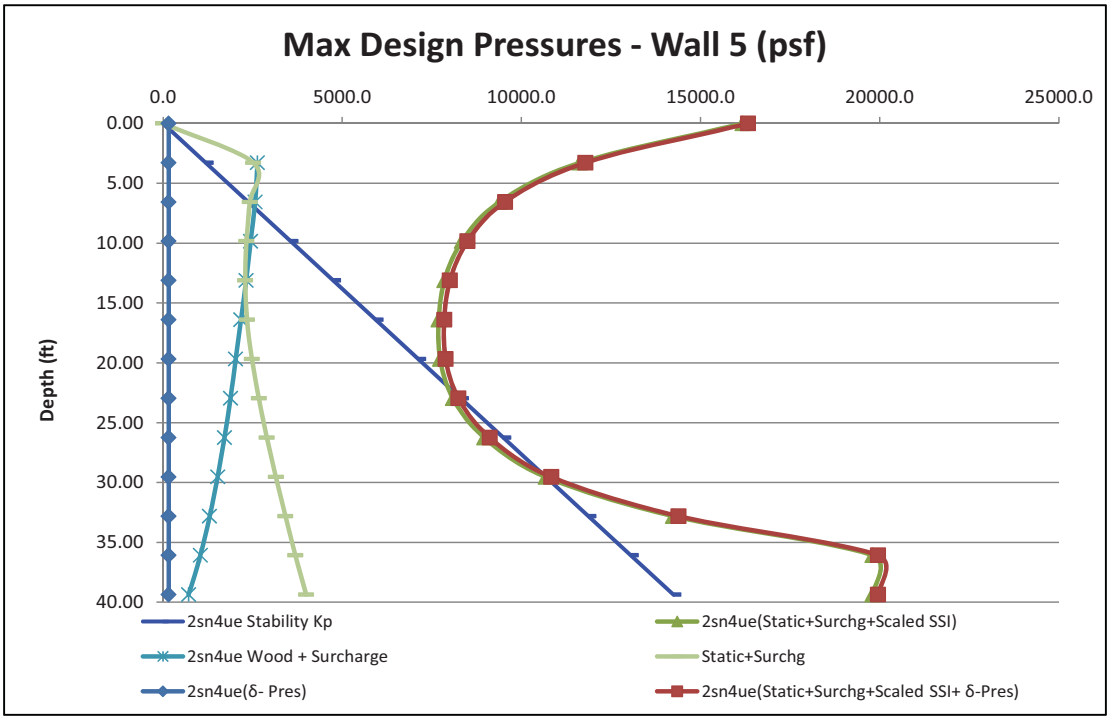

Figure 3.7.2-78-19: Wall 5 – 4uem (Cracked Concrete Case)

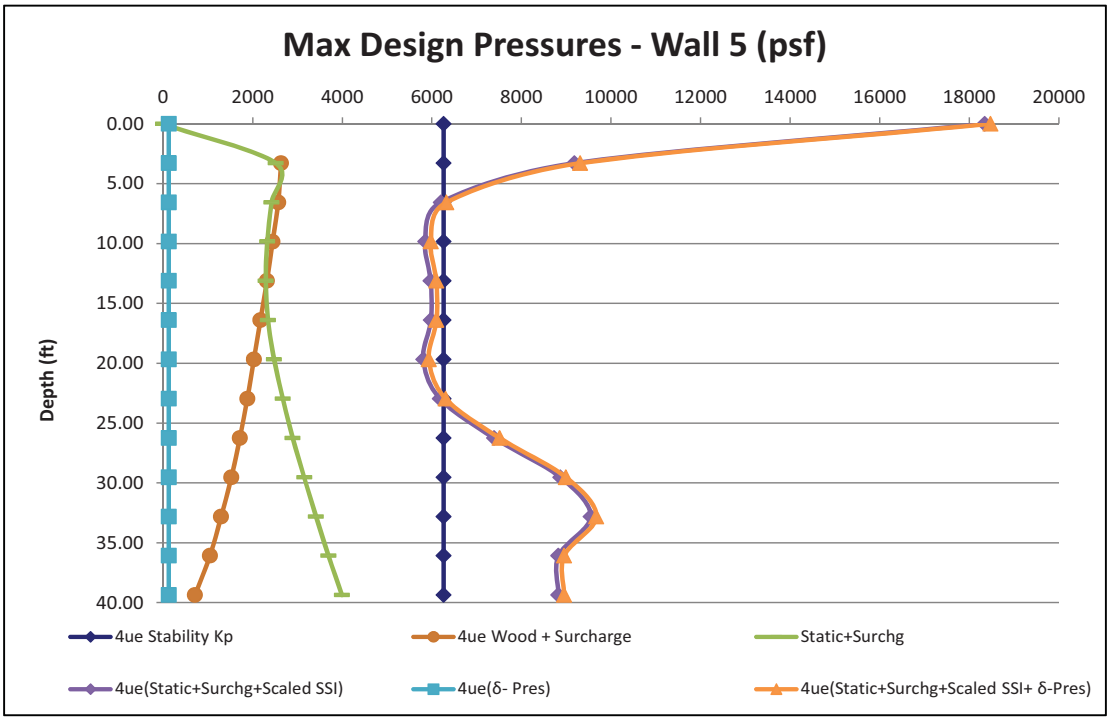

Figure 3.7.2-78-20: Wall 6 - Soil 1n2ue & 1n5aeh (Cracked Concrete Case)

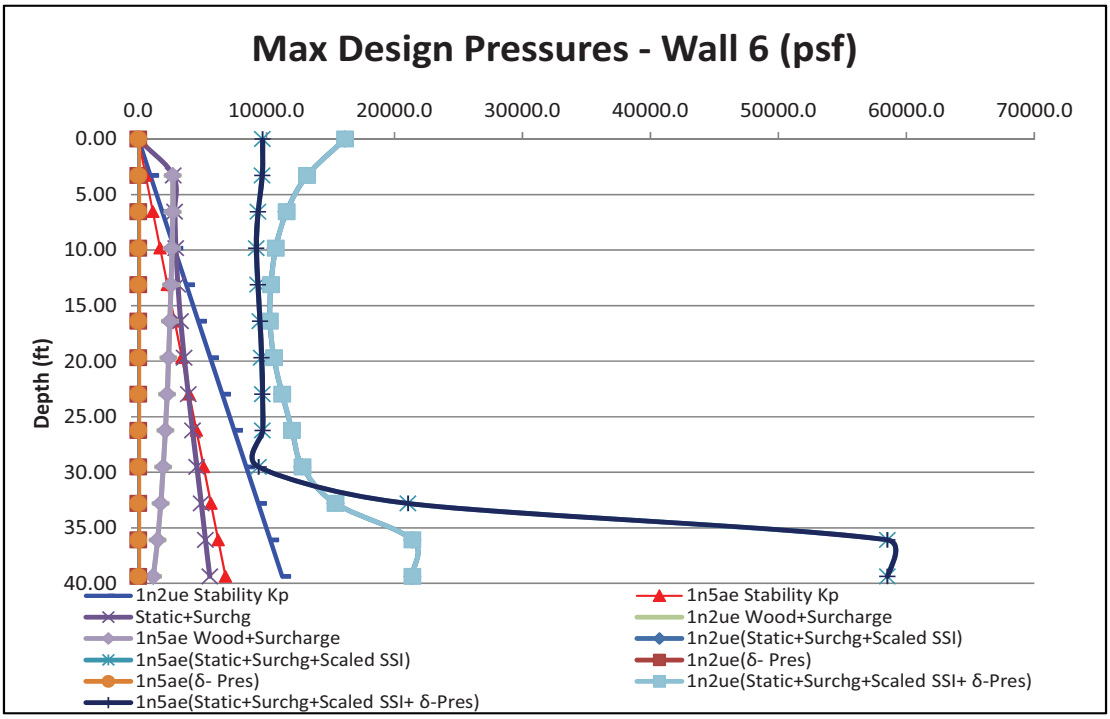

Figure 3.7.2-78-21: Wall 6 - Soil 2sn4uem (Cracked Concrete Case)

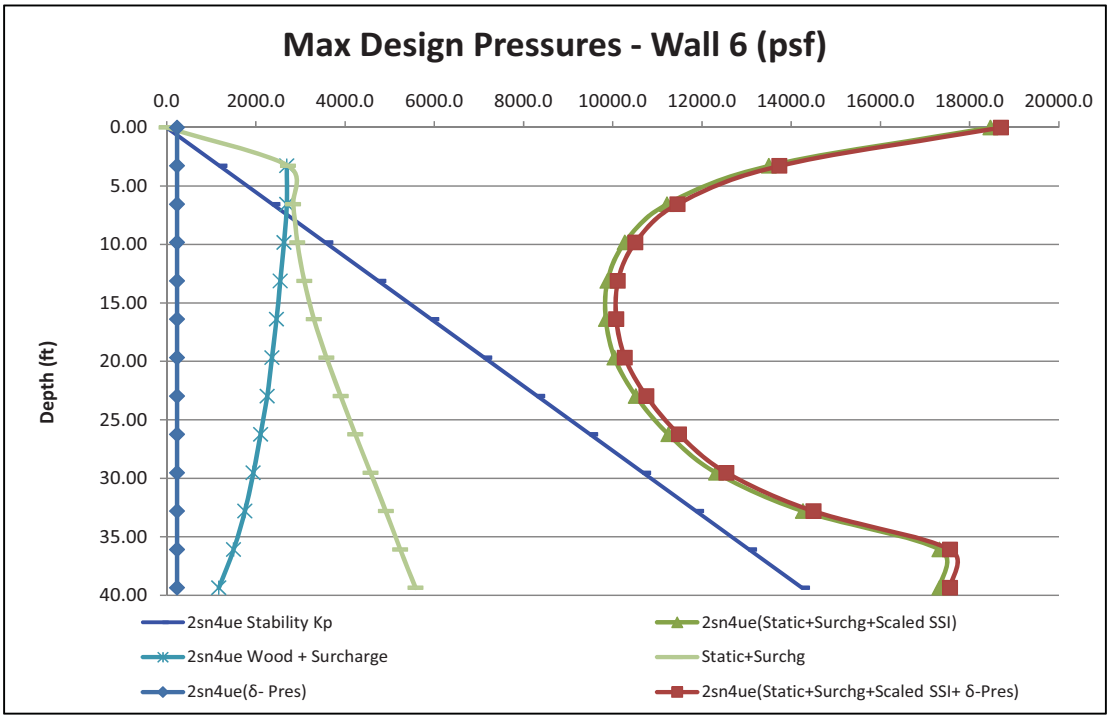

Figure 3.7.2-78-22: Wall 6 – 4uem (Cracked Concrete Case)

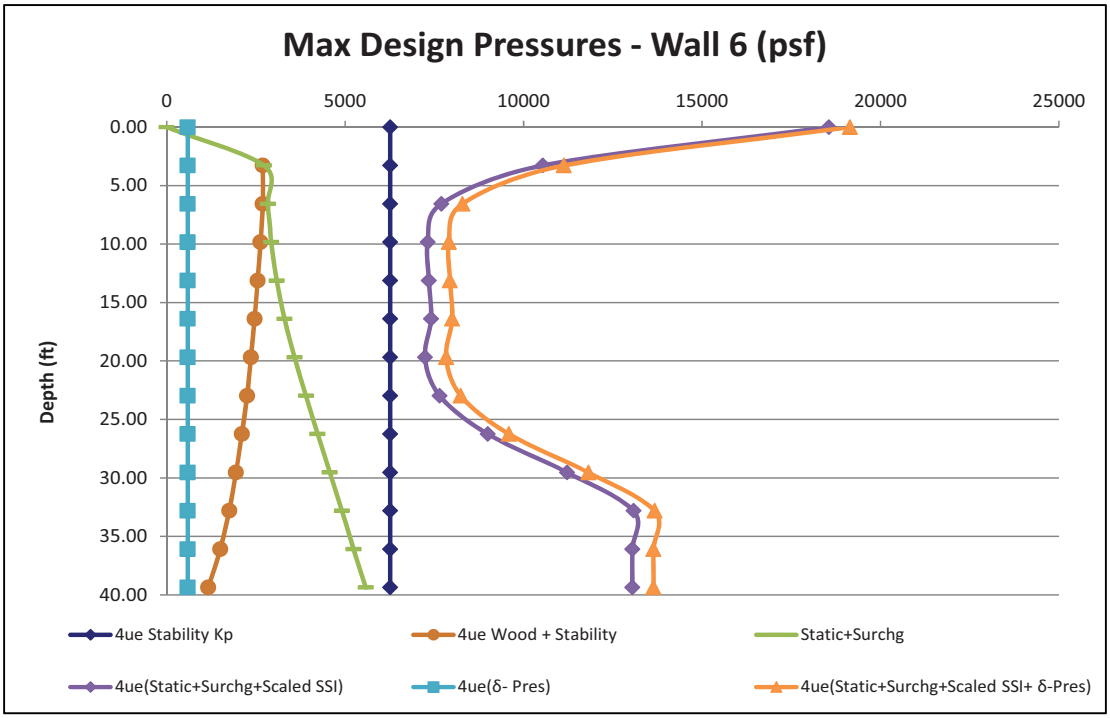

Figure 3.7.2-78-23: Wall 7 - Soil 1n2ue & 1n5aeh (Cracked Concrete Case)

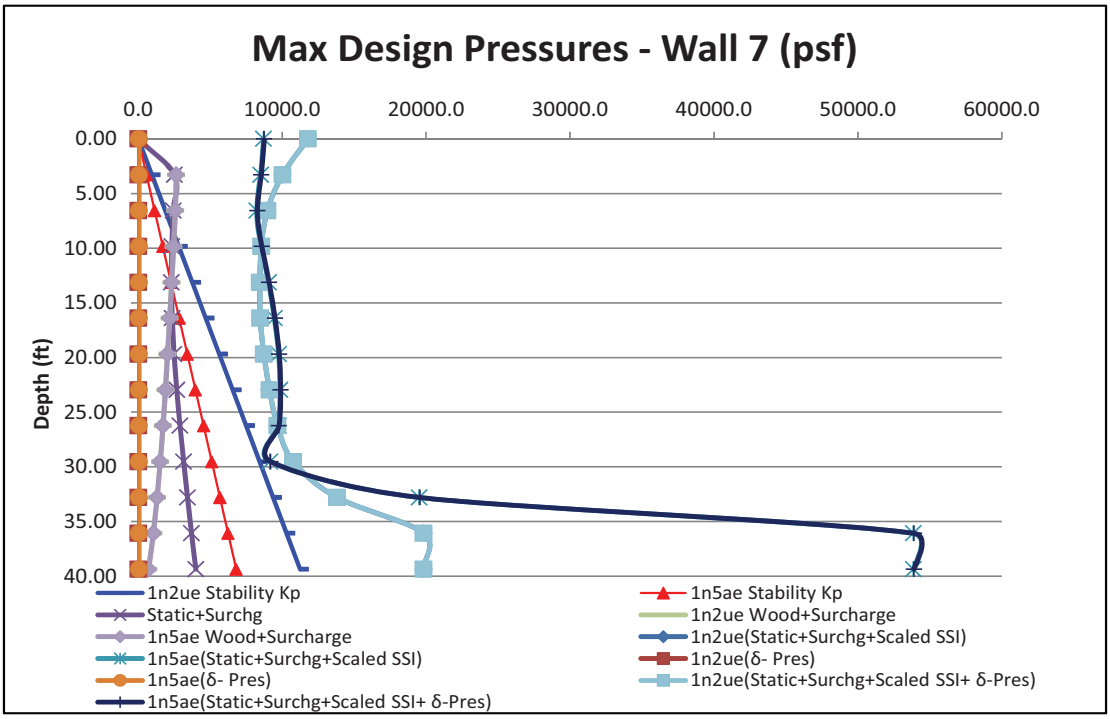

Figure 3.7.2-78-24: Wall 7 - Soil 2sn4uem (Cracked Concrete Case)

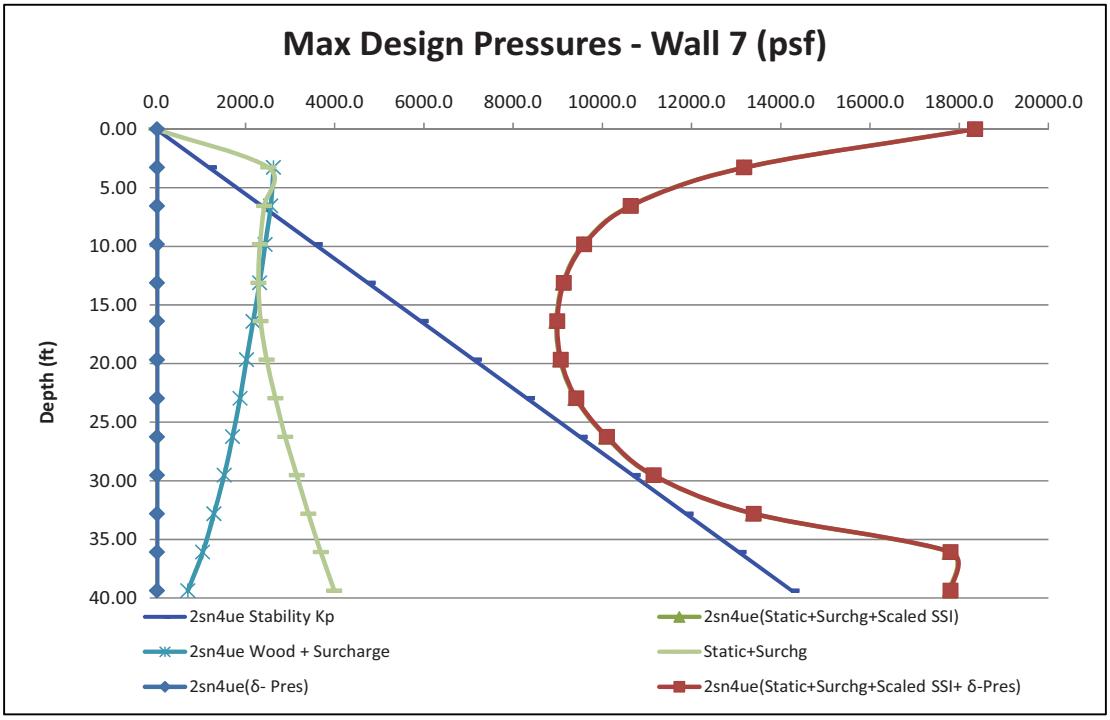

Figure 3.7.2-78-25: Wall 7 – 4uem (Cracked Concrete Case)

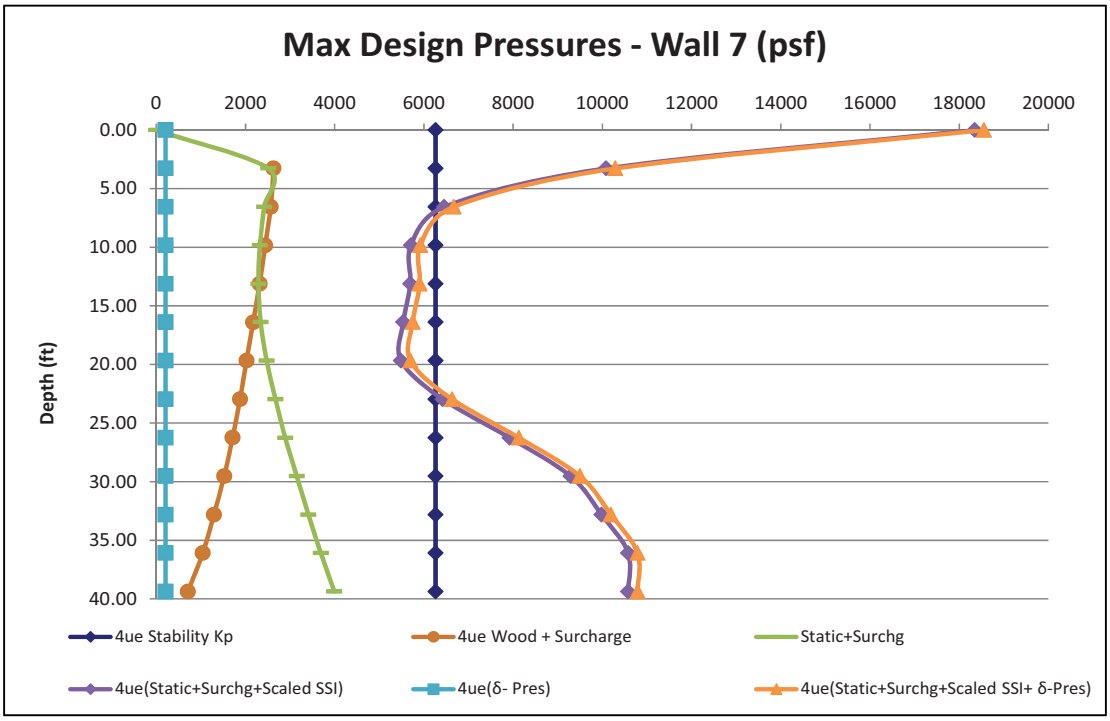

Figure 3.7.2-78-26: Wall 8 - Soil 1n2ue & 1n5aeh (Cracked Concrete Case)

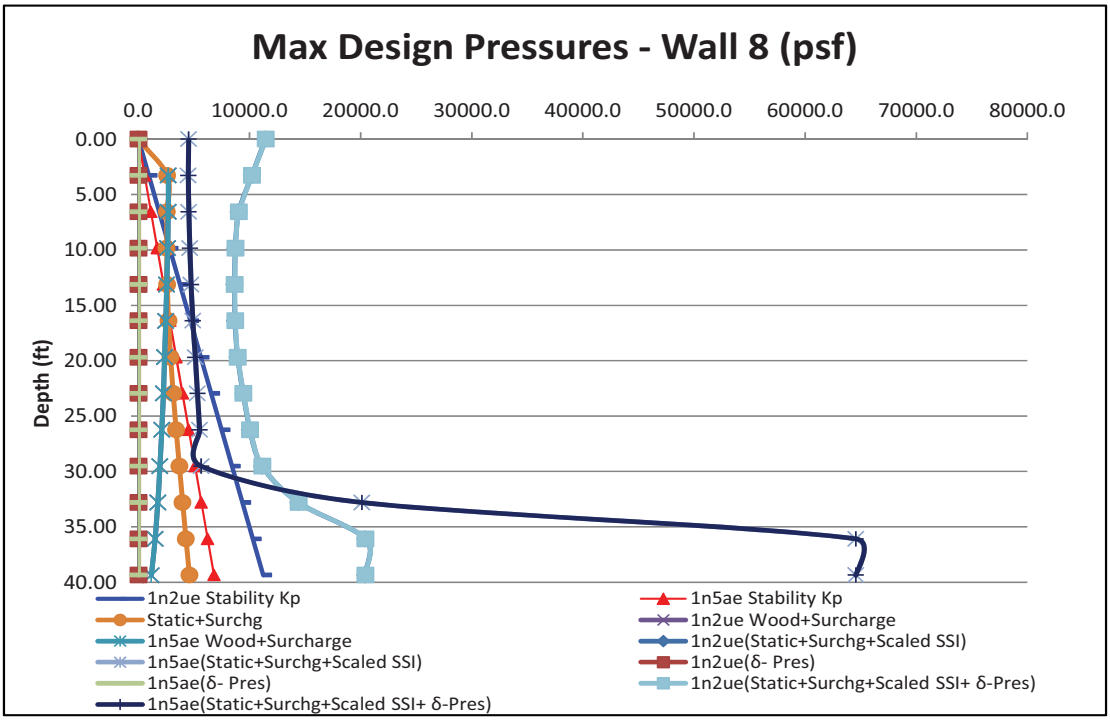

Figure 3.7.2-78-27: Wall 8 - Soil 2sn4uem (Cracked Concrete Case)

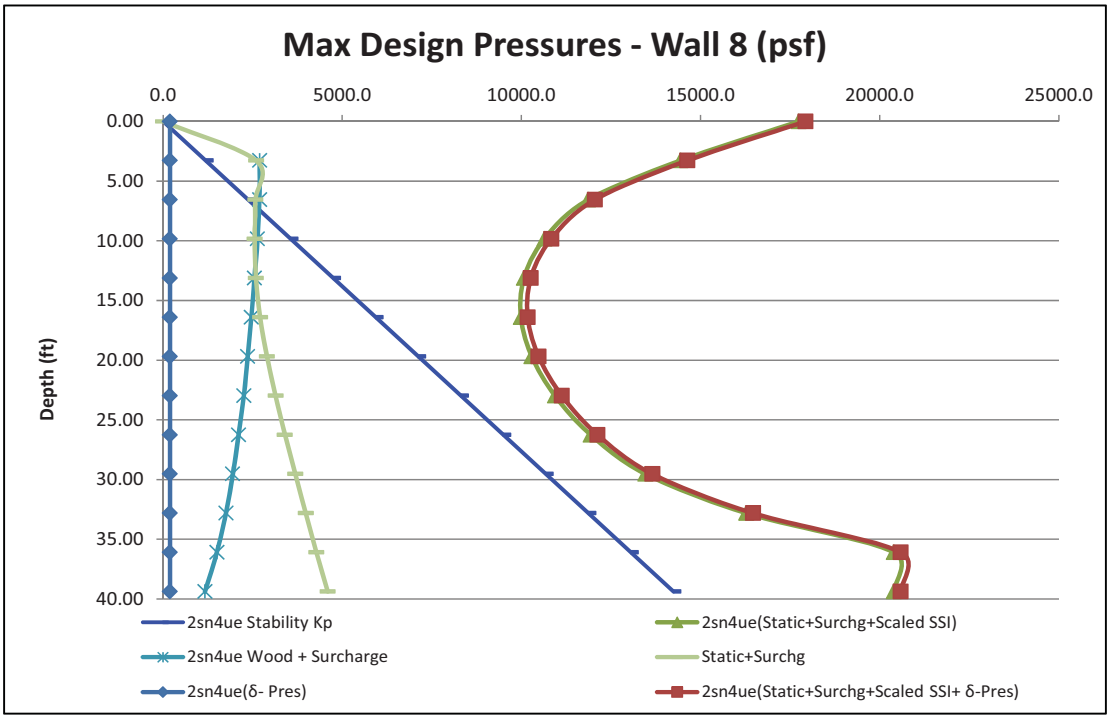

Figure 3.7.2-78-28: Wall 8 – 4uem (Cracked Concrete Case)

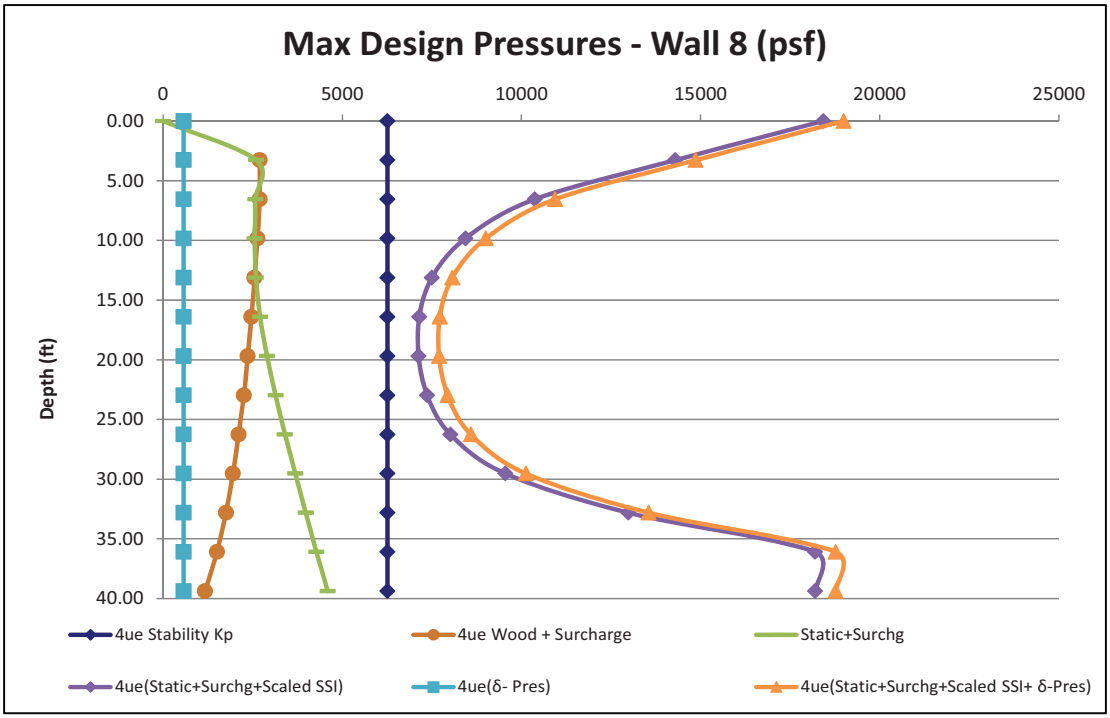

Figure 3.7.2-78-29: Wall 9 - Soil 1n2ue & 1n5aeh (Cracked Concrete Case)

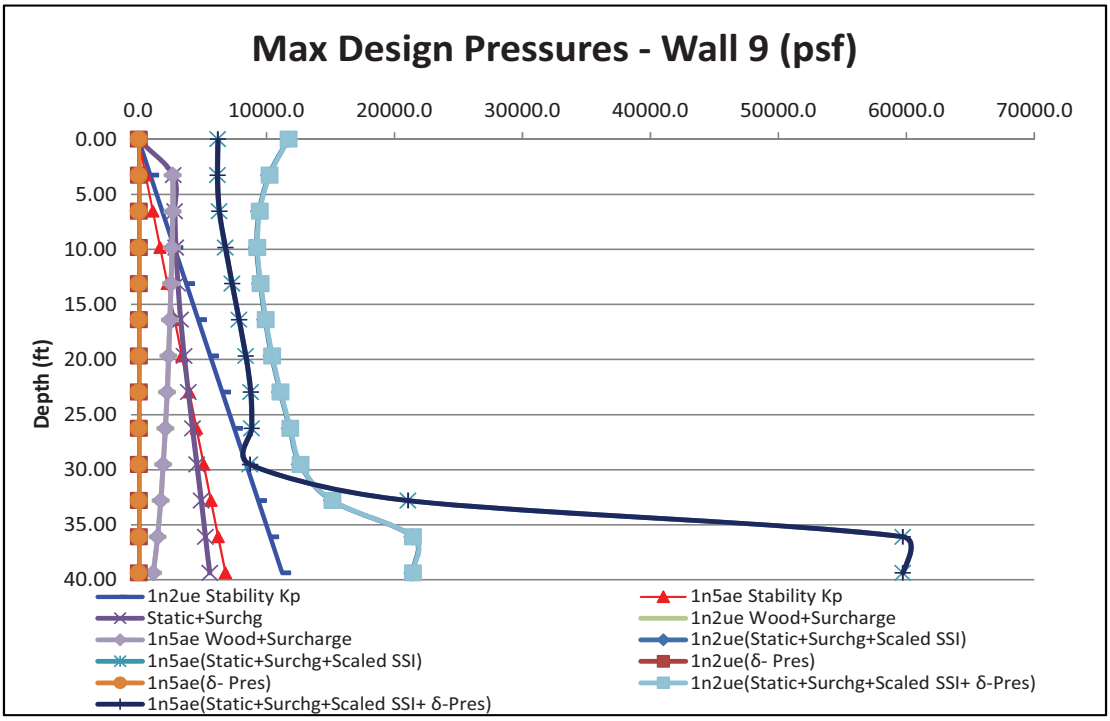

Figure 3.7.2-78-30: Wall 9 - Soil 2sn4uem (Cracked Concrete Case)

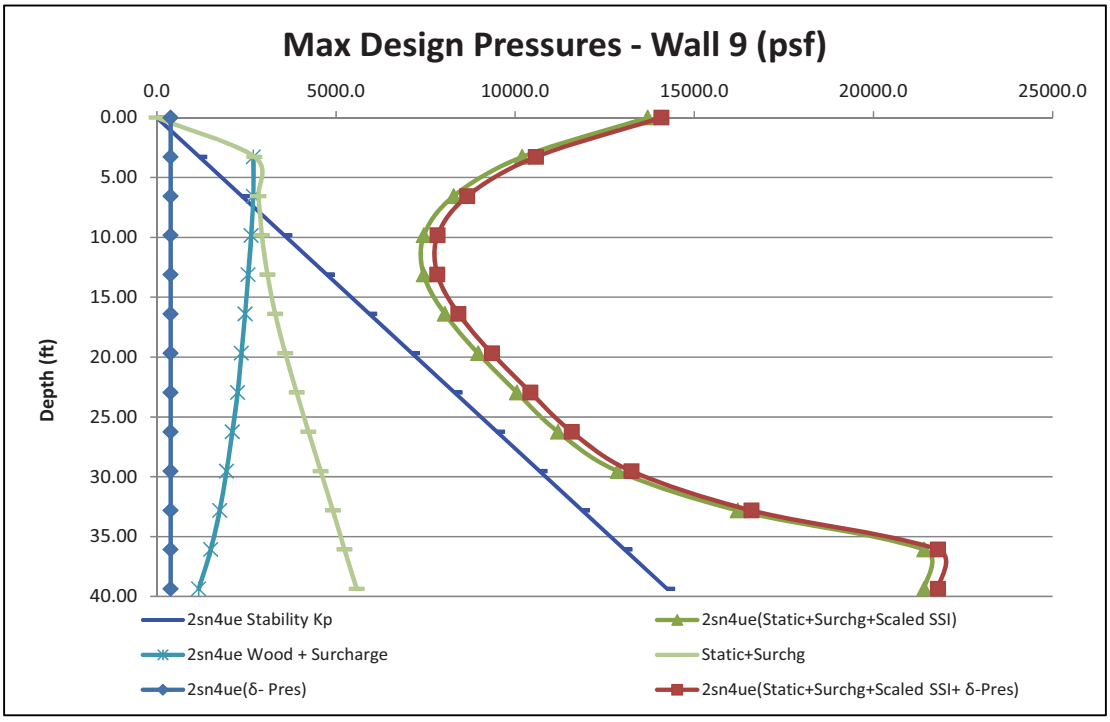

Figure 3.7.2-78-31: Wall 9 – 4uem (Cracked Concrete Case)

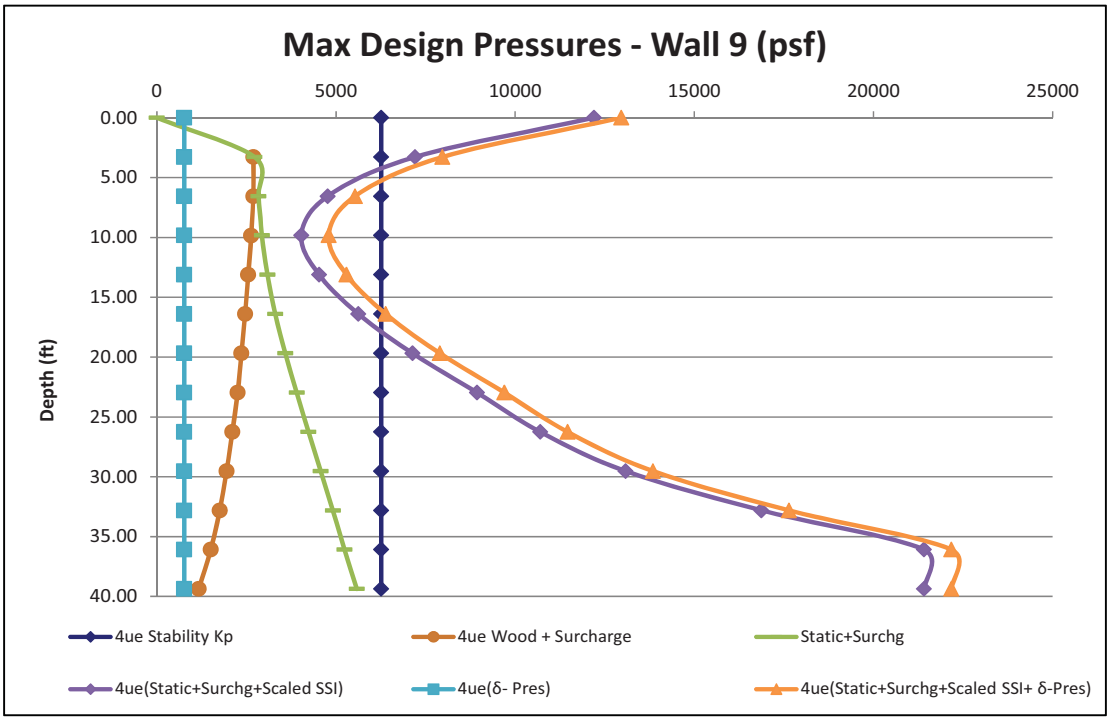

Figure 3.7.2-78-32: Wall 10 - Soil 1n2ue & 1n5aeh (Cracked Concrete Case)

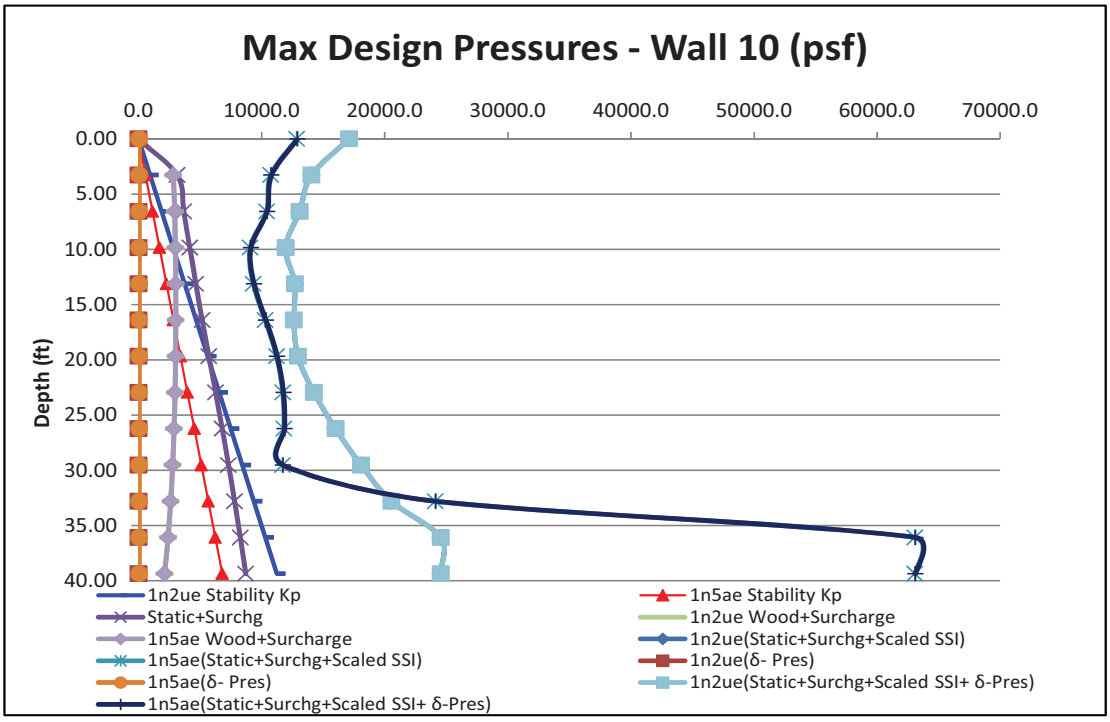

Figure 3.7.2-78-33: Wall 10 - Soil 2sn4uem (Cracked Concrete Case)

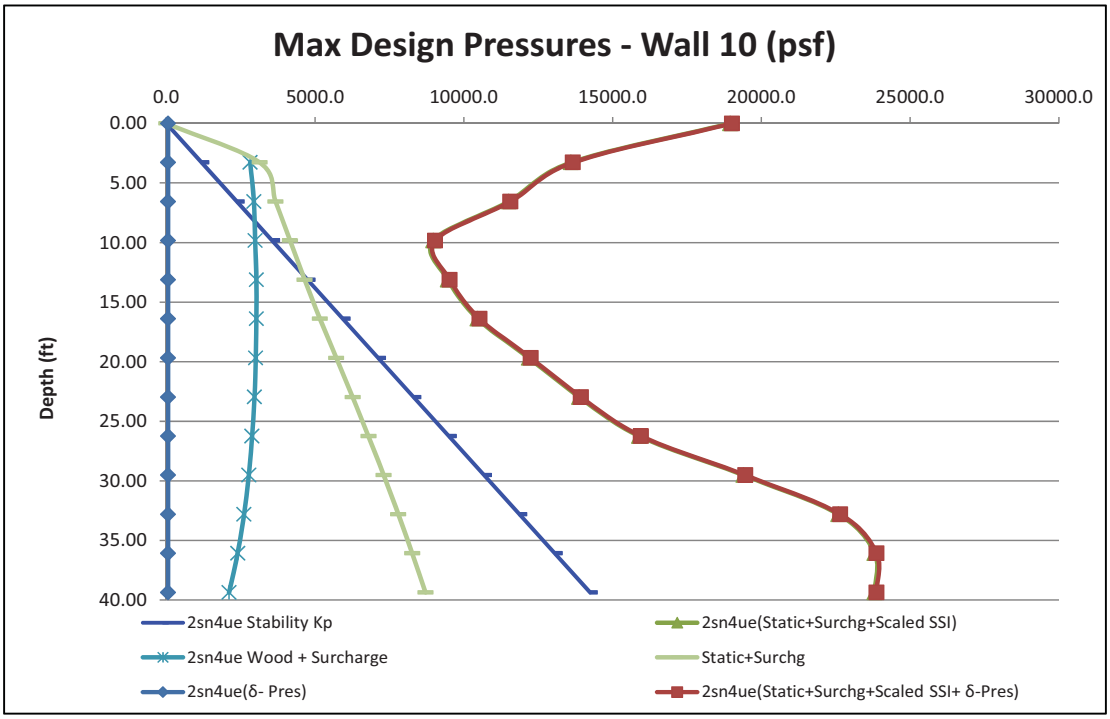

Figure 3.7.2-78-34: Wall 10 – 4uem (Cracked Concrete Case)

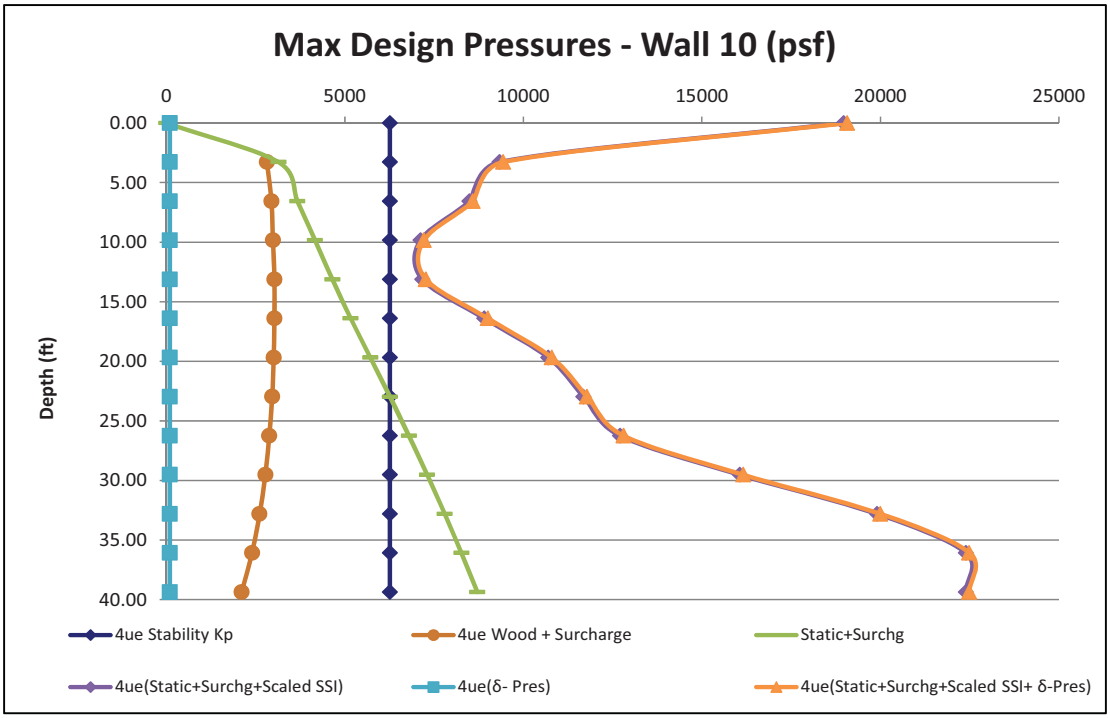

Figure 3.7.2-78-35: Wall 11 - Soil 1n2ue & 1n5aeh (Cracked Concrete Case)

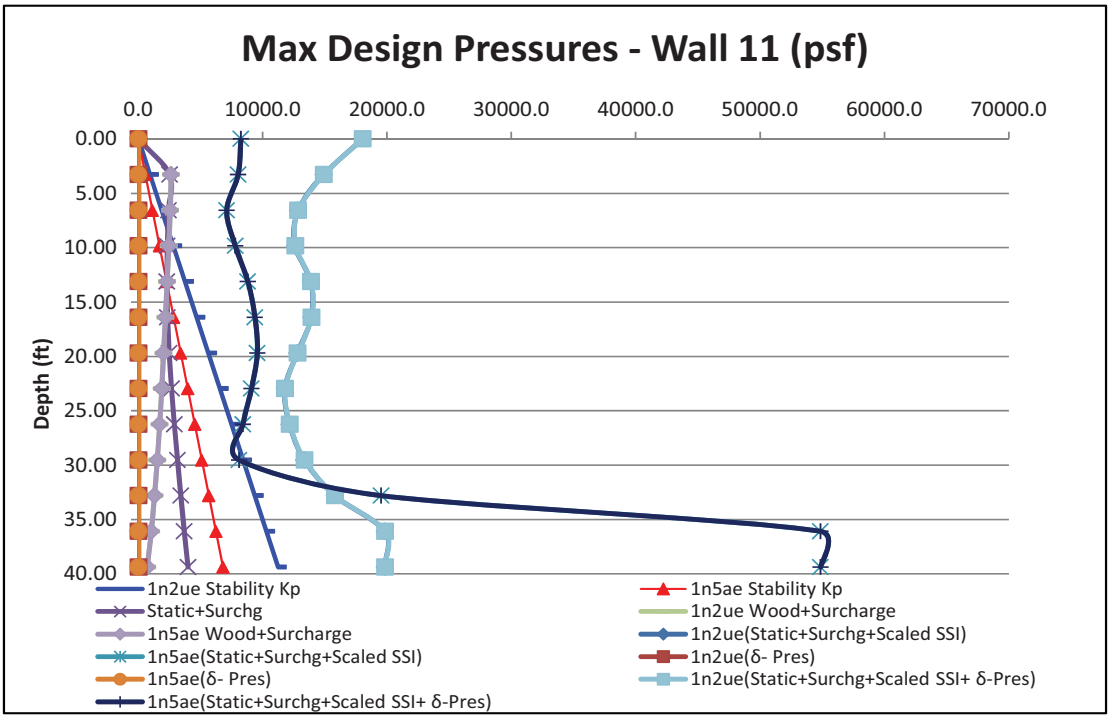

Figure 3.7.2-78-36: Wall 11 - Soil 2sn4uem (Cracked Concrete Case)

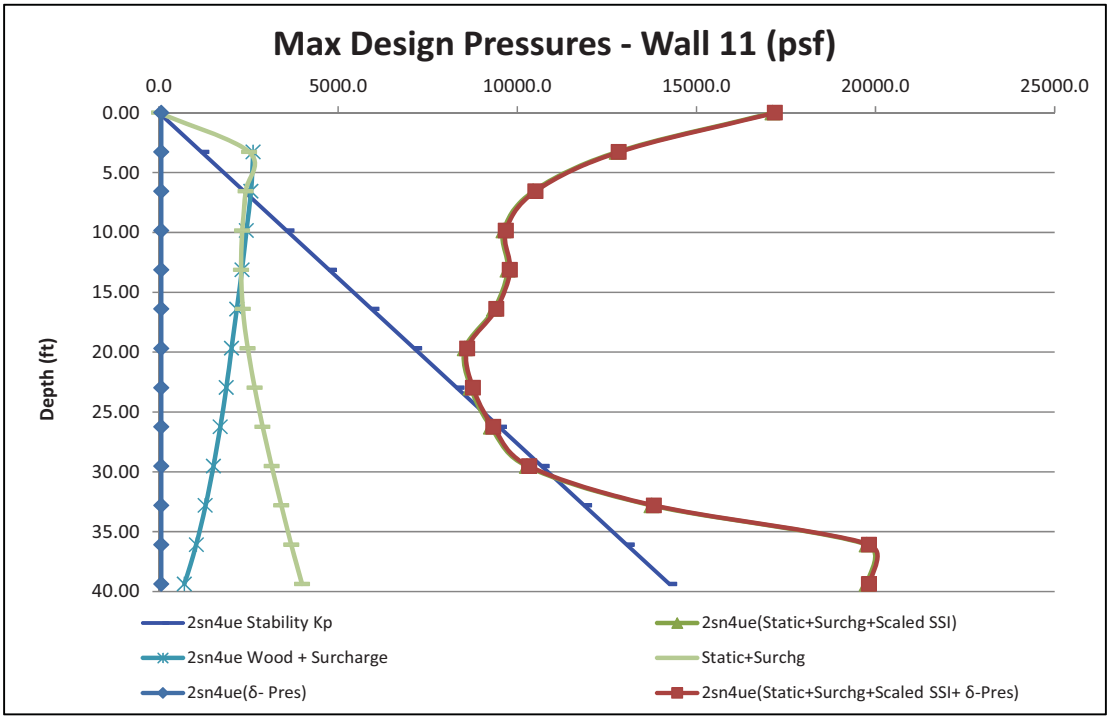

Figure 3.7.2-78-37: Wall 11 – 4uem (Cracked Concrete Case)

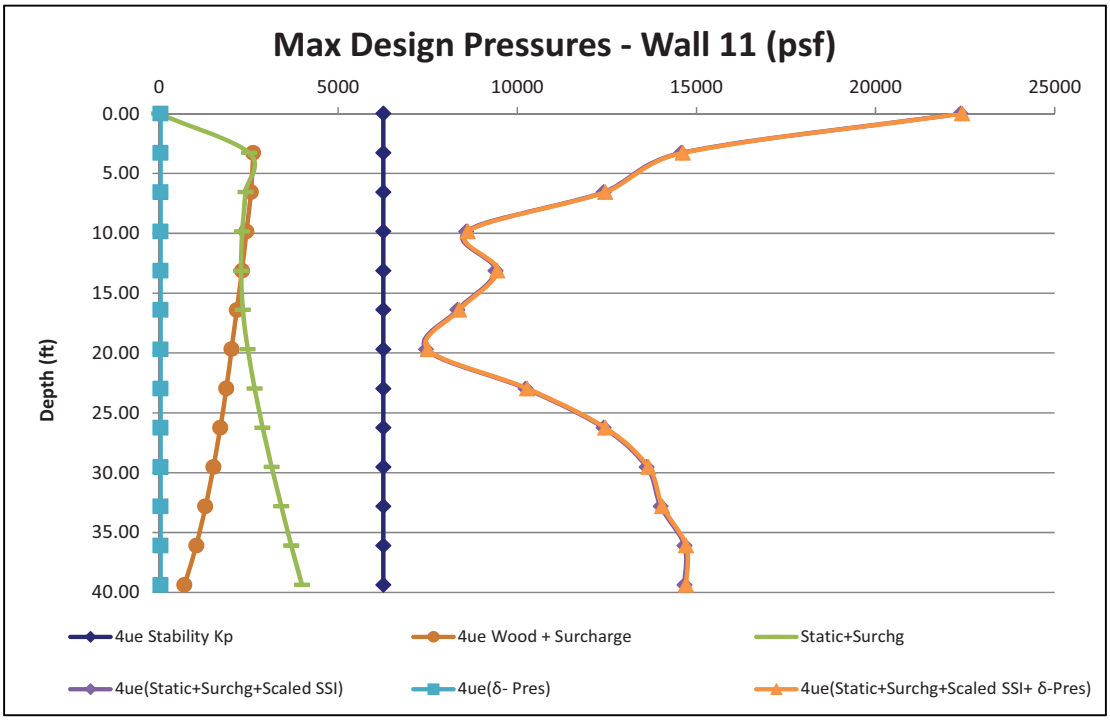

Figure 3.7.2-78-38: Inner Q1 – Soil 1n2ue, 2sn4uem, 4uem & 1n5aeh (Cracked Concrete Case)

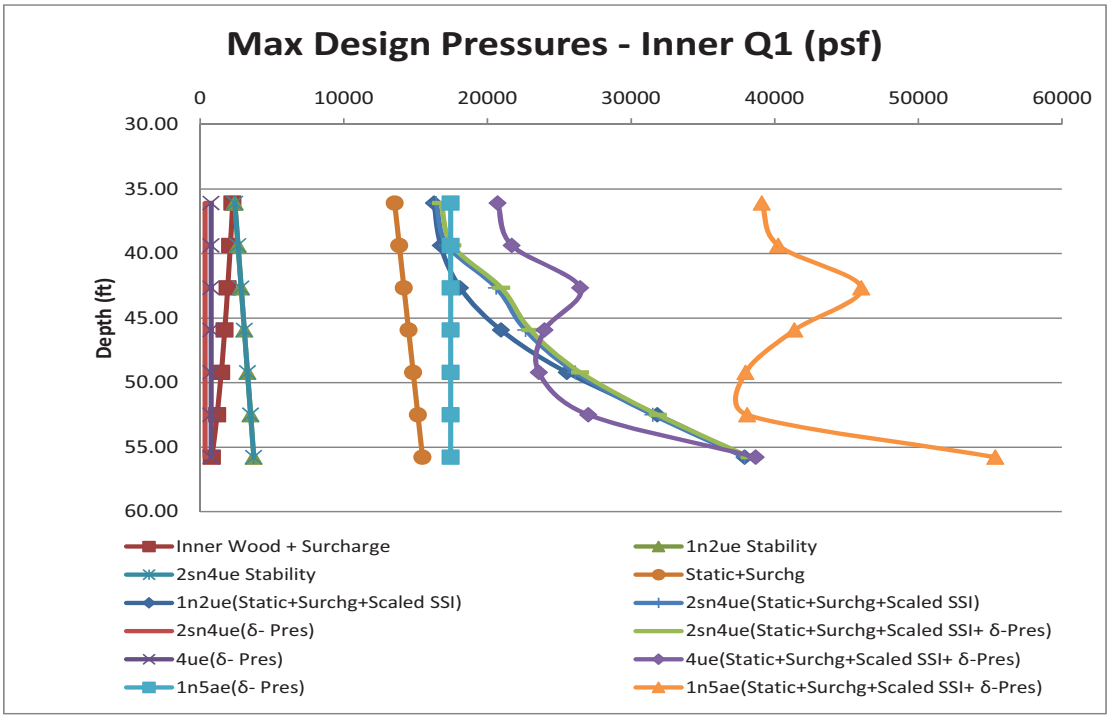

Figure 3.7.2-78-39: Inner Q2 – Soil 1n2ue, 2sn4uem, 4uem & 1n5aeh (Cracked Concrete Case)

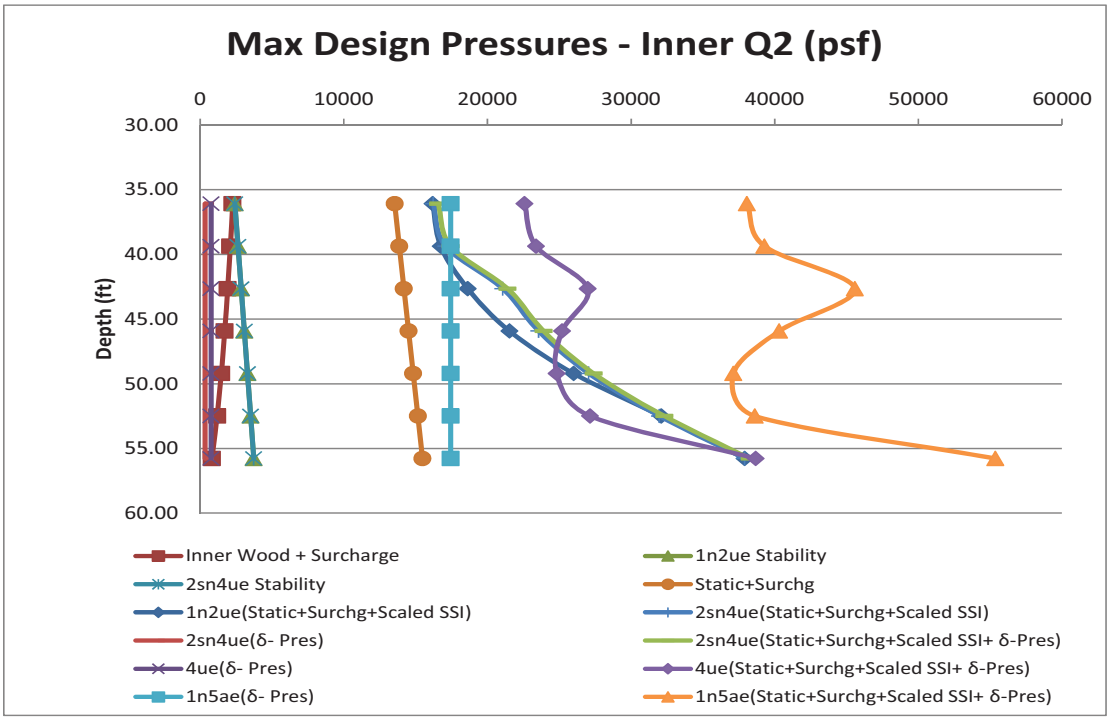

Figure 3.7.2-78-40: Inner Q3 – Soil 1n2ue, 2sn4uem, 4uem & 1n5aeh (Cracked Concrete Case)

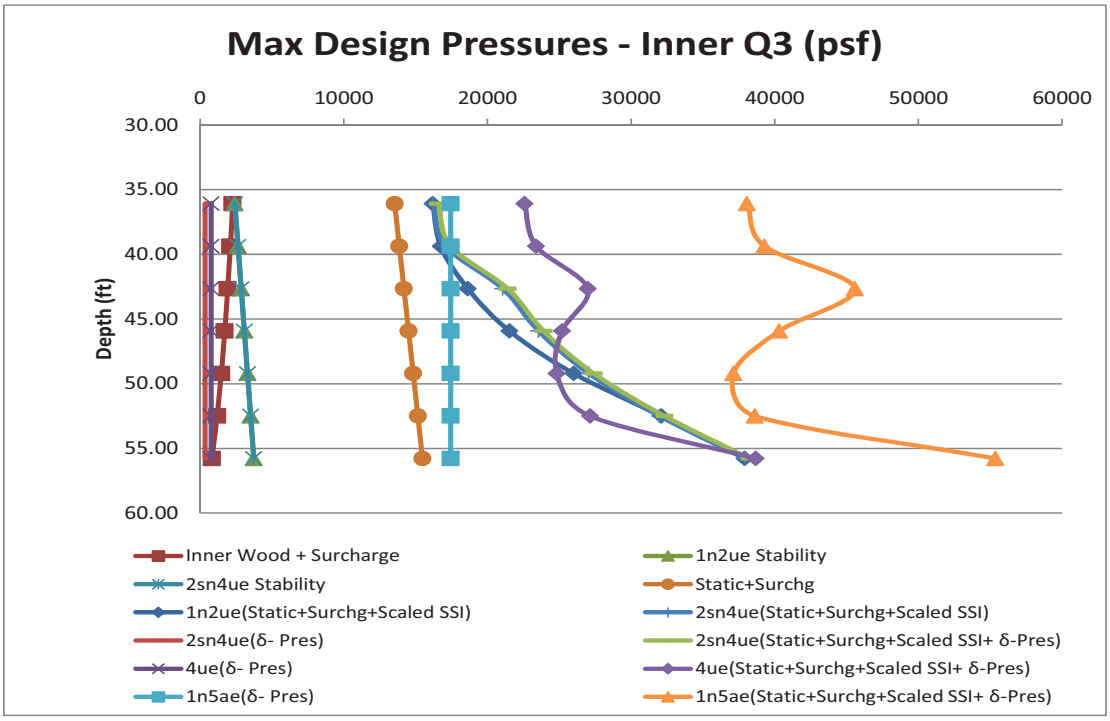

Figure 3.7.2-78-41: Inner Q4 – Soil 1n2ue, 2sn4uem, 4uem & 1n5aeh (Cracked Concrete Case)

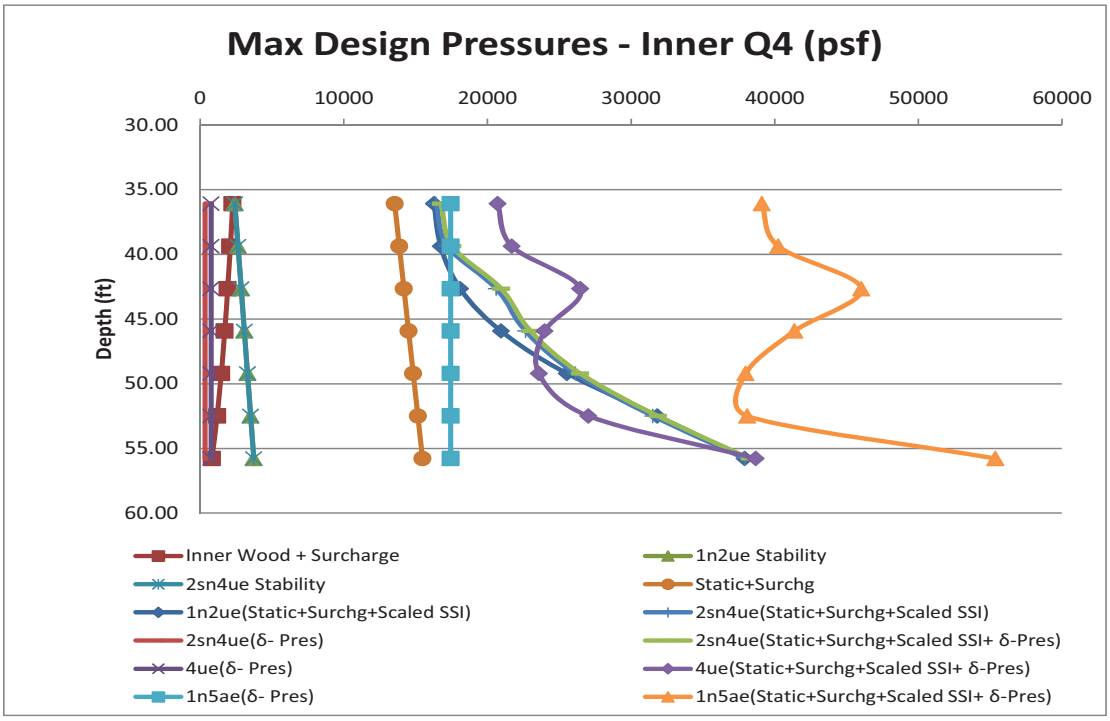

Figure 3.7.2-78-42: Outer Q1 – Soil 1n2ue, 2sn4uem, 4uem & 1n5aeh (Cracked Concrete Case)

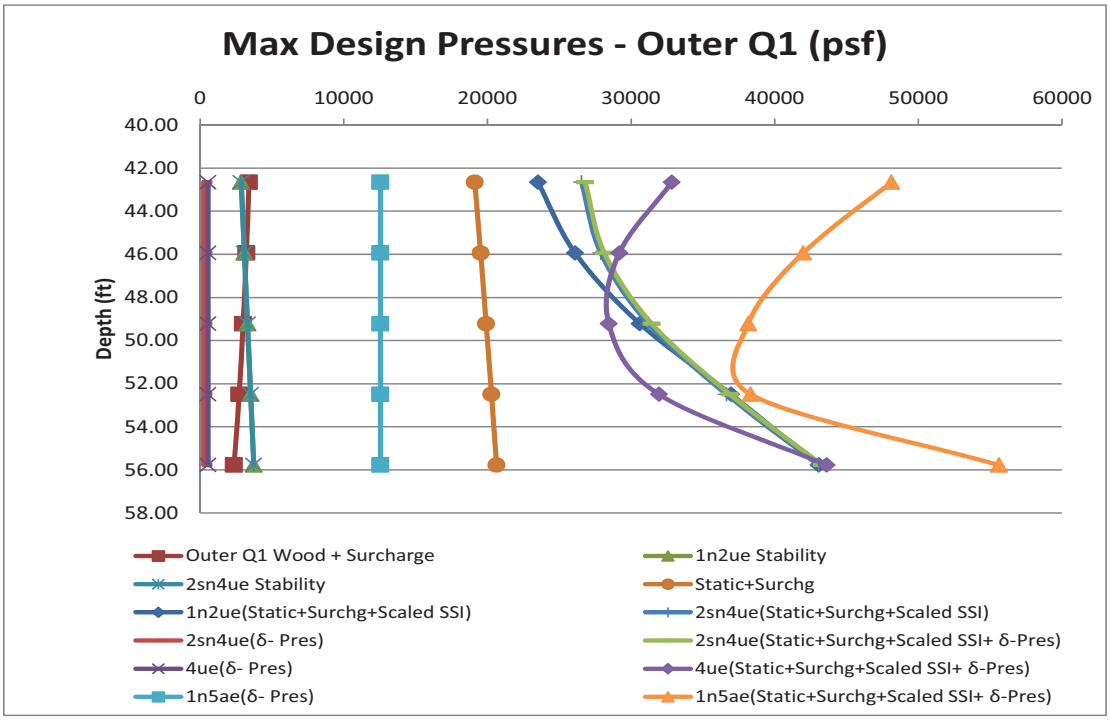

Figure 3.7.2-78-43: Outer Q2 – Soil 1n2ue, 2sn4uem, 4uem & 1n5aeh (Cracked Concrete Case)

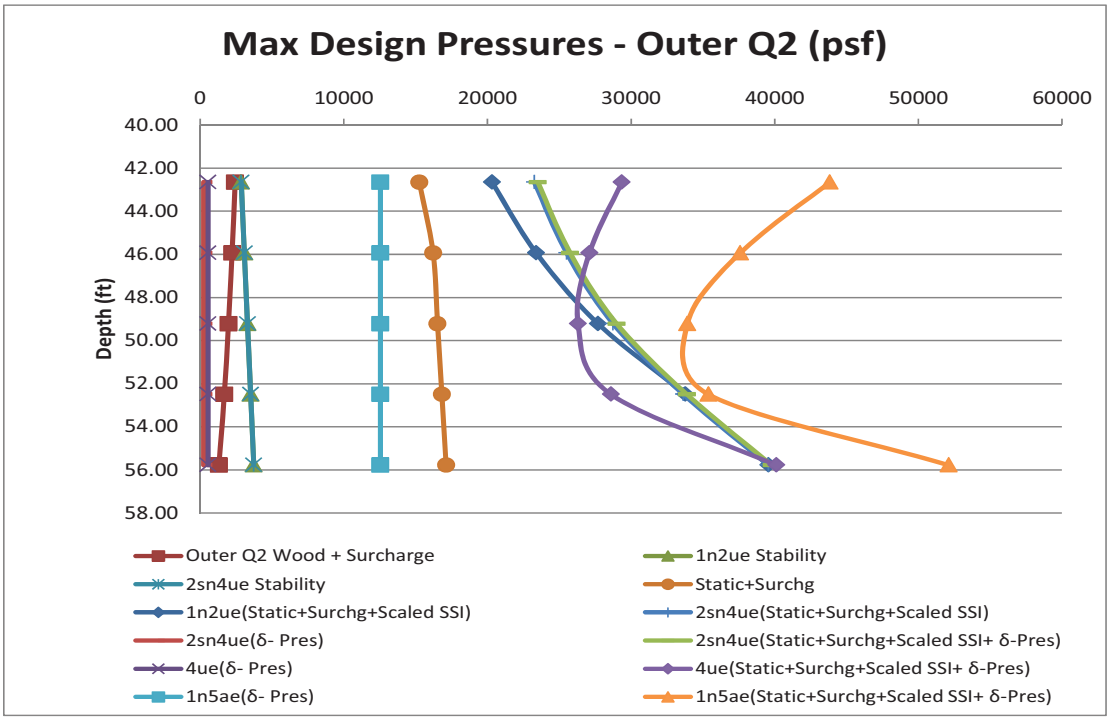

Figure 3.7.2-78-44: Outer Q3 – Soil 1n2ue, 2sn4uem, 4uem & 1n5aeh (Cracked Concrete Case)

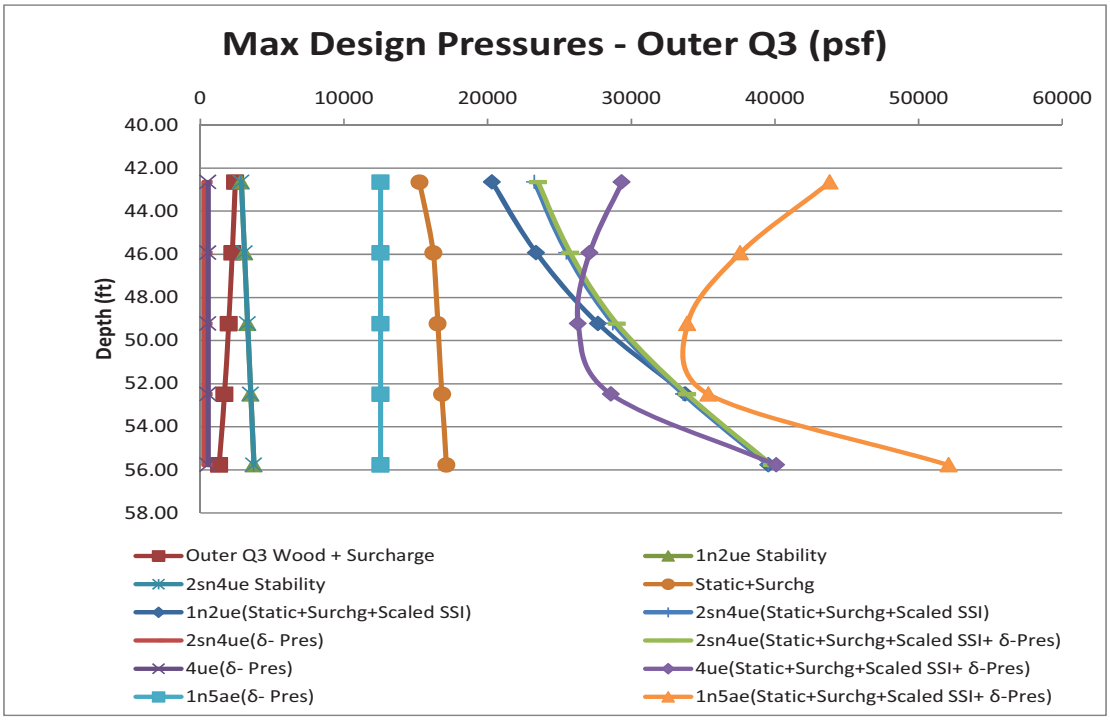

Figure 3.7.2-78-45: Outer Q4 – Soil 1n2ue, 2sn4uem, 4uem & 1n5aeh (Cracked Concrete Case)

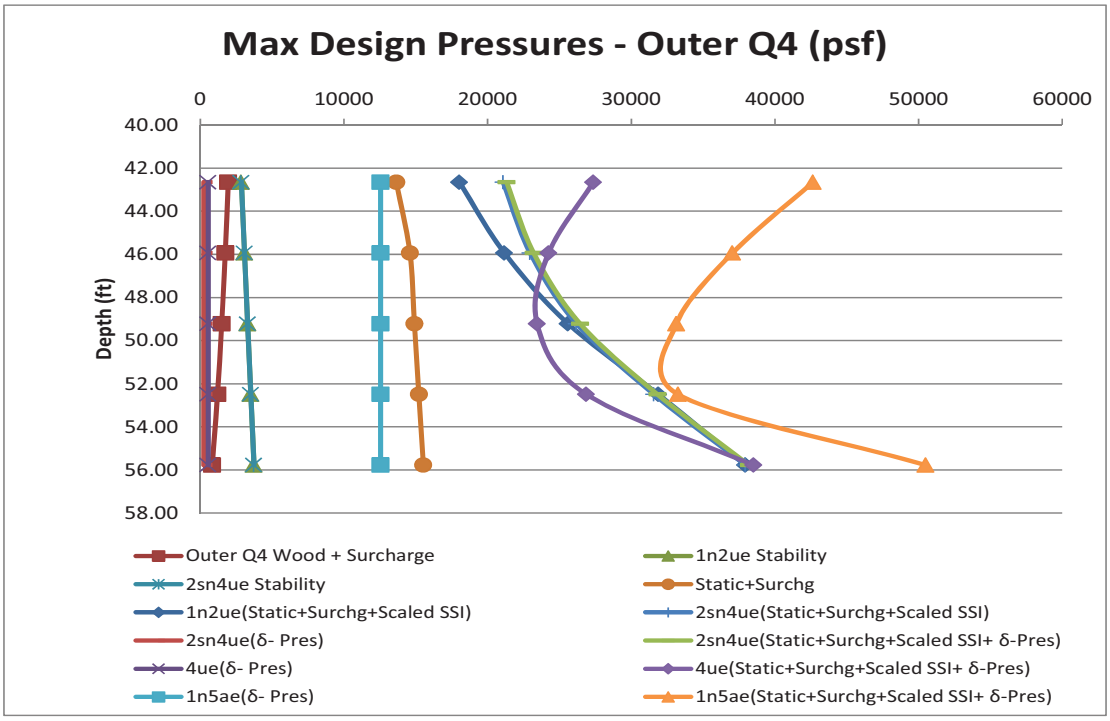

Figure 3.7.2-78-46: Wall 2 – Soil 4ue & 1n2ue (Cracked Concrete Case)

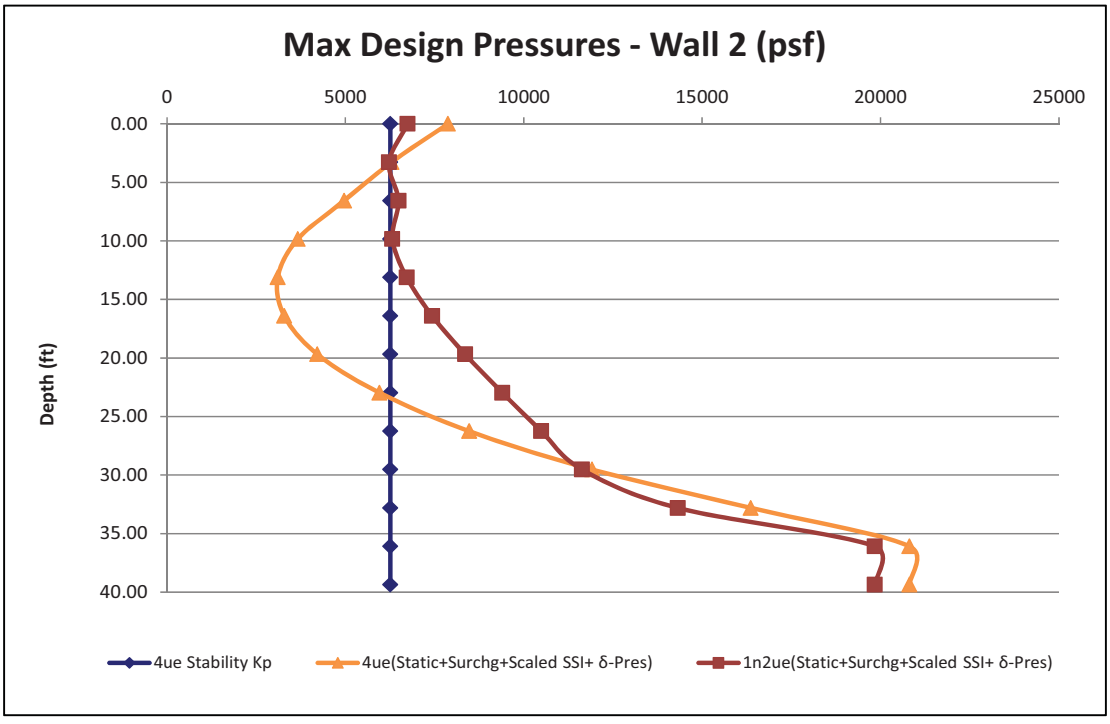

Figure 3.7.2-78-47: Wall 3 – Soil 4uem & 1n2ue (Cracked Concrete Case)

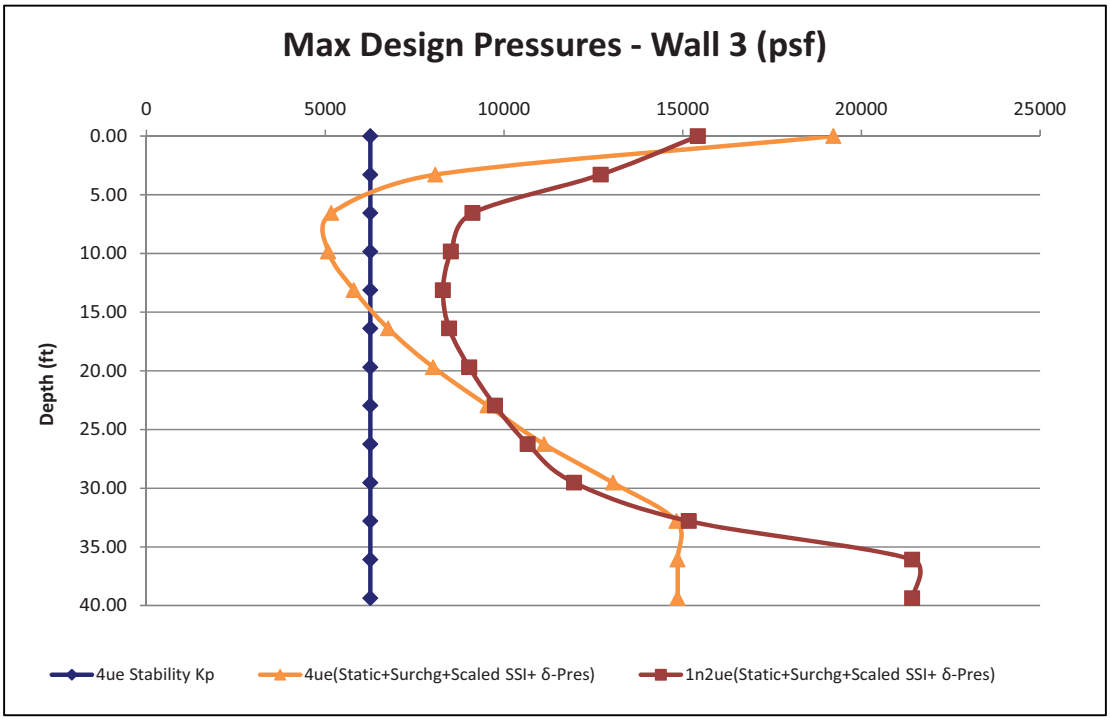

Figure 3.7.2-78-48: Wall 4 – Soil 4ue & 1n2ue (Cracked Concrete Case)

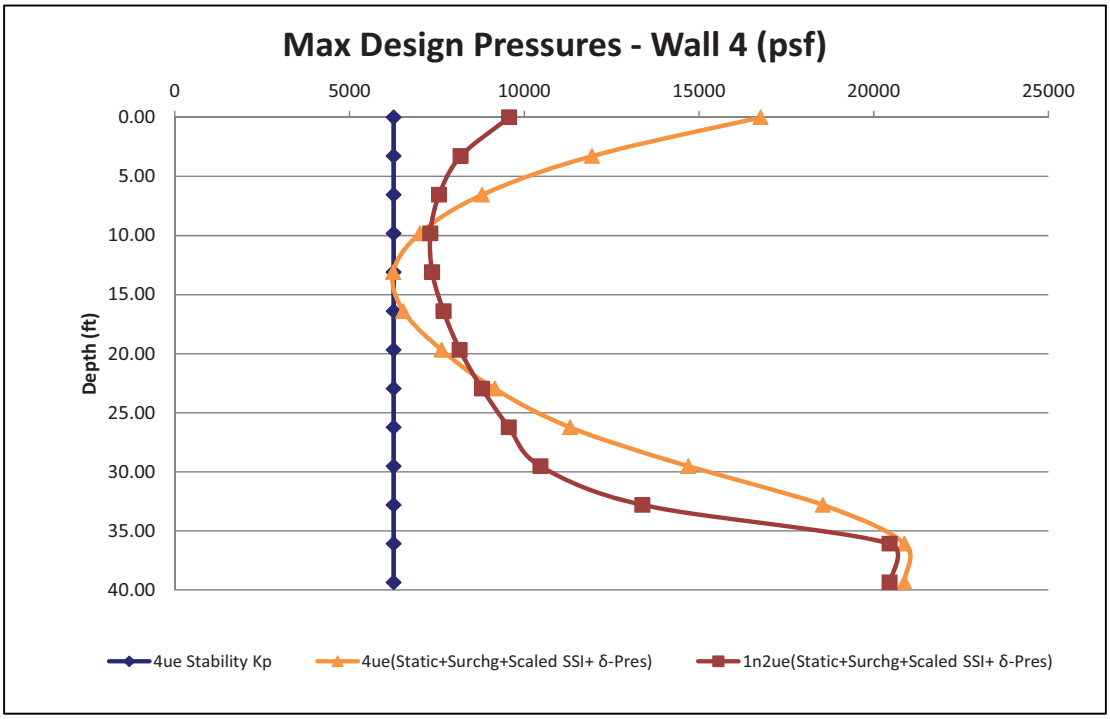

Figure 3.7.2-78-49: Wall 5 – Soil 4uem & 1n2ue (Cracked Concrete Case)

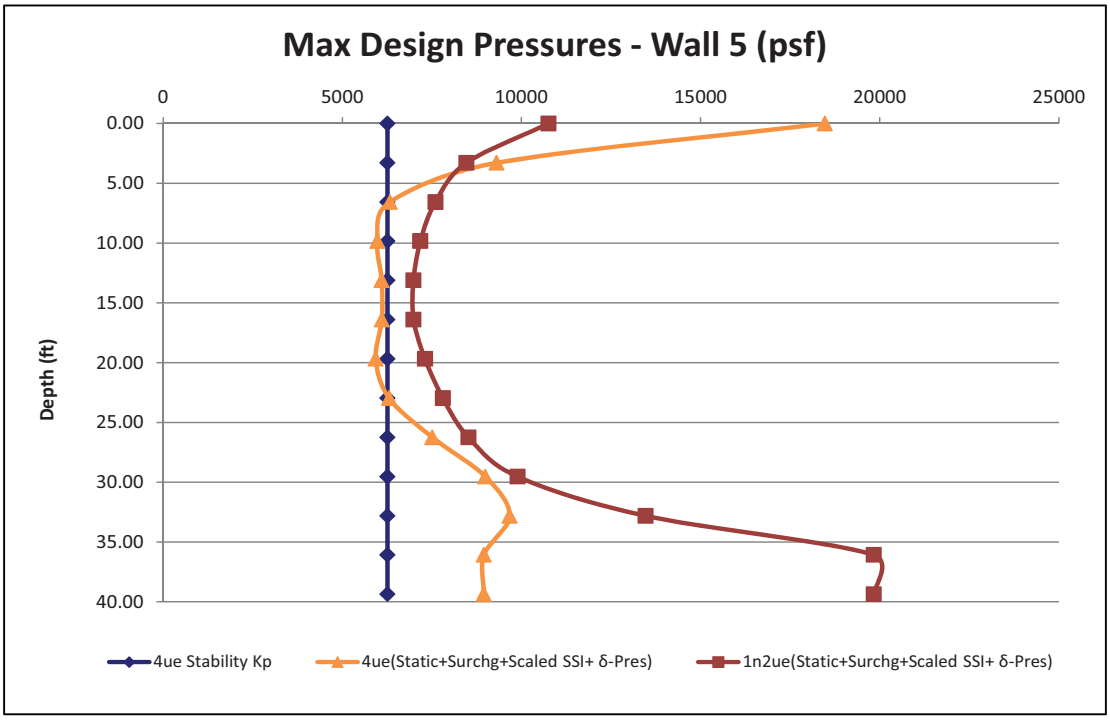

Figure 3.7.2-78-50: Wall 6 – Soil 4ue & 1n2ue (Cracked Concrete Case)

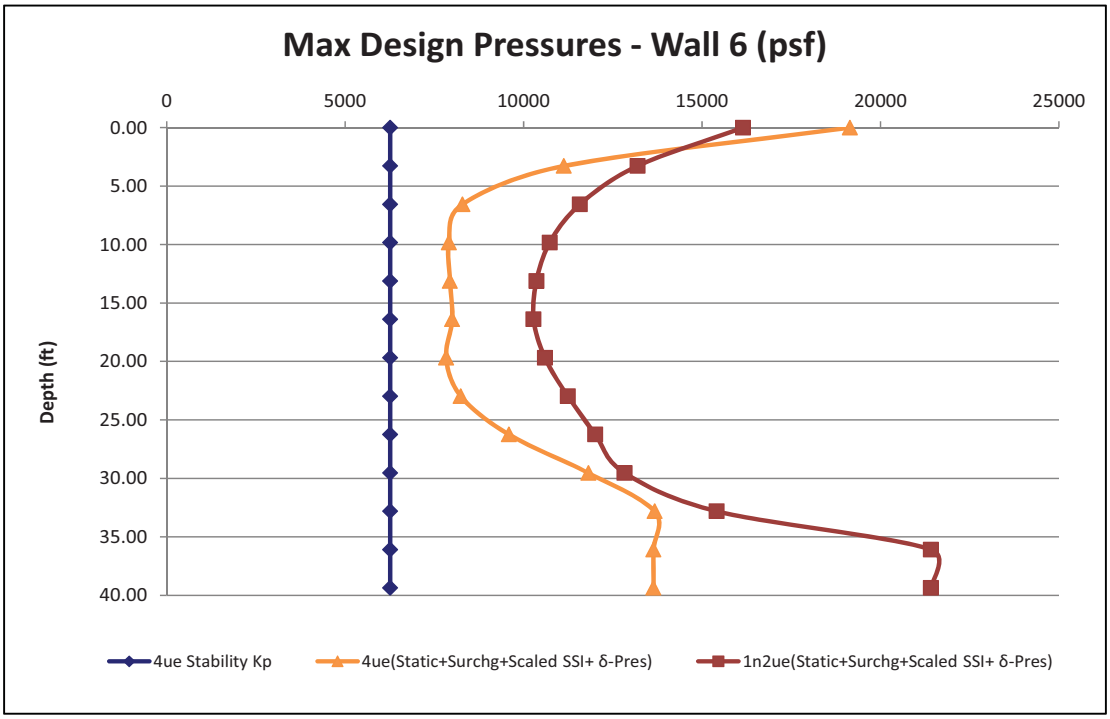

Figure 3.7.2-78-51: Wall 7 – Soil 4uem & 1n2ue (Cracked Concrete Case)

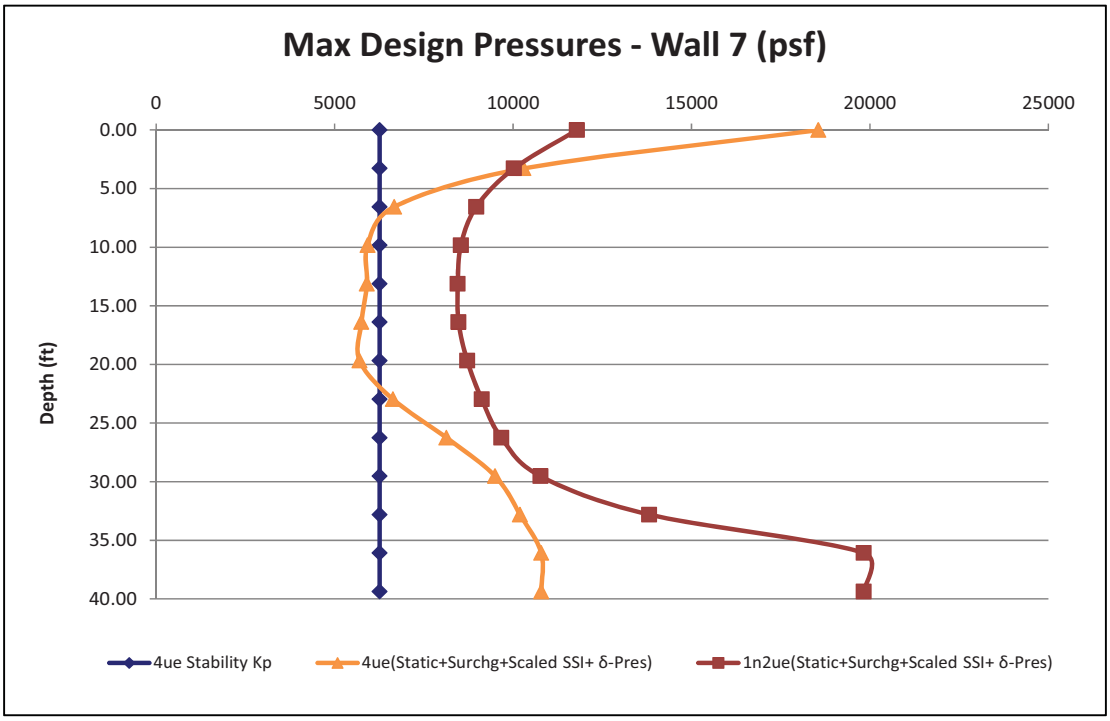

Figure 3.7.2-78-52: Wall 8 – Soil 4ue & 1n2ue (Cracked Concrete Case)

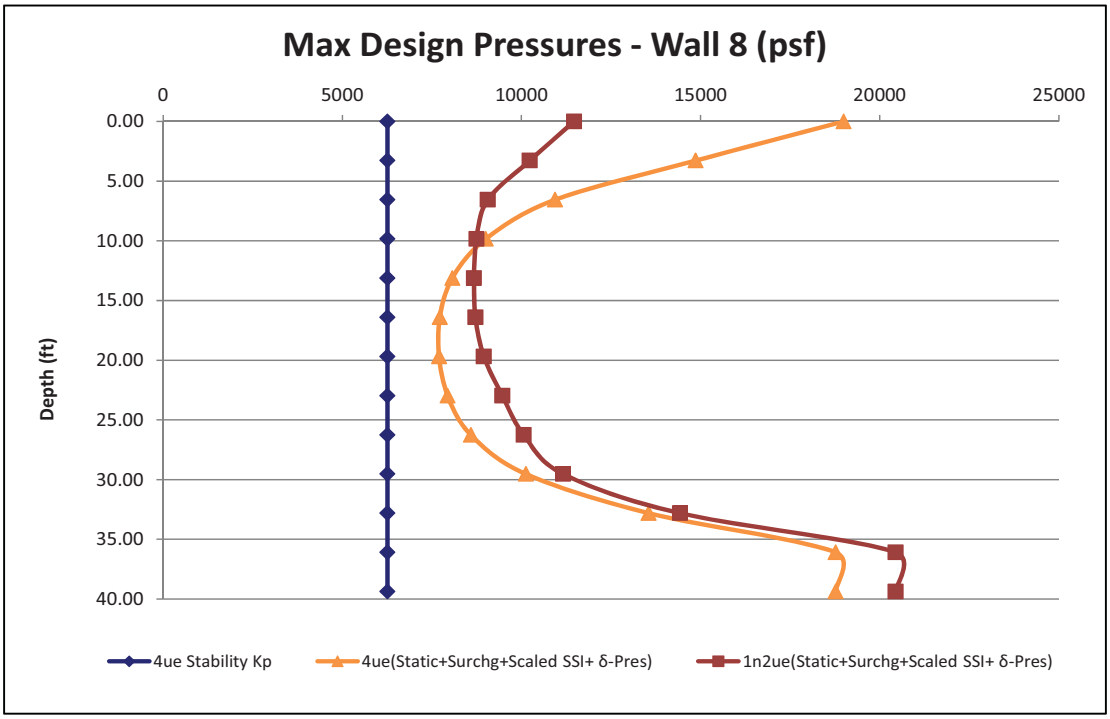

Figure 3.7.2-78-53: Wall 9 – Soil 4uem & 1n2ue (Cracked Concrete Case)

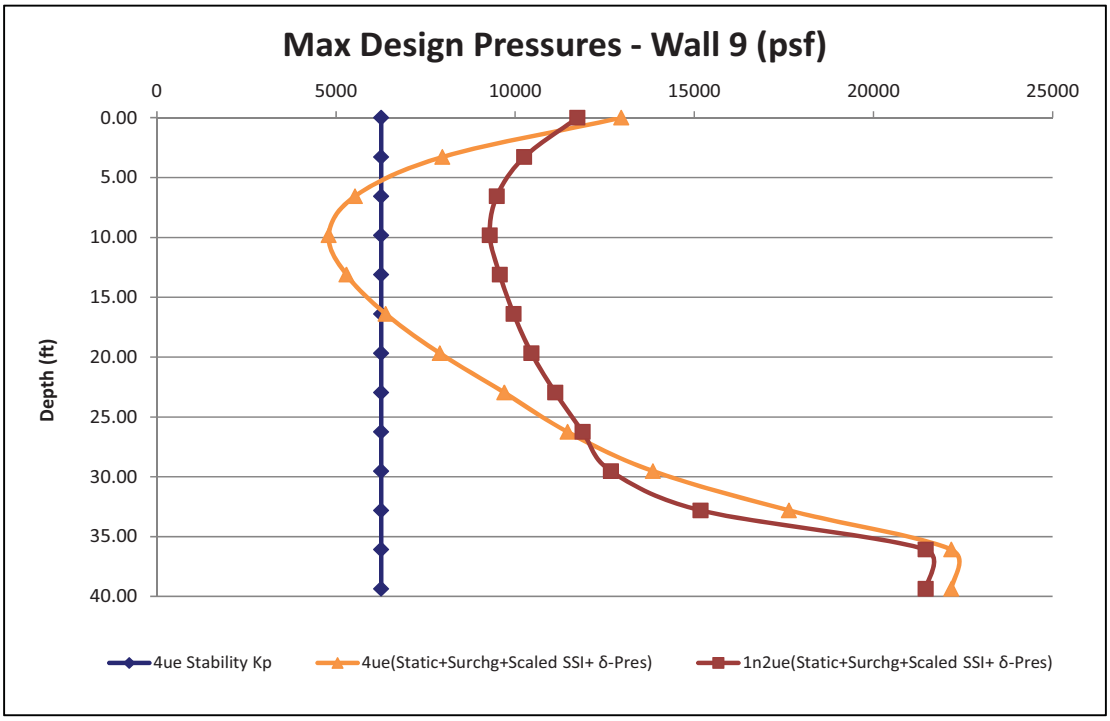

Figure 3.7.2-78-54: Wall 10 – Soil 4ue & 1n2ue (Cracked Concrete Case)

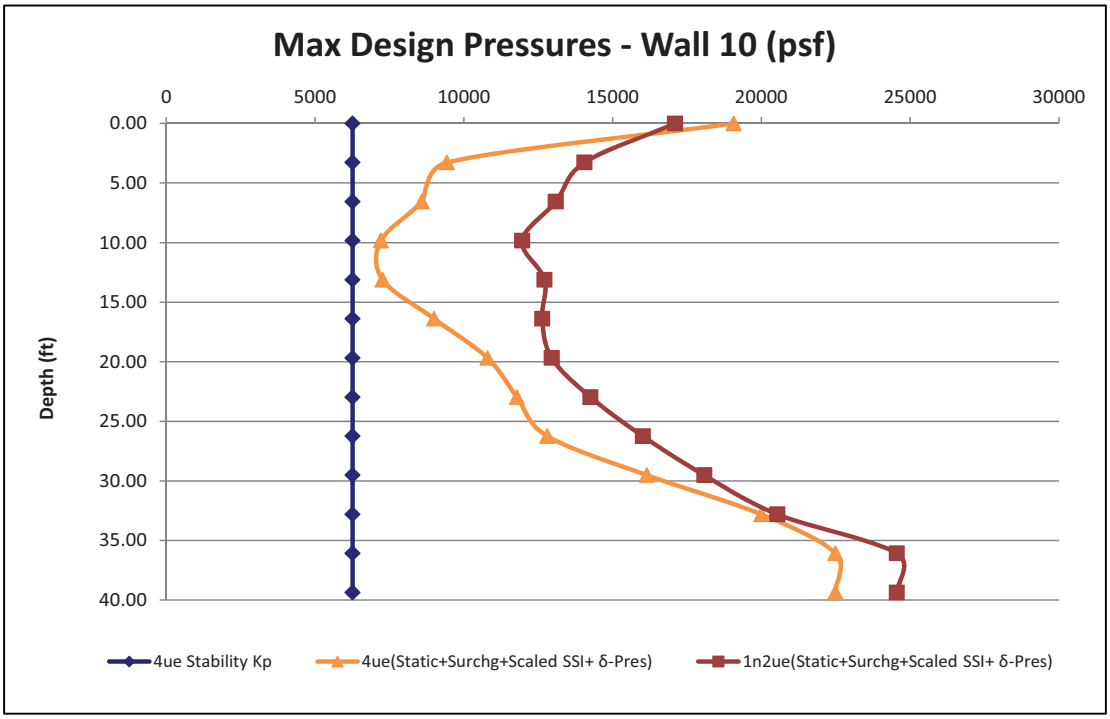

Figure 3.7.2-78-55: Wall 11 – Soil 4uem & 1n2ue (Cracked Concrete Case)

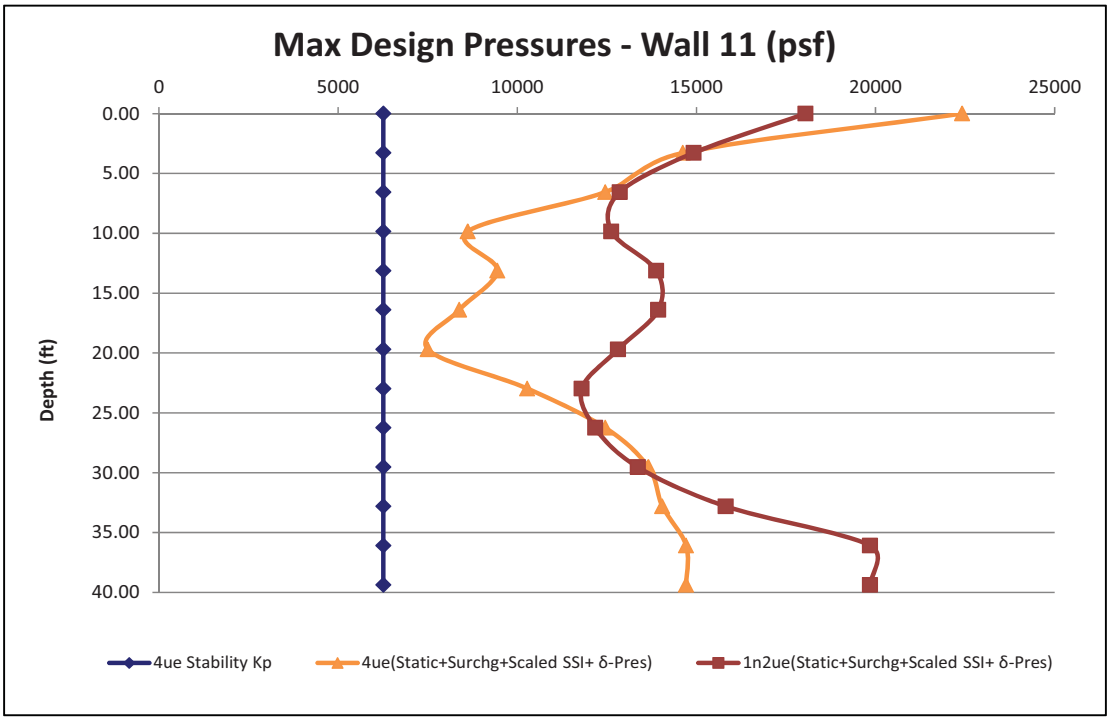

(e) In the design of the embedded walls and TG, the static soil pressure (earth pressure at rest) and effects of surcharge due to the weight of adjacent buildings (NI for the case of the TG) are applied as a separate load case. The dynamic load case corresponds to the passive pressures generated on the walls during the SSE condition. The passive soil pressures on the NI embedded walls (except for the TG) are calculated using the results from the SSI analysis. The SSI wall pressures are scaled up such that the maximum pressure on each wall is, at least, equal to the passive earth pressure obtained with K_p = 3. A comparison with Wood's soil pressures is performed to ensure that the applied passive soil pressures envelop the Wood's soil pressures. The dynamic load case corresponding to scaled SSI pressures and delta pressures due to uplift and sliding of the basemat is applied as a separate load case. The static and dynamic load cases are combined in the appropriate load combinations to obtain the design forces and moments of the walls. The above procedure was used for all soil cases except 5ae (rock case). For 5ae, the nodes of the embedded walls in contact with the excavation are laterally constrained to obtain design forces and moments of the walls.

The passive soil pressures and seismic design loads on the TG walls for all cases including the 5ae case are directly obtained from the nonlinear analysis of finite element model for NI common basemat foundation described in Section 3.7.2.3.1.4. These loads include the sidewall and delta pressures due to uplifting and sliding of the basemat. Rock case 5ae provides the maximum normal sidewall pressures on the TG walls. The maximum normal sidewall pressure over the entire time-history duration for case 5ae is roughly 75 ksf which envelops the maximum SASSI analysis value of 27 ksf. The seismic loads are combined with other static analysis load cases as described in Sections 3.8.1 through 3.8.4 to obtain the design forces and moments for the TG. U.S. EPR FSAR Tier 2, Section 3.8.5.4.2 will be revised to describe the design considerations for the NI embedded walls and TG.

(f) The apparent inconsistency between U.S. EPR FSAR Tier 2, Sections 3.8.5.4.1 and 3.8.5.4.2, has been corrected as indicated in the enclosed U.S. EPR FSAR markups.

4. The design of embedded walls will be addressed in the Response to RAI 155, Question 03.08.04-06.

5. The following clarification is provided to resolve the apparent inconsistency between the statements provided in the Responses to RAI 371, Question 03.07.02-66, Item (a) and RAI 376, Question 03.08.05-28, Item 3. The TG is designed to resist the maximum forces (shears and moments) due to the static pressure (including hydrostatic), surcharge effects, seismic SSI pressure, and additional pressure due to lifting/sliding of the basemat. As noted in Item (3) of the RAI (Question 03.07.02-78), the scaled SSI pressures always bound the Woods' (ASCE 4) solution.

   The BMAT model is used to derive the additional pressures on the TG due to lifting/sliding of the basemat. As stated in response to Item 2(g) of the RAI, static soil springs are used with the BMAT model to generate the forces and moments in the basemat due to various static load cases. The BMAT model with dynamic soil springs, derived using Gazetas method, was used to generate the delta pressures corresponding to the lifting/sliding of the basemat due to dynamic (seismic) loads.

6. In response to Question 6, the following additional information is provided:

   (a) The "edge" pressure in U.S. EPR FSAR Tier 2, Table 3.E.1-40, is the bearing pressure averaged over a strip of the basemat, representing five rows of elements or roughly 18% of the width of that section of the basemat excluding the corners. The bearing pressure contour plots in Figure 03.08.05-28-A through Figure 03.08.05-28-D in the Response to RAI 376, Question 03.08.05-28, show the edge pressures, as evidenced by the same color indicating uniform bearing pressure over that strip of the basemat. U.S. EPR FSAR Tier 2, Section 3E.1.9, will be revised (see enclosed FSAR markups) to include a description of the averaging process used in determining the edge pressures.

   (b) As reported in technical literature (see F.E. Richart and R.V. Whitman, "Footing Vibrations – Comparison of Test Results with Theory," University of Michigan, IP-755, November 1966) theoretical equations result in very high bearing pressures near the edges of the footing due to singularity. The authors present a more credible bearing (failure) pressure distribution shown in Figure 3.7.2-78-56 (reproduced from Richart's paper). In accordance with the postulated pressure distribution for combined static and dynamic loads, the bearing failure point moves away from the edge of the footing. Though the paper does not provide specific guidelines for averaging pressures near the edges (and corners), it does point to the need for a more realistic treatment of the theoretically derived peak pressures near the edges; and, thus, any FEM analysis. Therefore, averaging of the bearing pressures over the corner and edges of the basemat is considered to be a reasonable approach to estimate the corner and edge pressures.

Figure 3.7.2-78-56–Bearing Pressure Distribution for Foundations

(Reproduced from Richart and Whitman, University of Michigan, IP-755, September 1966)

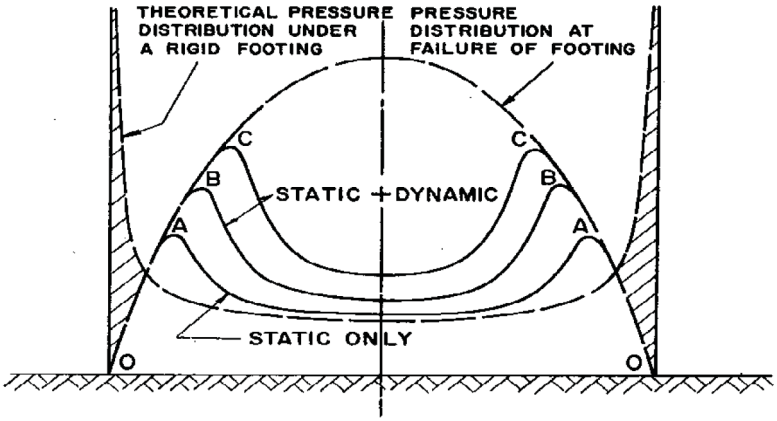

(a) DISTRIBUTION OF TOTAL LOAD

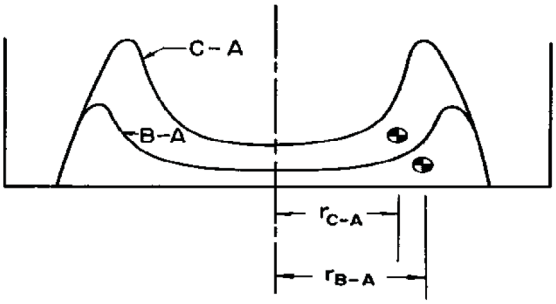

(b) REDUCTION OF THE EFFECTIVE RADIUS

(c) U.S. EPR FSAR Tier 2, Table 3E.1-40, includes the maximum edge pressures for the eight soil cases obtained from SASSI analyses. The bearing pressure contour plots (Response to RAI 376, Question 03.08.05-28, Figure 3.8.5-28-A through Figure 03.08.05-28-D) show the bearing pressures for the entire mat. The maximum edge pressure values reported in U.S. EPR FSAR Tier 2, Table 3E.1-40, are consistent with the bearing pressure contour plots. U.S. EPR FSAR Tier 2, Table 3E.1-40, has been updated and includes the corner pressures as shown in the enclosed U.S. EPR FSAR markup. The corner pressures were obtained by averaging the pressure over an area represented by a 6x6 corner grid.

The maximum dynamic bearing pressure demands shown in U.S. EPR FSAR Tier 1, Table 5.0-1, and U.S. EPR FSAR Tier 2, Table 2.1-1 and Section 2.5.4.10.1, have been updated as follows:

> "The maximum bearing pressure under safe shutdown earthquake loads combined with other loads, as described in Section 3.8.5, is 38,000 lbs/ft^2, for EUR soft soil, 48,000 lbs/ft^2 for EUR medium soil and 60,000 lbs/ft^2 for EUR hard soil. If a site with shear wave velocity that falls in between a soft and medium or between medium and hard soil conditions, the maximum dynamic bearing pressure demand is the larger of the two values. For sites not meeting the soil property requirements, a site-specific analysis is required."

(d) Bearing pressure contour plots generated from the ANSYS 3D FEM basemat model are shown in Figure 3.7.2-78-57 through Figure 3.7.2-78-60. These contour plots correspond to soil cases 1n2ue, 2sn4uem, 4uem, and 5aeh, respectively; and correspond to the SASSI-generated contour plots with similar soil cases shown in Figure 3.8.5-28-A though Figure 3.8.5-28-D in the Response to RAI 376, Question 03.08.05-28. The contour plots shown for the ANSYS results represent the bearing pressures without any averaging, whereas the SASSI contour plots show averaged corner and edge pressures. The two sets of results are comparable.

Figure 3.7.2-78-57: Case 1n2ue, Cracked, Time Snapshot of the Dynamic Bearing Pressure at Max Dynamic Bearing Pressure Time(s)

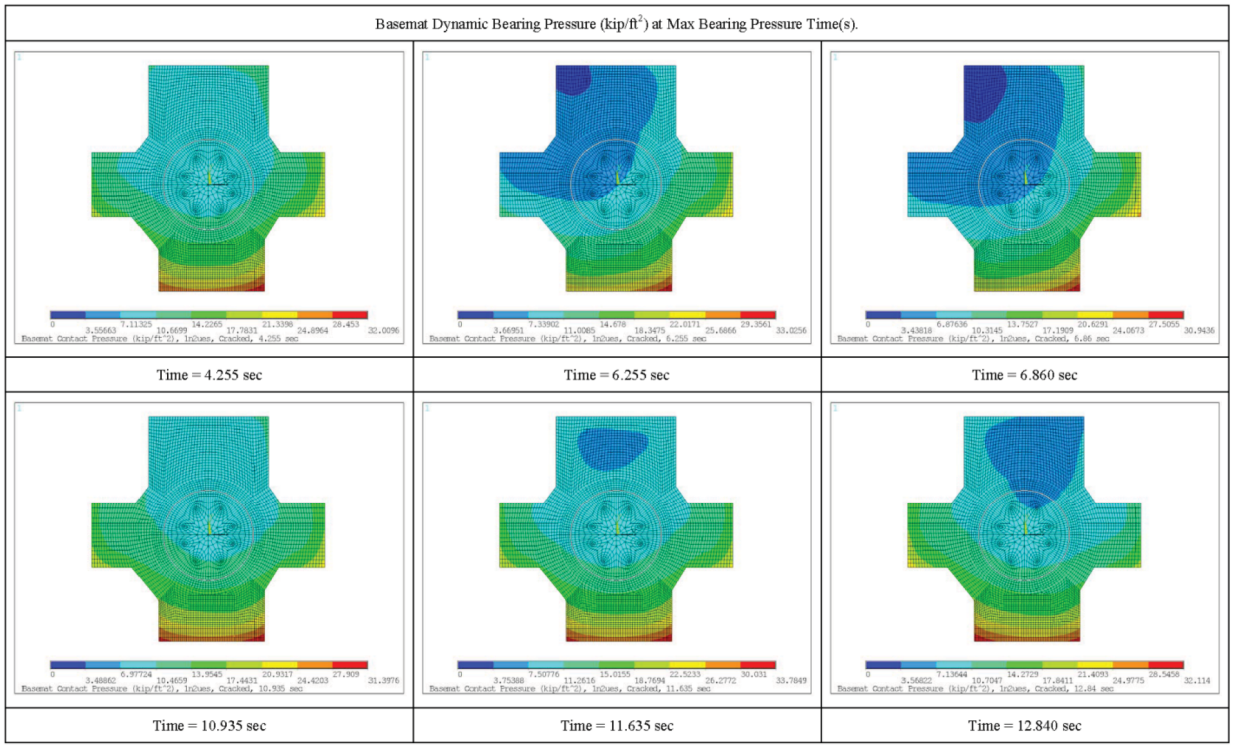

Figure 3.7.2-78-58: Case 2sn4uem, Cracked, Time Snapshot of the Dynamic Bearing Pressure at Max Dynamic Bearing Pressure Time(s)

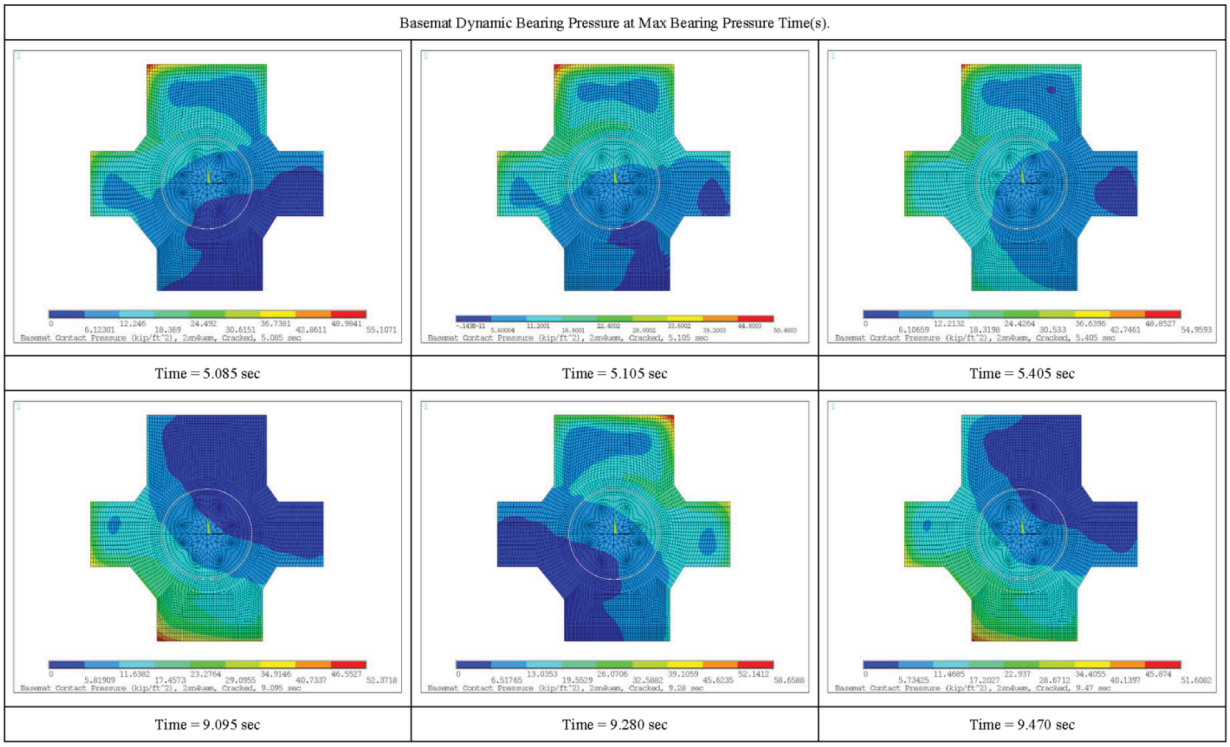

Figure 3.7.2-78-59: Case 4uem, Cracked, Time Snapshot of the Dynamic Bearing Pressure at Max Dynamic Bearing Pressure Time(s)